

# **Geno- and Phenotypic Characterisation of Coagulase-negative Staphylococci on Healthy Human Skin**

Dissertation

with the aim of achieving a doctoral degree at the

University of Hamburg

Department of Biology

submitted by

Charlotte Marie Ahle

Hamburg 2022

First evaluator: Prof. Dr. Wolfgang Streit

Second evaluator: Associate Prof. Dr. Holger Brüggemann

Date of oral defense: 07.07.2022

## **Eidesstattliche Versicherung**

Hiermit erkläre ich an Eides statt, dass ich die vorliegende Dissertationsschrift selbst verfasst und keine anderen als die angegebenen Quellen und Hilfsmittel benutzt habe.

*Declaration on oath*

*I hereby declare, on oath, that I have written the present dissertation by my own and have not used any other than the acknowledged resources and aid.*

Hamburg, 22.03.2022

---

Charlotte Marie Ahle

# Table of content

Zusammenfassung.....	5
Abstract.....	7
1 Introduction .....	8
1.1 The microbiome of healthy skin.....	8
1.2 Staphylococcal populations on human skin.....	9
1.3 Association of the skin microbiome with skin diseases.....	12
1.3.1 Atopic dermatitis .....	12
1.3.2 Acne.....	12
1.4 Health-beneficial traits of commensal staphylococci.....	13
1.4.1 Lantibiotics.....	14
1.4.2 Phenol-soluble modulins .....	15
1.4.3 Nonribosomal peptides.....	16
1.4.4 Signaling interferences.....	16
1.4.5 Interaction with the host immune system.....	18
1.4.6 Other modes of skin protection .....	19
1.5 Aim of this study .....	19
2 Publication I.....	21
3 Publication II.....	32
4 Manuscript I .....	45
5 Discussion .....	82
5.1 Establishment of a novel amplicon-based NGS approach for the characterisation of staphylococcal populations.....	82
5.2 Staphylococcal populations on healthy skin determined with culture-dependent and amplicon-based NGS approaches.....	84
5.3 <i>S. epidermidis</i> – skin guardian or infection-causing pathogen?.....	88

5.4	<i>C. acnes</i> populations on healthy skin .....	91
5.5	Interaction of CoNS and <i>C. acnes</i> on the skin.....	92
	References .....	96
	Appendix .....	107
	Danksagung.....	137

## Zusammenfassung

Staphylokokken gehören zu den am häufigsten vorkommenden Bakteriengattungen auf der gesunden menschlichen Haut. Während die Rolle von Staphylokokken bei Krankenhausinfektionen gut erforscht ist, fehlt es an umfassenden Kenntnissen über ihre Rolle als kommensale Hautbakterien. In dieser Studie wurden die Staphylokokken-Populationen von gesunder menschlicher Haut phäno- und genotypisch untersucht. Dazu wurde zunächst ein Next Generation Sequencing (NGS) Schema entwickelt, das auf der Amplifikation einer Teilsequenz des *tuf*-Gens beruht. Diese Methode wurde mit zwei zuvor veröffentlichten Methoden verglichen. In einer *in vivo* Studie wurden Hautabstriche von 30 Probanden mit gesunder Haut an Stirn, Wange, Unterarm und Rücken genommen. Im Anschluss wurden Staphylokokken-Stämme (n=557) kultivierungsbasiert isoliert und die Staphylokokken-Populationen mit dem neu entwickelten NGS-Schema analysiert. Die Ergebnisse zeigten, dass *Staphylococcus epidermidis* die häufigste Staphylokokken-Art war, gefolgt von *Staphylococcus capitis*, *Staphylococcus saccharolyticus* und *Staphylococcus hominis*. Interessanterweise wurde *Staphylococcus saccharolyticus* in früheren metagenomischen und (den meisten) kultivierungsbasierten Studien nicht beschrieben. Dies lässt sich vermutlich auf die anspruchsvollen Wachstumsanforderungen und das Fehlen eines Referenzgenoms von *S. saccharolyticus* zurückführen. In weiteren Experimenten wurden die Staphylokokken-Isolate auf ihre antimikrobielle Aktivität gegen *Staphylococcus aureus* und *Cutibacterium acnes* untersucht, die mit atopischer Dermatitis bzw. Akne assoziiert sind. Bemerkenswert ist, dass einige Staphylokokken-Stämme eine selektive antimikrobielle Aktivität gegen Akne-assoziierte *C. acnes*-Phylotypen zeigten. Interessanterweise wiesen Hautareale ohne Staphylokokken-Stämme mit nachweislich antimikrobieller Aktivität eine höhere Abundanz von Akne-assoziierten *C. acnes*-Phylotypen auf als Hautareale mit antimikrobiell aktiven Stämmen. Um einen Einblick in die zugrundeliegenden Mechanismen zu erhalten, wurde eine RNA-Sequenzierung eines antimikrobiell aktiven *S. epidermidis*-Stamms durchgeführt, der mit einem

Akne-assoziierten bzw. einem nicht Akne-assoziierten *C. acnes*-Stamm kultiviert wurde. Die Ergebnisse deuten auf eine Herabregulierung der Produktion und Aktivität antimikrobieller Peptide in *S. epidermidis* hin, solange dieser mit einem nicht Akne-assoziierten *C. acnes*-Stamm kultiviert wird.

## Abstract

Staphylococci belong to the most abundant bacterial genera present on healthy human skin. While the role of staphylococci in hospital-acquired infections is well studied, extensive knowledge of their role as skin commensals is lacking. In this study, staphylococcal populations of healthy human skin were pheno- and genotypically characterised. Therefore, a novel amplicon next-generation sequencing (NGS) scheme targeting the *tuf* gene was established and compared to two previously published methods. An *in vivo* study with 30 human volunteers with healthy skin was conducted. Skin swab samples were taken from the forehead, cheek, forearm and back to obtain staphylococcal isolates (n=557) and to analyze the staphylococcal populations via the amplicon-based NGS scheme. The results revealed *Staphylococcus epidermidis* as the most abundant staphylococcal species detected, followed by *Staphylococcus capitis*, *Staphylococcus saccharolyticus* and *Staphylococcus hominis*. Interestingly, *S. saccharolyticus* was not described in previous metagenomic and (most) culture-based studies. This can presumably be attributed to the fastidious growth requirements and the lack of a reference genome of *S. saccharolyticus*. In subsequent experiments, the staphylococcal isolates were screened for their antimicrobial activity against *Staphylococcus aureus* and *Cutibacterium acnes*, which are associated with atopic dermatitis and acne, respectively. Notably, some staphylococcal strains revealed a selective antimicrobial activity against acne-associated phlotypes of *C. acnes*. Interestingly, skin sites without staphylococcal strains with antimicrobial activity had a higher abundance of acne-associated phlotypes of *C. acnes*, compared to skin sites with antimicrobial active strains. To get mechanistic insights, RNA-sequencing of an antimicrobial active *S. epidermidis* strain co-cultured with an acne-associated and a non-acne-associated *C. acnes* strain, respectively, was performed. The results indicate a down-regulation of the production and activity of antimicrobial peptides in *S. epidermidis* when co-cultured with non-acne-associated *C. acnes*.



# 1 Introduction

## 1.1 The microbiome of healthy skin

As the most outer layer around our bodies, the human skin has many different functions. Our skin protects us from water loss, regulates body temperature, and prevents the entry of pathogens. The skin is made up of three main layers: epidermis, dermis and hypodermis. The top sub-layer of the epidermis consists of layers of corneocytes and is called stratum corneum. The skin surface is acidic with a high salt and low water content. Despite these seemingly inhospitable conditions, it is densely populated with microbes, the entirety of which is called the skin microbiome. The human skin microbiome consists of bacteria, fungi and viruses with the majority made up by bacteria (Byrd, Belkaid, & Segre, 2018). The three most abundant bacterial skin genera are *Staphylococcus*, *Corynebacterium* and *Cutibacterium* (Grice et al., 2009).

The composition of the skin microbiome differs highly between skin sites and skin conditions, which can be roughly divided in sebaceous, moist and dry skin sites (Byrd et al., 2018). Sebaceous skin sites are dominated by *Cutibacterium* and *Staphylococcus* species, while moist skin sites are mostly represented by *Corynebacterium* and *Staphylococcus* species (Grice et al., 2009). Dry skin sites reveal the highest diversity and are populated by a variety of different members from the phyla Actinobacteria, Proteobacteria, Firmicutes and Bacteroidetes. While the other skin sites are almost exclusively populated by Gram-positive bacteria, on dry skin sites some Gram-negative bacterial species can be found (Costello et al., 2009; Grice et al., 2009) (Fig. 1).

While it has long been assumed that the skin surface is  $\sim 2 \text{ m}^2$  in size, recent assessments factored in skin appendages and estimate the skin surface to  $\sim 25 \text{ m}^2$ , which gives a more realistic picture of the dimension of ecological niches for the microbiota (Gallo, 2017). Staphylococci are mostly located at the skin surface, while cutibacteria prefer the lipid-rich and anaerobic conditions of sebaceous glands

(Kearney, Harnby, Gowland, & Holland, 1984). Despite being exposed to many external influences, the skin microbiome of healthy skin is surprisingly stable over time (Costello et al., 2009; Oh et al., 2016).

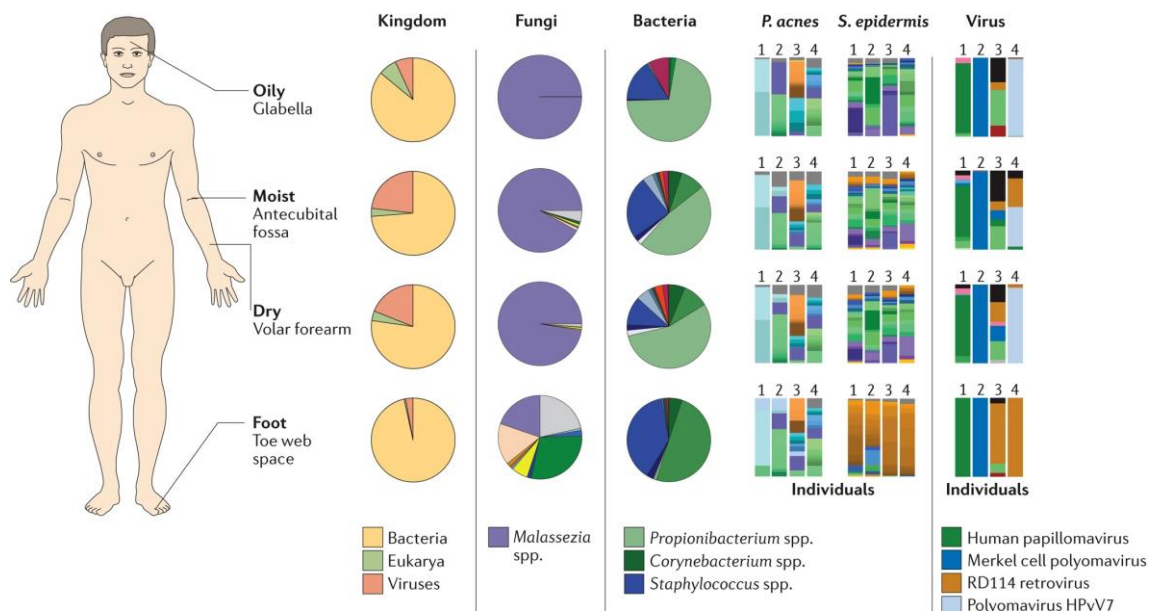


**Figure 1 Overview of the skin microbiome.** Composition of the skin microbiome on four skin sites (glabella, antecubital fossa, volar forearm, toe web space) is representative of oily, moist, dry and foot skin conditions. Pictured in pie charts is the mean composition of kingdom, fungi and bacteria on healthy skin. The bar charts show the *Cutibacterium acnes* (formerly *Propionibacterium acnes*), *Staphylococcus epidermidis* and virus populations of four individuals. Original figure from (Byrd et al., 2018). Reprinted with the permission of Springer Nature.

## 1.2 Staphylococcal populations on human skin

Staphylococci, the second most abundant skin genus can be found virtually on all body sites and individuals. They are Gram-positive, spherically shaped cluster forming bacteria. The species was named after their typical appearance under the microscope: “staphylo-” meaning “bunch of grapes” in ancient greek. At present, 61 different staphylococcal species are described in the NCBI taxonomy database (status: 10.02.2022) (Schoch et al., 2020). The genus is classified into coagulase-negative (CoNS) and coagulase-positive staphylococci (CoPS). As the name suggests, CoPS possess the ability to produce the enzyme coagulase, which converts fibrinogen to fibrin and thus results in the clotting of blood (Boden & Flock, 1989;

McDevitt, Vaudaux, & Foster, 1992). The main species of CoPS is *S. aureus*; its skin colonization is associated with skin disorders such as atopic dermatitis (Leyden, Marples, & Kligman, 1974). In contrast, staphylococci found on healthy skin belong almost exclusively to CoNS. Common CoNS found on skin are *Staphylococcus epidermidis*, *Staphylococcus hominis*, *Staphylococcus capitis*, *Staphylococcus warneri* and *Staphylococcus haemolyticus* (Kloss, 1975; K. H. K. Schleifer, W. E., 1975).

*S. epidermidis* is the most frequently isolated species from the skin, not only because of its abundance, but also because of its undemanding cultivation requirements. While very abundant on the skin, *S. epidermidis* can also act as an opportunistic pathogen involved in nosocomial infections (Otto, 2009). Especially, infections of implanted devices are in two thirds of cases caused either by *S. epidermidis* or *S. aureus* (Campoccia, Montanaro, & Arciola, 2006). They often cause persistent infection, which are difficult to treat because *S. epidermidis* can form biofilms on these devices (Mack et al., 2006). Of all CoNS species *S. epidermidis* causes the highest number of infections (Rogers, Fey, & Rupp, 2009).

There is great interest in understanding the differences between infection and skin commensal isolates of *S. epidermidis*, to get a better insight into their pathogenicity and skin beneficial functionality, respectively. The population of *S. epidermidis* can be divided into three clades (A, B and C). The B-clade consists mainly of skin isolates, while the A- and C-clades harbor isolates from various sources (Conlan et al., 2012; Espadinha et al., 2019). Furthermore, *S. epidermidis* strains are assigned to sequence types (ST), determined by multilocus sequence typing (MLST). *S. epidermidis* strains assigned to the ST types ST2, ST5 and ST23 are particularly often isolated from infections (Lee et al., 2018). Certain virulence genes such as the methicillin-resistance gene *mecA*, biofilm operon *icaADBC* and insertion sequence element IS256 are also more prevalent in *S. epidermidis* isolates from infections compared to skin commensals (Conlan et al., 2012; Rohde et al., 2004).

Staphylococci are also commensal colonizers of animals, but the species differ from those species commonly found on human skin. For example, *Staphylococcus arlettae*, *Staphylococcus auricularis* and *Staphylococcus devriesei* found on cows (Verdier-

Metz et al., 2012) are not commonly found on human skin. The same applies to *Staphylococcus equorum* and *Staphylococcus cohnii*, which are dominant on pig skin (Strube, Hansen, Rasmussen, & Pedersen, 2018).

Most *Staphylococcus* species possess a high salt tolerance and grow aerobically and facultative anaerobically. These capabilities make them highly adapted to the harsh conditions present on the skin. First analyses of staphylococcal populations on the skin were done with culture-based methods, and species were characterised based on phenotypic properties (Kloos & Musselwhite, 1975; Kloss, 1975; K. H. K. Schleifer, W. E., 1975). First phylogenetic characterisations of the skin microbiota were performed on single isolates via Sanger sequencing by using the full 16S rRNA gene (~1500 kb) (Lane et al., 1985). Next-generation sequencing (NGS) technologies made it possible to analyse not only the culturable skin bacteria, but also difficult or non-culturable ones. Furthermore, NGS enabled the sequencing of mixed bacterial communities. However, NGS methods often run on the Illumina MiSeq platform, which is restricted to a limited read length of around 300 kb. Hence, only a fraction of the 16S rRNA gene can be used as a phylogenetic marker (Meisel et al., 2016). These 16S rRNA gene fragments do not vary extensively between most staphylococcal species, which makes it difficult to differentiate beyond the genus level by using 16S rRNA amplicon-based NGS (Meisel et al., 2016). In contrast, whole genome shotgun sequencing makes it possible to analyse the microbiome consisting of bacteria, fungi, virus and the host genome simultaneously and with high resolution. However, this method is still comparatively costly, and a higher bioinformatic effort is needed to analyse the large extent of data created. Furthermore, the input DNA concentration needed for whole genome shotgun metagenomics is higher than for amplicon-based NGS, which is sometimes not feasible on skin sites with low bacterial numbers as, e.g. observed on the forearm.

### 1.3 Association of the skin microbiome with skin diseases

While the microbiome on healthy skin is stable over time (Oh et al., 2016), a shift in the skin microbiome, called dysbiosis, can be associated with skin diseases. The most common skin diseases linked to a pronounced microbiome shift are atopic dermatitis and acne.

#### 1.3.1 Atopic dermatitis

Atopic dermatitis is a multifactorial skin disease with a high prevalence of around 20 % in children of developed countries (Laughter, Istvan, Tofte, & Hanifin, 2000; Schultz Larsen, Diepgen, & Svensson, 1996; Sugiura et al., 1998). Common phenotypes/manifestations of atopic dermatitis are dry skin and a severe itch at the face, neck or inner side of elbow/knee (Spergel & Paller, 2003). Atopic dermatitis lesions are often colonized with *S. aureus* (Leyden et al., 1974). *S. aureus* colonization density correlates with atopic dermatitis disease severity (Tauber et al., 2016). Several virulence factors of *S. aureus* have been associated with atopic dermatitis. The alpha-toxin of *S. aureus* induces cell death in keratinocytes (Brauweiler, Goleva, & Leung, 2014). Additionally, *S. aureus* produces toxins that can act as superantigens such as Staphylococcal enterotoxin B or Toxic Shock Syndrome Toxin-1, which lead to hyperactivation of T cells and thus significant inflammation (Travers, 2014). A genetic predisposition in atopic dermatitis patients results in a deficient skin barrier, which can be exploited by *S. aureus* to penetrate into deeper skin layers and trigger the production of inflammatory cytokines (Nakatsuji et al., 2016). Furthermore, *S. aureus* can contribute to a deficient skin barrier by inducing serine protease activity in keratinocytes (Williams, Nakatsuji, Sanford, Vrbanac, & Gallo, 2017). These findings indicate that *S. aureus* skin colonization contributes to atopic dermatitis disease severity. This species thus provides a promising target for antibacterial therapies in atopic dermatitis.

#### 1.3.2 Acne

Acne is a chronic skin disease, affecting approximately 85% of adolescents and young adults (White, 1998). Typical skin manifestations are comedones, papules and pustules, which are formed in the pilosebaceous unit and sometimes can result

in scarring. While there is no evidence for a change in overall *C. acnes* populations density on acne affected skin compared to healthy controls, a decrease in *C. acnes* strain type diversity can be observed (Dagnelie et al., 2019). *C. acnes* can be divided into the six main phylotypes IA<sub>1</sub>, IA<sub>2</sub>, IB, IC, II and III (Lomholt & Kilian, 2010; McDowell, Nagy, Magyari, Barnard, & Patrick, 2013). These phylotypes can be subdivided into different single-locus sequence type (SLST) classes (A to L), where A to E corresponds to the phylotype IA<sub>1</sub>, F to IA<sub>2</sub>, G to IC, H to IB, K to II and L to III (Scholz, Jensen, Lomholt, Bruggemann, & Kilian, 2014). On acne-affected skin, strains of *C. acnes* A-class, C-class and F-class are enriched, while strains of H-class and K-class *C. acnes* are more prevalent on healthy skin (Dagnelie et al., 2018; Lomholt, Scholz, Bruggemann, Tettelin, & Kilian, 2017; McDowell et al., 2012; McDowell et al., 2011; Nakase et al., 2020; Nakase, Hayashi, Akiyama, Aoki, & Noguchi, 2017). Acne-associated F-class strains produce higher amounts of porphyrins than non-acne associated K-class strains (T. Johnson, Kang, Barnard, & Li, 2016). Porphyrins are increased on acne-affected skin and can induce inflammation in keratinocytes through the production of reactive oxygen species (ROS) (Meyer et al., 2015; Schaller et al., 2005). Furthermore, acne-associated *C. acnes* strains harbor more virulence genes than non-acne-associated strains (Tomida et al., 2013). Hence, not the whole species, but certain *C. acnes* strain-classes are associated with acne.

#### **1.4 Health-beneficial traits of commensal staphylococci**

For decades, most research focused on the pathogenicity of staphylococci and their involvement in hospital-acquired infections. However, recent findings showed the importance of commensal staphylococcal species on the skin, most notably *S. epidermidis*. They play a central role in maintaining the skin microbiome homeostasis, e.g. in atopic dermatitis: An early colonization with commensal staphylococcal species lowers the risk of developing atopic dermatitis (Kennedy et al., 2017). Some staphylococcal strains possess antagonistic properties against potentially disease-causing skin bacteria, e.g. *S. aureus* and *C. acnes*. These mechanisms may play a central role in preventing skin diseases such as acne and

atopic dermatitis associated with skin dysbiosis. The different antagonistic mechanisms of CoNS are explained in the following paragraphs.

#### 1.4.1 Lantibiotics

Many staphylococcal strains produce antimicrobial peptides, which most commonly belong to the group of lantibiotics. The study of Nakatsuji et al. (2017) showed that colonization with staphylococcal strains that possess antimicrobial activity occur less frequently on atopic dermatitis patient skin compared to healthy controls, demonstrating their importance in protecting against skin disease.

Lantibiotics are post-translationally modified peptides and named after their unusual amino acids lanthionine and methyllanthionine. They can be classified according to their structure into groups A and B. Group A lantibiotics show an elongated structure, while group B lantibiotics are globular (Bierbaum & Sahl, 2009). Most lantibiotics produced by CoNS belong to the group A lantibiotics. The so far best described staphylococcal lantibiotic is epidermin, produced by certain strains of *S. epidermidis* (Schnell et al., 1988), which shows activity against *S. aureus* and *C. acnes* (Kellner et al., 1988) (Fig. 2). Other lantibiotics expressed by certain *S. epidermidis* strains are lantibiotics pep5, epicidin 280, epilancin K7, epidermicin NI01 and epilancin 15x (Heidrich et al., 1998; Kaletta et al., 1989; Sandiford & Upton, 2012; van de Kamp et al., 1995). Bacterial mechanisms to hinder the activity of lantibiotics occur mostly not lantibiotic-specific, such as the alteration of the cell wall or composition of the membrane (Draper, Cotter, Hill, & Ross, 2015). One example is the multiple peptide resistant factor (MprF) in *S. aureus*, which enables the esterification of lysine in phosphatidylglycerol in the membrane. This leads to a reduced negative charge of the cell membrane, making it less susceptible to cationic peptides (Peschel et al., 2001). However, specific resistance to lantibiotics is very rare, making them an important potential alternative to antibiotics (Draper et al., 2015).

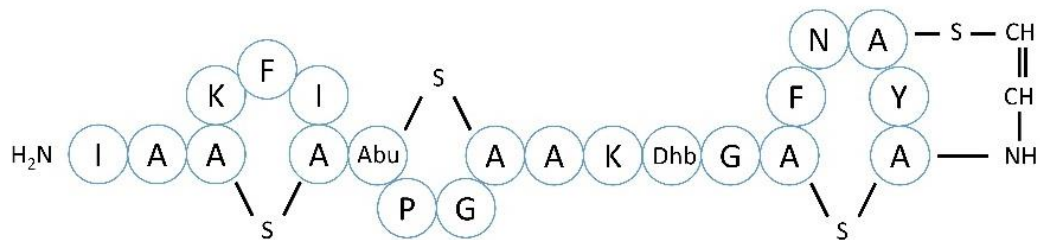


**Figure 2 Primary structure of the lantibiotic epidermin.** Dhb: 2,3-didehydroalanine, A-S-A: lanthionine, Abu-S-A: 3-methylanthionine.

#### 1.4.2 Phenol-soluble modulins

Phenol-soluble modulins (PSMs) are amphipathic,  $\alpha$ -helical peptides produced by staphylococci. There are two different types of PSMs, which differ in their size. The  $\alpha$ -type PSMs are 20 to 25 amino acids in length, while  $\beta$ -type PSMs are 43 to 44 amino acids long. *S. epidermidis* produces four  $\alpha$ -type PSMs (PSM $\alpha$ , PSM $\gamma$ , PSM $\delta$ , PSM $\epsilon$ ,) and two  $\beta$ -type PSMs (PSM $\beta$ 1, PSM $\beta$ 2) (Mehlin, Headley, & Klebanoff, 1999; Yao, Sturdevant, & Otto, 2005). Especially for *S. aureus*, PSMs have been described as a virulence factor, e.g. PSM $\gamma$  (called  $\delta$ -toxin) secreted by *S. aureus* can cause lysis of membranes (Alouf, Dufourcq, Siffert, Thiaudiere, & Geoffroy, 1989; Yoshida, 1963). Furthermore, they are important in biofilm formation and dissemination of *S. epidermidis* (R. Wang et al., 2011). All *Staphylococcus* species and strains are capable of expressing PSMs. However, different PSM-types are produced, which differ in their properties. It is important to note that the name of PSM-types describe different peptides in different species, e.g. PSM $\beta$ s in *S. epidermidis* are different from PSM $\beta$ s in *S. capitis*.

While *S. aureus* secretes high amounts of cytolytic PSMs (PSM $\alpha$ 3 and PSM $\delta$ ), *S. epidermidis* mostly produces non-cytolytic PSM $\beta$ s (Cheung et al., 2010). Expression of *S. epidermidis* PSM $\beta$ s is directly controlled by the quorum sensing *agr* system (Queck et al., 2008). PSMs in commensal CoNS can exhibit antimicrobial activity, often in synergy with other antimicrobial peptides (AMPs) (Cogen, Yamasaki, Muto, et al., 2010; Cogen, Yamasaki, Sanchez, et al., 2010; O'Neill et al., 2020). Therefore, they could play a role in inhibiting the colonization of potential



pathogens on the skin. *S. capitis* secretes four different PSM $\beta$ s with antimicrobial activity against *C. acnes* (O'Neill et al., 2020). Furthermore, an *S. epidermidis* strain was found, whose produced PSM $\gamma$  act synergistically together with host AMPs against group A streptococci (Cogen, Yamasaki, Sanchez, et al., 2010).

#### 1.4.3 Nonribosomal peptides

Nonribosomal peptides are directly synthesized by nonribosomal peptide synthetases, thus their synthesis is independent of mRNA. Their properties range from antimicrobial, cytostatic or immunosuppressant. Recently, a *Staphylococcus lugdunensis* strain derived from the nose was found to produce a nonribosomal antimicrobial peptide, designated lugdunin, with activity against *S. aureus* (Zipperer et al., 2016). Lugdunin enhances the expression of human AMPs in keratinocytes and induces the innate immune response. Both mechanisms reveal a strong potential of preventing and reducing *S. aureus* colonization on the skin (Bitschar et al., 2019).

#### 1.4.4 Signaling interferences

The *agr* (accessory gene regulator) system represents the main quorum sensing system of staphylococci. *S. aureus* virulence factors such as PSM $\alpha$  and PSM $\delta$  can promote skin inflammation in atopic dermatitis and are controlled by the *agr* system (Nakagawa et al., 2017; Nakamura et al., 2013; Yarwood & Schlievert, 2003). It was recently shown that the *agr* system of *S. aureus* is critical for epidermal colonization and inflammation in atopic dermatitis (Y. Nakamura et al., 2020). Therefore, the *agr* system provides a potential target to alleviate symptoms triggered through *S. aureus* in atopic dermatitis.

The *agr* system locus is composed of the *agrBDCA* operon. The pro-peptide precursor AgrD gets exported out of the cell and modified by the integral membrane peptidase AgrB to become the autoinducing peptide (AIP). The AIP is detected by the histidine kinase AgrC. The latter phosphorylates the response regulator AgrA, which in turn activates the expression of the *agrBDCA* operon and RNAlII (reviewed in: (Thoendel, Kavanaugh, Flack, & Horswill, 2011)). RNAlII is a regulatory RNA and the main effector of the *agr* system. Part of the RNAlII sequence is the *hld* gene, which codes for the  $\delta$ -toxin (Janzon, Lofdahl, & Arvidson, 1989). While most gene

expression is regulated through RNAIII, AgrA also directly activates the expression of PSM genes (Queck et al., 2008) (Fig. 3). Interestingly, it was observed that AIPs of other strains or species function as competitive antagonists of the *agr* system, by binding to AgrC, thereby blocking the receptor (Ji, Beavis, & Novick, 1997) (Fig. 3).

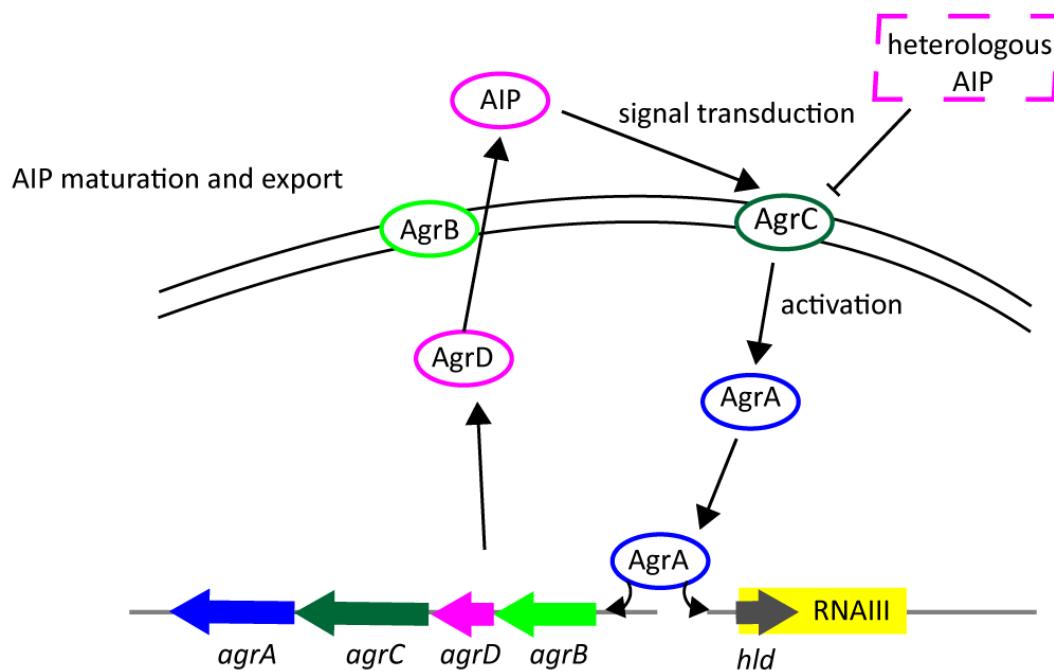


**Figure 3 Scheme of quorum sensing and quenching of the *agr* system in staphylococci.** AIP pre-cursor peptide (coded in *agrD*) gets exported and matured through the membrane peptidase AgrB. AIP binds to the histidine kinase AgrC, which activates AgrA. AgrA activates the expression of the *agrBDCA* operon and RNAIII. Heterologous AIP can bind to AgrC and thus, can inhibit the *agr* system.

Allelic variants of the AIP gene are present in staphylococcal species and hence, the AIP length can vary between seven to nine amino acids (Yarwood & Schlievert, 2003). In the case of *S. aureus* and *S. epidermidis*, four different AIP types (*agr*-I, -II, -III and -IV) are described for each species (Yarwood & Schlievert, 2003; Zhou et al., 2020). Analyses of the structure and activity of the AIP/AgrC interaction showed that the AIP conformation is essential for the ability to activate or inhibit AgrC (J. G. Johnson, Wang, Debelouchina, Novick, & Muir, 2015).

Through these different AIP types, staphylococcal strains can interfere with the *S. aureus agr* system and inhibit the expression of virulence factors involved in

atopic dermatitis. This cross-species quorum quenching between *S. epidermidis* and *S. aureus* was first described by Otto, Sussmuth, Vuong, Jung, and Gotz (1999). In addition, strains of other commensal CoNS species from the skin, such as *S. hominis*, *S. simulans* or *S. caprae*, showed a potent inhibition of *S. aureus agr* signaling (Brown et al., 2020; Paharik et al., 2017; Williams et al., 2019). Staphylococcal species derived from animal skin such as *Staphylococcus hycius* and *Staphylococcus lentus* were also shown to inhibit the *S. aureus* quorum sensing system (Peng et al., 2019). It was shown that *S. epidermidis agr-I* type is able to inhibit *S. aureus agr-I*, *agr-I* and *agr-III* type systems (Otto, Echner, Voelter, & Gotz, 2001). Interestingly, metagenomic analysis of the atopic dermatitis patient's skin microbiome revealed that a reduced abundance of *S. epidermidis agr-I* is associated with a higher disease severity in atopic dermatitis (Williams et al., 2019).

#### 1.4.5 Interaction with the host immune system

So far, most research on the interaction between the human immune system and microorganisms focusses on pathogens. However, it was suggested that most interactions occur in a symbiotic manner with commensal bacteria of the human microbiome (Belkaid & Hand, 2014).

It was shown that colonization with *S. epidermidis* enhances the human innate immunity through dendritic cells which prime CD8+ T cells. The CD8+ T cells migrate to the skin, enhance the antimicrobial defense of keratinocytes and thus, inhibiting the invasion of pathogenic bacteria (Naik et al., 2015). In addition, it was shown that *S. epidermidis* inhibit toll-like receptor 3 (TLR3) induced inflammation through lipoteichoic acid (Lai et al., 2009). The study of Pastar et al. (2020) showed that *S. epidermidis* upregulates perforin-2 expression in skin cells, which in turn leads to an increased killing of intracellular *S. aureus* (Pastar et al., 2020). Staphylococcal species were shown to provoke an increased antimicrobial defense of the host in a TLR2-mediated manner (Lai et al., 2010). Furthermore, *S. epidermidis* induced the expression of the microRNA miR-143 in keratinocytes, which can inhibit *C. acnes*-induced inflammation in acne (Xia et al., 2016).

#### 1.4.6 Other modes of skin protection

Besides the production of antimicrobial peptides, signaling interferences and interaction with the immune system, other mechanisms through CoNS are thought to have a beneficial impact on skin health. *S. epidermidis* produces the short-chain fatty acid succinic acid with antimicrobial properties against *C. acnes*, implicated in acne (Y. Wang et al., 2014). *S. epidermidis* secretes an Esp serine protease with the ability to degrade *S. aureus* biofilm and thus, hinders the colonization of *S. aureus* (Iwase et al., 2010). Additionally, *S. epidermidis* produces a sphingomyelinase, which may facilitate the production of protective ceramides, preventing skin dehydration and skin barrier disruption (Zheng et al., 2022).

### 1.5 Aim of this study

The aim of this study was to characterise the staphylococcal populations on healthy human skin. Therefore, an *in vivo* study with 30 healthy volunteers was conducted and skin swab samples were taken from the skin of forehead, cheek, forearm and back. Subsequently, the staphylococcal populations were characterised with culture-dependent and -independent approaches. For the culture-independent approach a novel amplicon-based NGS scheme was established. Staphylococcal isolates were collected from the skin for phenotypic and genotypic characterisation. The pathogenic potential of *S. epidermidis* isolates from healthy skin was assessed by genome sequencing and compared to the genomes of *S. epidermidis* isolates derived from infections. Isolated staphylococcal strains were screened *in vitro* for their antimicrobial properties against different strains of *S. aureus* and *C. acnes*, involved in atopic dermatitis and acne, respectively. To get insight into the interaction mechanisms between CoNS and *C. acnes*, RNA-sequencing of a *S. epidermidis* strain in co-culture with acne- and non-acne-associated *C. acnes* strains was performed.

The geno- and phenotypic characterisation of staphylococci on healthy skin resulted in the following two publications and one manuscript:

**Publication I:**

**Ahle CM et al.** Comparison of three amplicon sequencing approaches to determine staphylococcal populations on human skin. *BMC Microbiol* 21, 221 (2021).

**Publication II:**

**Ahle CM et al.** *Staphylococcus saccharolyticus*: An Overlooked Human Skin Colonizer. *Microorganisms* 8, (2020).

**Manuscript I:**

**Ahle CM et al.** Interference and co-existence of staphylococci and *Cutibacterium acnes* within the healthy human skin microbiome. (submitted)

## 2 Publication I

### **Comparison of three amplicon sequencing approaches to determine staphylococcal populations on human skin**

Charlotte Marie Ahle, Kristian Stødkilde-Jørgensen, Anja Poehlein, Wolfgang R. Streit, Jennifer Hüpeden, Holger Brüggemann

**Published in:**

BMC Microbiology (2021)

**DOI:**

10.1186/s12866-021-02284-1

**Contributions to the article:**

- Writing of manuscript
- Planning and conducting the study
- Isolation and species characterisation of staphylococcal isolates from skin
- DNA extraction of skin swabs and staphylococcal isolates
- Assembling of mock communities
- Analysis and visualization of amplicon NGS data
- Phylogenomic analysis

---

Associate Prof. Dr. Holger Brüggemann

## METHODOLOGY ARTICLE

## Open Access

# Comparison of three amplicon sequencing approaches to determine staphylococcal populations on human skin



Charlotte Marie Ahle<sup>1,2</sup>, Kristian Stødtkilde-Jørgensen<sup>3</sup>, Anja Poehlein<sup>4</sup>, Wolfgang R. Streit<sup>2</sup>, Jennifer Hüpeden<sup>1</sup> and Holger Brüggemann<sup>3\*</sup> 

## Abstract

**Background:** Staphylococci are important members of the human skin microbiome. Many staphylococcal species and strains are commensals of the healthy skin microbiota, while few play essential roles in skin diseases such as atopic dermatitis. To study the involvement of staphylococci in health and disease, it is essential to determine staphylococcal populations in skin samples beyond the genus and species level. Culture-independent approaches such as amplicon next-generation sequencing (NGS) are time- and cost-effective options. However, their suitability depends on the power of resolution.

**Results:** Here we compare three amplicon NGS schemes that rely on different targets within the genes *tuf* and *rpsK*, designated *tuf1*, *tuf2* and *rpsK* schemes. The schemes were tested on mock communities and on human skin samples. To obtain skin samples and build mock communities, skin swab samples of healthy volunteers were taken. In total, 254 staphylococcal strains were isolated and identified to the species level by MALDI-TOF mass spectrometry. A subset of ten strains belonging to different staphylococcal species were genome-sequenced. Two mock communities with nine and eighteen strains, respectively, as well as eight randomly selected skin samples were analysed with the three amplicon NGS methods. Our results imply that all three methods are suitable for species-level determination of staphylococcal populations. However, the novel *tuf2*-NGS scheme was superior in resolution power. It unambiguously allowed identification of *Staphylococcus saccharolyticus* and distinguishing phylogenetically distinct clusters of *Staphylococcus epidermidis*.

**Conclusions:** Powerful amplicon NGS approaches for the detection and relative quantification of staphylococci in human samples exist that can resolve populations to the species and, to some extent, to the subspecies level. Our study highlights strengths, weaknesses and pitfalls of three currently available amplicon NGS approaches to determine staphylococcal populations. Applied to the analysis of healthy and diseased skin, these approaches can be useful to attribute host-beneficial and -detrimental roles to skin-resident staphylococcal species and subspecies.

## Background

Studying the skin microbiome is regarded increasingly important in understanding skin diseases as well as skin health. The genus *Staphylococcus* is one of the most abundant bacterial genera in the human skin

microbiome; it plays a central role on human skin and in health and disease [1–17]. While the skin colonization by *Staphylococcus aureus* is correlated with disease severity, as seen for example in atopic dermatitis [1], coagulase-negative staphylococci (CoNS) are regarded as having rather health-beneficial roles on human skin. Common CoNS species that can be found on human skin are *Staphylococcus epidermidis*, *Staphylococcus*

\* Correspondence: [brueggemann@biomed.au.dk](mailto:brueggemann@biomed.au.dk)

<sup>3</sup>Department of Biomedicine, Aarhus University, 8000 Aarhus, Denmark  
Full list of author information is available at the end of the article



© The Author(s). 2021 **Open Access** This article is licensed under a Creative Commons Attribution 4.0 International License, which permits use, sharing, adaptation, distribution and reproduction in any medium or format, as long as you give appropriate credit to the original author(s) and the source, provide a link to the Creative Commons licence, and indicate if changes were made. The images or other third party material in this article are included in the article's Creative Commons licence, unless indicated otherwise in a credit line to the material. If material is not included in the article's Creative Commons licence and your intended use is not permitted by statutory regulation or exceeds the permitted use, you will need to obtain permission directly from the copyright holder. To view a copy of this licence, visit <http://creativecommons.org/licenses/by/4.0/>. The Creative Commons Public Domain Dedication waiver (<http://creativecommons.org/publicdomain/zero/1.0/>) applies to the data made available in this article, unless otherwise stated in a credit line to the data.

*hominis*, *Staphylococcus capitis* and *Staphylococcus haemolyticus* and others [18, 19]. As an important host-beneficial mechanism of certain CoNS, colonization resistance can prevent the expansion of potential pathogens on the skin; this is achieved by different CoNS properties such as the production of bacteriocins and phenol-soluble modulins [2–5] and quorum-sensing interference [6, 7]. Other host beneficial mechanisms of CoNS include, for example, the training and fortification of skin immunity [8–11], supporting wound healing [12, 13], and, possibly, anti-cancer effects [14]. Such host-interacting functions of CoNS are often species-, subspecies-, phylotype- and even strain-specific [2, 11, 14, 20, 21].

It was shown that one individual is not only colonised by an array of different staphylococcal species, but also by different strains of each species, in particular of *S. epidermidis* [22, 23]. The population of *S. epidermidis* species consists of strains belonging to three main phylogenetically distinct clades (A, B and C) [24–26]. In addition, a myriad of individual strains within each clade can be distinguished that differ in the core genome by single nucleotide polymorphisms (SNPs) and in the flexible genome by strain-specific genomic islands and extrachromosomal plasmids [20, 24, 25, 27].

To comprehensively map staphylococci on human skin, specific methods are needed to determine populations beyond the genus and species level. Traditionally, studies concerning the determination of staphylococci employed cultivation approaches with solid agar-based media [28, 29]. This makes it possible to investigate the isolated strains regarding their geno- and phenotypes. Depending on the choice of media and growth conditions, cultivation methods can underrepresent slow-growing and fastidious microorganisms. In contrast, culture-independent methods employing next-generation sequencing (NGS) achieve a more comprehensive picture of the skin microbiome [30]. Previous culture-independent studies have often relied on the 16S rRNA gene. However, this gene is inadequate to sufficiently distinguish several different staphylococcal species, and does not discriminate populations beyond the species level [31, 32]. Alternative target genes for identification and differentiation of staphylococcal isolates were evaluated and proposed such as *kat* [33], *gap* [31, 34, 35], *hsp60* [36, 37], *rpoB* [38, 39] and *sodA* [40]. One of the most established gene targets is *tuf*, which codes for elongation factor Tu (EF-Tu) [41]. The *tuf* gene, or rather fragments thereof, is also used as a target for analysing mixed staphylococcal communities with NGS methods, hereafter referred to as amplicon NGS [42–45]. Furthermore, the staphylococcal *rpsK* gene that encodes the 30S ribosomal protein S11 was recently proposed for amplicon NGS [46].

Here, we first isolated staphylococcal strains obtained from skin swabs of healthy volunteers, in order to assemble staphylococcal mock communities. We then compared three amplicon NGS schemes for their suitability to determine the staphylococcal populations of these mock communities. Two tested amplicon NGS schemes target different *tuf* gene fragments; one was developed by Martineau et al. [41] and the other one by Ahle et al. [47], designated here *tuf1* and *tuf2* scheme, respectively. The third tested scheme, designated *rpsK* scheme, targets a fragment of the *rpsK* gene and was developed by Ederveen et al. [46]. Lastly, the three amplicon NGS schemes were tested on skin swab samples obtained from healthy volunteers.

## Results

### Origin of targets for amplicon NGS

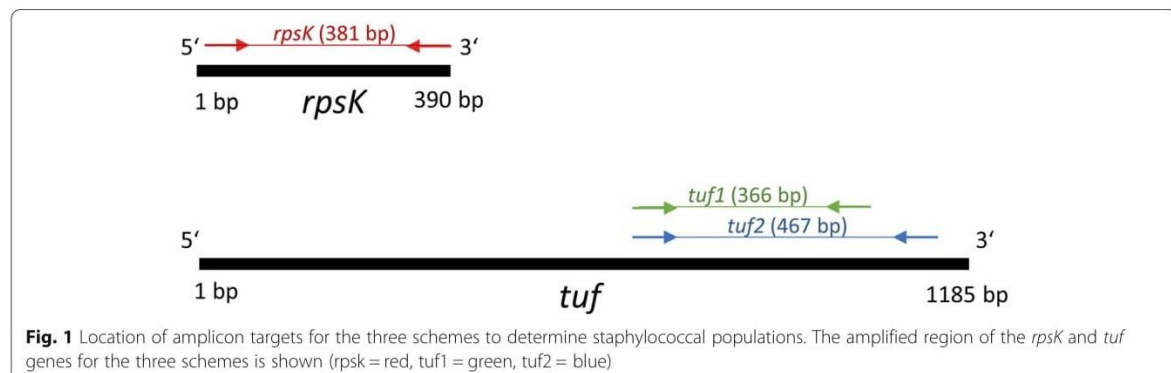
Here, we compared three different amplicon NGS schemes, all previously published and designed for determining staphylococcal populations in mixed communities: *tuf1* and *tuf2* schemes target the *tuf* gene and the *rpsK* scheme targets the *rpsK* gene. The *rpsK* and *tuf1* amplicon targets have a similar length with 381 and 366 bp, respectively, while the *tuf2* amplicon target is with 467 bp the longest among the three targets (Fig. 1). The amplicon targets *tuf1* and *tuf2* overlap to some extent (position 688 to 1053 bp and 685 to 1151 bp, respectively).

### Amplicon NGS of bacterial mock communities

Two different bacterial mock communities (M1/M2) were prepared, containing DNA of nine (M1) and 18 (M2) different staphylococcal strains, respectively (Additional file 1). All utilized strains belonged to staphylococcal species commonly found on human skin. They originated either from publicly accessible collections or were isolated here from healthy skin. Strains isolated here, in total 254 strains, were first identified to the species level by MALDI-TOF mass spectrometry (Additional file 2). A subset of ten strains belonging to different staphylococcal species were subsequently genome sequenced to obtain a complete genome database for the two mock communities (Additional file 3).

To test whether the three NGS schemes can distinguish between staphylococci on species level, the mock community M1 was analysed. The mock community M1 contained one strain each of *S. aureus*, *S. capitis*, *S. epidermidis*, *S. haemolyticus*, *S. hominis*, *Staphylococcus saccharolyticus*, *Staphylococcus saprophyticus*, *Staphylococcus simulans* and *Staphylococcus warneri* (Additional file 1). DNA was pooled in equimolar ratios and the three amplicon NGS pipelines were applied. All three schemes were able to identify and distinguish each of the nine species. The *rpsK* and the *tuf1* schemes slightly





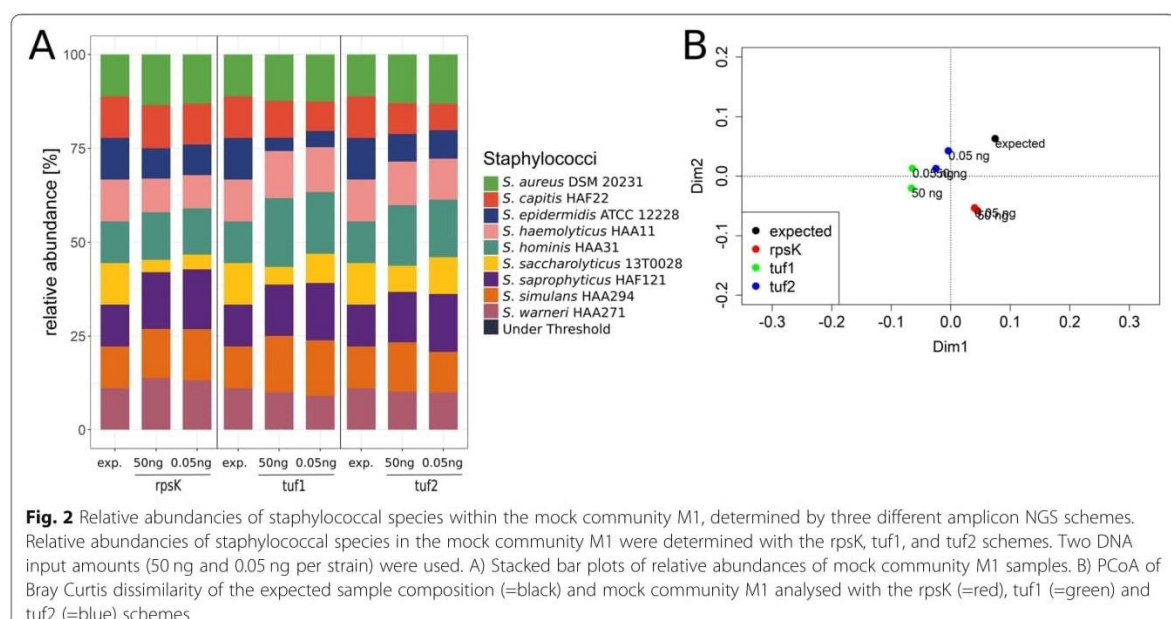
underrepresented *S. saccharolyticus* and *S. epidermidis*, respectively (Fig. 2A). A principal coordinate analysis (PCoA) plot of Bray Curtis dissimilarity was constructed to examine how accurate each scheme can represent the expected staphylococcal composition of mock community M1. The *tuf2* scheme represented the expected sample composition more accurately than the other two schemes. We repeated the experiment with different DNA input amounts, varying from 0.05 ng to 50 ng DNA per strain. The DNA input amount did only mildly influence the detected relative abundancies by the three schemes (Fig. 2 A and B).

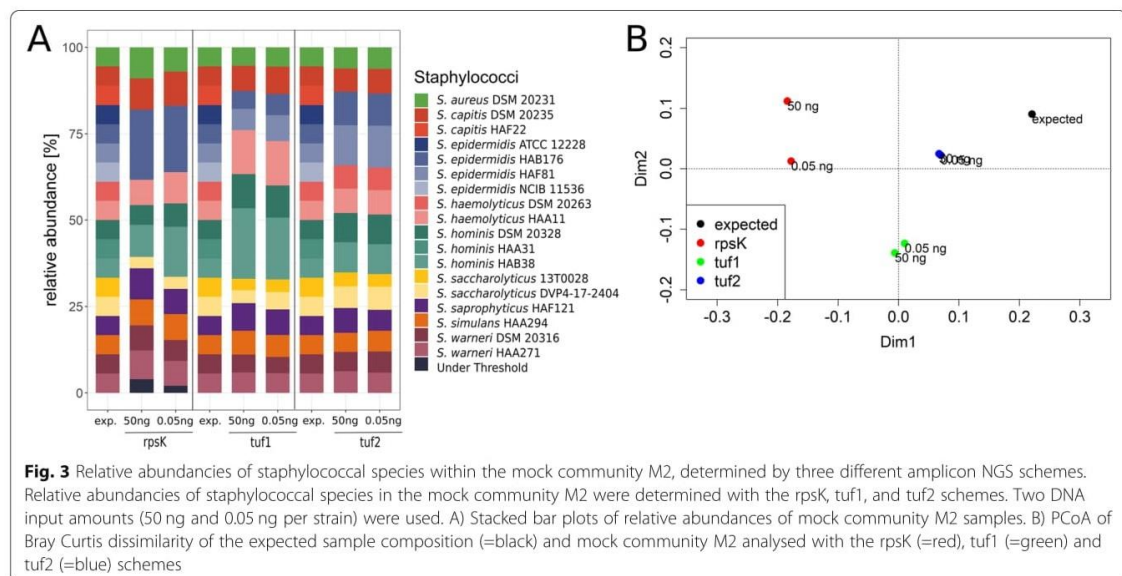
The second mock community M2 was composed of 18 strains to investigate whether the schemes were able to resolve diversity of samples beyond the species level. The mock community M2 included genomic DNA of

one *S. aureus* strain, two *S. capitis* strains, four *S. epidermidis* strains, two *S. haemolyticus* strains, three *S. hominis* strains, two *S. saccharolyticus* strains, one *S. saprophyticus* strain, one *S. simulans* strain and two *S. warneri* strains (Additional file 1).

First, we calculated the theoretical resolution power of each scheme regarding the M2 community. To do so, we extracted the three target alleles of each of the 18 genomes present in M2 and built phylogenetic trees. The trees showed that the *rpsK*, *tuf1* and *tuf2* schemes should distinguish 12, 14 and 15 strains, respectively (Additional file 4). Thus, in silico, the *tuf2* scheme is superior in resolution power.

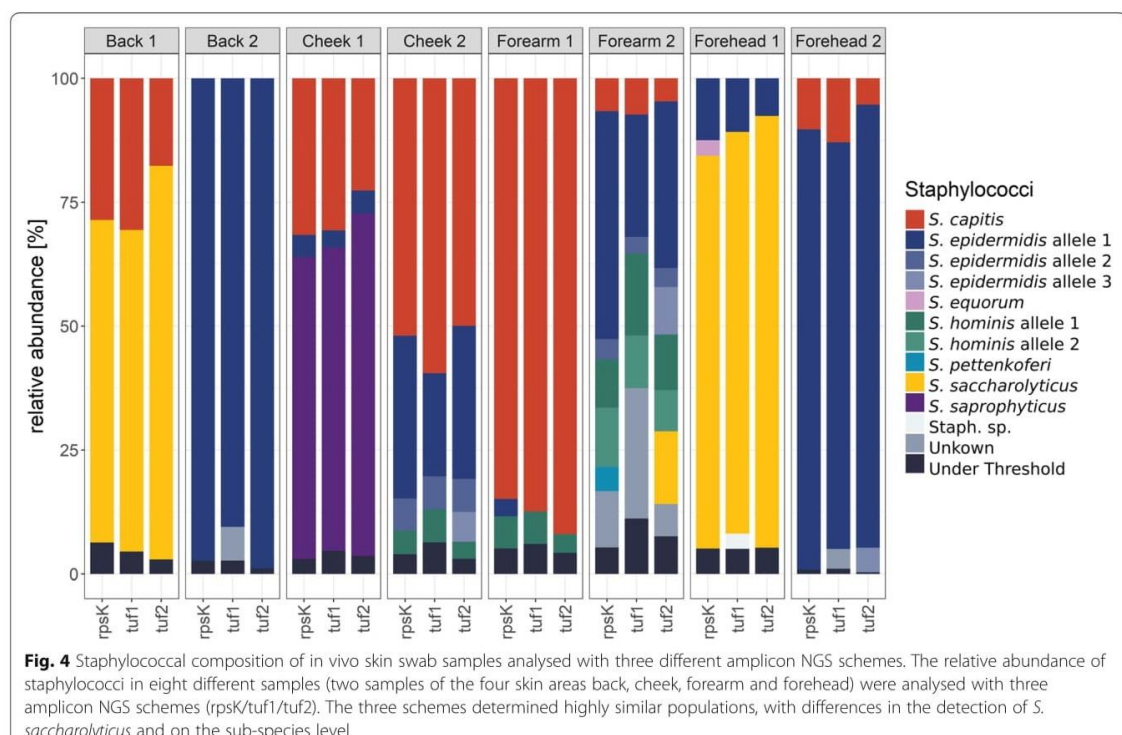
Next, we applied the three schemes to analyse the DNA cocktail of the mock community M2. The *rpsK* scheme detected 11 strains, while the *tuf1* and *tuf2*





schemes detected 13 and 14 strains, respectively (Fig. 3A). The PCoA plot from Bray Curtis dissimilarity showed that the expected sample composition was best reflected by the data generated with the tuf2 scheme.

Furthermore, compared to the two tuf schemes, data generated with the rpsK scheme showed a higher divergence when different DNA input amounts were used (Fig. 3 A and 3B).



### Amplicon NGS of human skin swab samples

Next, we applied the three schemes for the determination of staphylococcal populations in vivo. Eight skin swab samples from eight different volunteers were randomly selected. These eight samples included two samples from each of the four skin sites investigated (forehead, cheek, forearm, back).

Overall, all three schemes detected a similar staphylococcal species composition in the analysed skin swab samples (Fig. 4). The most prominent differences were seen in one of the forearm samples ("forearm 2"); here, the *tuf2* scheme detected *S. saccharolyticus*, whereas the *rpsK* and *tuf1* schemes did not. Moreover, small differences were noted: first, the *rpsK* scheme detected *S. epidermidis* and *Staphylococcus pettenkoferi* in forearm samples, and *Staphylococcus equorum* in a forehead sample ("forehead 1"), all of which with low relative abundances; in contrast, these three species were not detected by the two *tuf* schemes. Second, the *tuf2* scheme detected three different *S. epidermidis* alleles in one cheek ("cheek 2") and one forearm sample ("forearm 2"). In addition, in one forehead sample ("forehead 2"), the *tuf2* scheme found two different *S. epidermidis* alleles. In contrast, the other two schemes detected one *S. epidermidis* allele less in each sample.

### In silico comparison of *S. epidermidis* amplicon targets

We observed that three different alleles of *S. epidermidis* were detected with the *tuf2* scheme (Fig. 4). Since *S. epidermidis* is the most dominating staphylococcal species on human skin and its phylogenetic diversification into three clades (designated A, B and C) is well reported, we performed a detailed analysis of the resolution power of the three amplicon NGS schemes regarding *S. epidermidis*. A phylogenetic tree based on the core genome of 308 publicly available *S. epidermidis* genomes (Additional file 5) was built and analysed regarding the question whether the amplicon schemes can mirror the population structure. The data showed that the *rpsK* scheme could unambiguously identify B clade strains of *S. epidermidis*, but it could not distinguish strains of the A and C clades (Fig. 5). The *tuf1* and *tuf2* schemes could both unambiguously identify most strains regarding their assignment to the phylogenetic clades A, B and C. However, the *tuf1* scheme could distinguish less A and B clade strains compared to the *tuf2* scheme. Overall, the *tuf2* scheme was superior in resolution power.

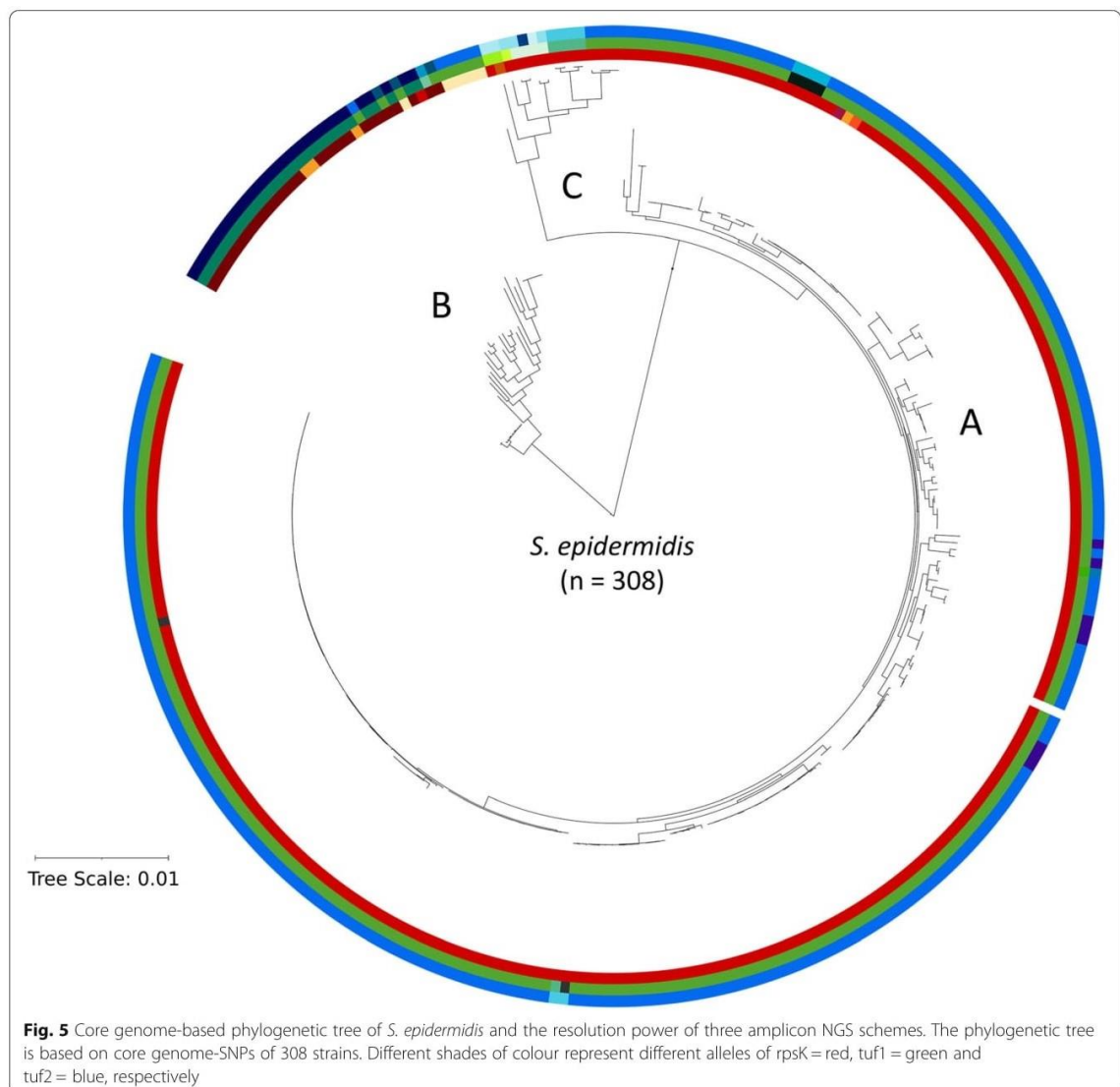
### Discussion

Staphylococcal populations are an important part of the human skin microbiome and play a central role in health and disease, in a species- and often also in a strain-dependent manner [1–14]. There is a need for efficient tools to determine and discriminate staphylococcal

populations on human skin, ideally beyond the species level. Here, we compared three culture-independent amplicon NGS schemes to investigate their suitability and accuracy for analysing staphylococcal populations in human skin samples.

The *tuf1* gene fragment was first used for the identification of staphylococcal isolates to the species level [41]. Later, this *tuf1* target sequence was applied in an amplicon NGS approach for determining staphylococcal populations of pig skin and pig noses [42]. A modified scheme, relying on a different *tuf* gene fragment (*tuf2*) was recently developed [47]. In the latter study, samples from healthy skin were analysed, and a surprising finding was the identification of the species *S. saccharolyticus* in relatively high quantities, which was not seen before in other amplicon NGS studies or in culture-dependent studies. In the third scheme analysed here, a *rpsK* gene fragment was used, derived from a prediction with a bioinformatics pipeline [46]. The scheme was used for determining staphylococcal populations of atopic dermatitis affected skin versus healthy skin.

Overall, we could show that all three amplicon NGS schemes accurately identified staphylococcal populations of mock communities as well as of in vivo skin swab samples. All three methods performed comparably well, regardless of DNA input amounts. However, a few differences were detected regarding the detection of *S. saccharolyticus* and different alleles of *S. epidermidis*. First, on the species level, two schemes, the *rpsK* and *tuf1* scheme, were unable to detect *S. saccharolyticus* in all samples, while the *tuf2* scheme was able to detect this species. This could be due to a mismatch in the primers to amplify *rpsK* and *tuf1*: both reverse primers have one mismatch with the corresponding regions in the genome sequence of *S. saccharolyticus* DVP4-17-2404 and 13 T0028 (data not shown). Second, the *tuf1* scheme had problems to accurately detect *S. epidermidis* in both mock communities. A reason could be a mismatch of the reverse *tuf1* primer with the corresponding region in the genome sequences of the *S. epidermidis* strains included in mock community M2. Such primer mismatches can lead to an amplification bias and thus an underestimation of the corresponding target [48, 49]. Another reason for the higher resolution power of the *tuf2* scheme can also be the amplicon size: it is longer (467 bp), compared to the other two schemes (*rpsK* = 381 bp; *tuf1* = 366 bp). This leads to a better resolution due to a higher number of SNPs in the amplicon, compared to the *tuf1* and *rpsK* amplicons. This is likely the reason why the *tuf2* scheme could distinguish more strains in mock community M2 and was able to differentiate between more *S. epidermidis* alleles in in vivo skin samples.



On the other hand, the longer tuf2 amplicon length can create a potential problem, since it leads to fewer usable paired-end reads after quality processing, due to a low sequence quality of reads at the 3' ends with the applied Illumina MiSeq sequencing approach. The analysis of the sequence data obtained with the rpsK and tuf1 schemes showed that a similar portion of paired-end reads passed the quality processing, in average 21.7 and 21.0% respectively (Additional file 6). The proportion of passed reads for the tuf2 scheme was lower compared to rpsK and tuf1 schemes, with an average of 11.6%. This did not seem to have an impact on the quality of results generated in this study, since the mock community

populations were best determined by the tuf2 scheme, but could lead to problems when the input DNA concentration of in vivo samples is extremely low.

We further investigated whether the three amplicon NGS schemes can not only detect overall staphylococcal populations on species level, but also whether they can differentiate subspecies and phylogenetic clades of CoNS. Exemplarily, we focused on *S. epidermidis*, because of its abundance on skin and the extensive knowledge about its population structure [24–26]. Previous studies have shown that the population of *S. epidermidis* can be divided in three main clades (A, B and C) [24–26] and that each individual and each skin site is

colonised by multiple founder lineages of *S. epidermidis* of different phylogenetic clades [50]. In Espadinha et al. [25] it was shown that *S. epidermidis* strains from the A and C clades were more often associated with hospital-infections, while the B clade was mainly associated with commensal *S. epidermidis* strains. We analysed in silico if the schemes can give an accurate picture of the genetic diversity regarding the three phylogenetic clades of *S. epidermidis*. The *tuf2* scheme was superior in differentiating the three main clades of *S. epidermidis*, probably due to a longer amplicon sequence and thus higher resolution power. Thus, the *tuf2* scheme is able to analyse the presence of each *S. epidermidis* clade and could show which clade is mainly present e.g. in skin samples. However, all schemes including the *tuf2* schemes have only limited powers to resolve the population structure of *S. epidermidis*. A species-specific scheme would need to be employed, such as the duplex-amplicon NGS scheme developed by Rendboe et al. [51] to more accurately resolve the diversity of *S. epidermidis*.

Besides the three amplicon NGS schemes analysed here, other studies have used different *tuf* gene fragments for the analysis of staphylococcal populations [43–45]. For example, the *tuf* gene fragment used by McMurray et al. [43] was predicted to distinguish fourteen out of eighteen strains of mock community M2 (data not shown). Two additional *tuf* schemes were developed in the last year [44, 45]; these schemes were predicted to distinguish both 13 strains of mock community M2 (data not shown). Thus, these additional three schemes based on *tuf* gene fragments were predicted to distinguish fewer strains of the mock community M2 than the *tuf2* scheme.

The overall limitation of the amplicon NGS schemes analysed here is that they cannot resolve staphylococcal populations to the strain level. This could be achieved by shotgun metagenomic sequencing; however, it relies on a sufficiently high DNA input amount and high sequencing depth and is thus still expensive.

## Conclusion

All three schemes included in this study performed well when analysing staphylococcal populations in mock communities as well as in skin swab samples. However, the *tuf2* amplicon NGS scheme determined the expected sample composition best; it could distinguish between more *S. epidermidis* alleles in in vivo samples and detected *S. saccharolyticus* most reliably.

## Methods

### Participants and skin swabbing

Skin swab samples with moistened cotton tips were taken from 13 volunteers (female,  $n = 5$ ; male,  $n = 8$ ) with an age range of 22–43 years from forehead, cheek,

back and forearm, as described previously [47]. None of the volunteers had a history of skin disease; none had undergone treatment with topical medicine or antibiotics during the last 6 months. Written informed consent was obtained from all volunteers and the study was approved by the International Medical & Dental Ethics Commission GmbH (IMDEC), Freiburg (Study no. 67885).

### Cultivation of swab sample and species identification

Skin swab samples obtained were diluted in 0.9% NaCl solution and plated out on Columbia agar with 5% sheep blood and cultivated at 37 °C for 24 h. Up to five colonies that resembled staphylococci based on colony size and colour were randomly picked of each plate and pure cultures were obtained by sub-cultivation on the same agar, cultivated at 37 °C for 24 h. Each isolate (254 in total) was assigned to species level by MALDI-TOF mass spectrometry (Additional file 2).

### DNA extraction from skin swab samples

Eight skin swab samples were randomly selected for DNA extraction. Prior to DNA extraction, skin swab samples were centrifuged, and the supernatant was discarded. The pellets were lysed by using lysostaphin (0.05 mg/mL, Sigma) and lysozyme (9.5 mg/mL, Sigma). DNA was extracted using the DNeasy PowerSoil Kit (QIAGEN), following the manufacturer's instructions. DNA concentrations were measured with the Qubit dsDNA HS Assay (ThermoFisher Scientific) at a Qubit fluorometer.

### Whole genome sequencing

Bacterial isolates were grown on Columbia agar with 5% sheep blood for 24 h at 37 °C. Bacteria were harvested and lysed with lysostaphin (0.05 mg/mL, Sigma). DNA extraction was performed using DNeasy UltraClean Microbial Kit by following manufacturer's instructions. DNA concentration and purity were measured by Nanodrop. DNA integrity was examined with Genomic DNA ScreenTape (Agilent) at the 4200 TapeStation System. The extracted bacterial DNA was used to generate Illumina shotgun libraries; they were prepared using the Nextera XT DNA Sample Preparation Kit and subsequently sequenced on a MiSeq system using the v3 reagent kit with 600 cycles (Illumina, San Diego, CA, USA) as recommended by the manufacturer. Quality filtering was done with version 0.36 of Trimmomatic [52]. Assembly was performed with version 3.13.0 of the SPAdes genome assembler software [53]. Version 2.2.1 of Quali-map [54] was used to validate the assembly and determine the sequence coverage. Additional file 3 contains information regarding the sequencing and genome

**Table 1** Primer sets used in this study (without adapter sequences)

Primer pair name	Amplicon position <sup>a</sup>	Target gene	5' --> 3'	Amplicon length [bp]	reference	
rpsK	2–382	rpsK	fw	TGGCACGTAAACAAGTATC	381	[46]
			rev	GACGACGTTTGGTGGAC		
tuf1	688–1053	tuf	fw	GGCCGTGTTGAACGTGGTCAAATC	366	[41, 42]
			rev	TIACCATTTCAGTACCTTCTGGTAA		
tuf2	685–1151	tuf	fw	ACAGGCCGTGTTGAACGTG	467	[47]
			rev	ACAGTACGTCCACCTTCACG		

<sup>a</sup> Amplicon position in genes (*tuf/rpsK*) of *S. epidermidis* ATCC 12228 (GCA\_000007645.1)

statistics, i.e. coverage, contig number, N50 and GenBank accession numbers.

#### Bacterial mock communities

Genomic DNA of 18 strains was used to build two mock communities. The DNA was combined in equimolar ratios, with 0.05 ng or 50 ng DNA of each strain. The following bacterial strains were used for two mock communities M1 and M2 (Additional file 1).

The nine-strain-community (M1) contained: *S. epidermidis* ATCC 12228, *S. hominis* HAA31, *S. capitis* HAF22, *S. aureus* DSM 20231, *S. warneri* HAA271, *S. haemolyticus* HAA11, *S. saprophyticus* HAF121, *S. simulans* HAA294 and *S. saccharolyticus* 13 T0028. The 18-strain mixture (M2) contained the same strains as above plus the additional strains: *S. epidermidis* NCIB 11536, *S. epidermidis* HAF81, *S. epidermidis* HAB176, *S. hominis* DSM 20328, *S. hominis* HAB38, *S. capitis* DSM 20325, *S. warneri* DSM 20316, *S. haemolyticus* DSM 20263 and *S. saccharolyticus* DVP4-17-2404. GenBank accession numbers of all genomes of the listed strains are given in Additional file 1.

#### Amplicon polymerase chain reaction (PCR) and sequencing

The target fragments, designated tuf1 [41], tuf2 [47], and rpsK [46], were amplified using specific primer sets (Table 1). PCR reaction mixtures were made in a total volume of 25 µl and comprised 5 µl of DNA sample, 2.5 µl AccuPrime PCR Buffer II (Invitrogen, Waltham, MA, USA), 1.5 µl of each primer (10 µM) (DNA Technology, Risskov, Denmark), 0.15 µl AccuPrime Taq DNA Polymerase High Fidelity (Invitrogen, Waltham, MA, USA), and 14.35 µl of PCR grade water. The PCR reaction was performed using the following cycle conditions: an initial denaturation at 94 °C for 2 min, followed by 35 cycles of denaturation at 94 °C for 20 s, annealing at 55 °C for 30 s, elongation at 68 °C for 1 min, and a final elongation step at 72 °C for 5 min. PCR products were verified on an agarose gel and purified using the Qiagen GeneAid™ Size Selection kit (Qiagen, Hilden, Germany). The concentration of the purified PCR products was

measured with a NanoDrop 2000 spectrophotometer (ThermoFisher Scientific, Waltham, MA, USA). Amplicon NGS was performed as described previously [47].

#### Amplicon NGS data analysis and visualization

FASTQ sequences were processed using QIIME2 (v. 2019.7) [55] as described previously [47]. A cut-off of 99% identity against *tuf* and *rpsK* gene databases was used. The database was built based on all closed staphylococcal genomes available in GenBank (status 02/01/2021). Mock community samples were analysed with a database which contained the rpsK/tuf1/tuf2 allele for each strain. Data was normalized, low abundant features were filtered with a threshold of 2.5%, and figures were prepared in R (v. 4.0.1) with the packages ggplot2 [56] and gplots [57]. Bray-Curtis dissimilarity of mock community sample data was calculated in the vegan package [58] and ordinated in a principal coordinate analysis (PCoA).

#### Phylogenomic amplicon target analysis

For phylogenomic analyses, all closed and scaffold genome sequence data of *S. epidermidis* was obtained from NCBI RefSeq (status 07.01.2021). GenBank accession numbers of all used genomes are given in Additional file 5. Genomes were aligned and clustered based on SNPs in their core genome using Parsnp (v 1.0) [59]. The different amplicon alleles were identified for each strain using Blast+ (v 2.11.0). Visualization of the tree was done with iTOL (v 5.7).

#### Abbreviations

CoNS: coagulase-negative staphylococci; EF-Tu: elongation factor Tu; MALDI-TOF: Matrix-Assisted Laser Desorption – Ionization - Time of Flight; NGS: Next-generation sequencing; PCoA: principal coordinate analysis; PCR: polymerase chain reaction; SNP: single nucleotide polymorphism; SRA: Sequence Read Archive

#### Supplementary Information

The online version contains supplementary material available at <https://doi.org/10.1186/s12866-021-02284-1>.

**Additional file 1.** Table S1: Composition of two staphylococcal mock communities.

**Additional file 2.** Table S2: Cultivation results of skin swabs from 13 volunteers.

**Additional file 3.** Table S3: Genome statistics of sequenced staphylococcal genomes.

**Additional file 4.** Fig. S1: Phylogenetic trees of the alleles of three amplicon targets (*tuf1*, *tuf2* and *rpsK*), extracted from 18 staphylococcal genomes present in the M2 mock community.

**Additional file 5.** Table S4: Accession numbers of *S. epidermidis* genomes included in the phylogenomic analysis.

**Additional file 6.** Table S5: Amplicon sequencing statistics of the mock communities.

#### Acknowledgements

We thank Lise Hald Schultz for excellent technical assistance. Data processing was performed on the GenomeDK cluster; we would like to thank GenomeDK and Aarhus University for providing computational resources that contributed to these research results.

#### Authors' contributions

Conceptualization, CA, JH, WRS, HB; methodology and experiments, CA, AP; data analysis, CA, KS, AP, HB; writing—original draft preparation, CA, HB; writing—review and editing, KS, AP, WRS, JH; supervision, JH, WRS, HB; project administration, JH, WRS, HB; funding acquisition, HB. All authors have read and agreed to the published version of the manuscript.

#### Funding

This work was supported by grants from the NovoNordisk Foundation (grant no. NNF18OC0053172).

#### Availability of data and materials

Whole genome sequences generated for this project are available in the NCBI BioProject database under the project ID PRJNA702288, and NCBI GenBank accession numbers are listed in Additional file 3. Whole genome sequences of strains used in the mock communities were obtained from NCBI GenBank, and all NCBI GenBank accession numbers are listed in Additional file 1. Amplicon sequencing data are available in the NCBI Sequence Read Archive (SRA) under the project ID PRJNA702649. Whole genome sequences of *S. epidermidis* used for the phylogenomic analysis were obtained from NCBI RefSeq, and NCBI RefSeq accession numbers are listed in Additional file 5.

#### Declarations

##### Ethics approval and consent to participate

Written informed consent was obtained from all volunteers and the study was approved by the International Medical & Dental Ethics Commission GmbH (IMDEC), Freiburg (Study no. 67885).

##### Consent for publication

Not applicable.

##### Competing interests

Conflicts of Interest: CA and JH are employees at Beiersdorf AG. The other authors declare no conflict of interest.

##### Author details

<sup>1</sup>Beiersdorf AG, Research & Development, Front End Innovation, 20245 Hamburg, Germany. <sup>2</sup>Department of Microbiology and Biotechnology, University of Hamburg, 22609 Hamburg, Germany. <sup>3</sup>Department of Biomedicine, Aarhus University, 8000 Aarhus, Denmark. <sup>4</sup>Department of Genomic and Applied Microbiology, Institute of Microbiology and Genetics, University of Göttingen, 37073 Göttingen, Germany.

Received: 25 March 2021 Accepted: 21 July 2021

Published online: 28 July 2021

##### References

- Bunikowski R, Mielke ME, Skarabis H, Worm M, Anagnostopoulos I, Kolde G, et al. Evidence for a disease-promoting effect of *Staphylococcus aureus*-

derived exotoxins in atopic dermatitis. *J Allergy Clin Immunol.* 2000;105(4): 814–9. <https://doi.org/10.1067/mai.2000.105528>.

- Nakatsuji T, Chen TH, Narala S, Chun KA, Two AM, Yun T, et al. Antimicrobials from human skin commensal bacteria protect against *Staphylococcus aureus* and are deficient in atopic dermatitis. *Sci Transl Med.* 2017;9(378):eaah4680. <https://doi.org/10.1126/scitranslmed.aah4680>.
- Schnell N, Entian KD, Schneider U, Gotz F, Zahner H, Kellner R, et al. Prepeptide sequence of epidermin, a ribosomally synthesized antibiotic with four sulphide-rings. *Nature.* 1988;333(6170):276–8. <https://doi.org/10.1038/333276a0>.
- Sandiford S, Upton M. Identification, characterization, and recombinant expression of epidermin N101, a novel unmodified bacteriocin produced by *Staphylococcus epidermidis* that displays potent activity against staphylococci. *Antimicrob Agents Chemother.* 2012;56(3):1539–47. <https://doi.org/10.1128/AAC.05397-11>.
- O'Neill AM, Nakatsuji T, Hayachi A, Williams MR, Mills RH, Gonzalez DJ, et al. Identification of a human skin commensal bacterium that selectively kills *Cutibacterium acnes*. *J Invest Dermatol.* 2020.
- Brown MM, Kwiecinski JM, Cruz LM, Shahbandi A, Todd DA, Cech NB, et al. Novel peptide from commensal *Staphylococcus simulans* blocks methicillin-resistant *Staphylococcus aureus* quorum sensing and protects host skin from damage. *Antimicrob Agents Chemother.* 2020;64(6). <https://doi.org/10.1128/AAC.00172-20>.
- Peng P, Baldry M, Gless BH, Bojer MS, Espinosa-Gongora C, Baig SJ, et al. Effect of Co-inhabiting Coagulase Negative Staphylococci on *S. aureus* agr Quorum Sensing, Host Factor Binding, and Biofilm Formation. *Front Microbiol.* 2019;10:2212. <https://doi.org/10.3389/fmicb.2019.02212>.
- Scharschmidt TC, Vasquez KS, Truong HA, Gearty SV, Pauli ML, Nosbaum A, et al. A wave of regulatory T cells into neonatal skin mediates tolerance to commensal microbes. *Immunity.* 2015;43(5):1011–21. <https://doi.org/10.1016/j.immuni.2015.10.016>.
- Naik S, Bouladoux N, Linehan JL, Han SJ, Harrison OJ, Wilhelm C, et al. Commensal-dendritic-cell interaction specifies a unique protective skin immune signature. *Nature.* 2015;520(7545):104–8. <https://doi.org/10.1038/nature14052>.
- Stacy A, Belkaid Y. Microbial guardians of skin health. *Science.* 2019; 363(6424):227–8. <https://doi.org/10.1126/science.aat4326>.
- Parlet CP, Brown MM, Horswill AR. Commensal staphylococci influence *Staphylococcus aureus* skin colonization and disease. *Trends Microbiol.* 2019;27(6):497–507. <https://doi.org/10.1016/j.tim.2019.01.008>.
- Leonel C, Sena IFG, Silva WN, Prazeres P, Fernandes GR, Mancha Agresti P, et al. *Staphylococcus epidermidis* role in the skin microenvironment. *J Cell Mol Med.* 2019;23(9):5949–55. <https://doi.org/10.1111/jcmm.14415>.
- Lai Y, Di Nardo A, Nakatsuji T, Leichte A, Yang Y, Cogen AL, et al. Commensal bacteria regulate toll-like receptor 3-dependent inflammation after skin injury. *Nat Med.* 2009;15(12):1377–82. <https://doi.org/10.1038/nm.2062>.
- Nakatsuji T, Chen TH, Butcher AM, Trzoss LL, Nam SJ, Shirakawa KT, et al. A commensal strain of *Staphylococcus epidermidis* protects against skin neoplasia. *Sci Adv.* 2018;4:eaa04502.
- Grice EA, Kong HH, Conlan S, Deming CB, Davis J, Young AC, et al. Topographical and temporal diversity of the human skin microbiome. *Science.* 2009;324(5931):1190–2. <https://doi.org/10.1126/science.1171700>.
- Byrd AL, Belkaid Y, Segre JA. The human skin microbiome. *Nat Rev Microbiol.* 2018;16(3):143–55. <https://doi.org/10.1038/nrmicro.2017.157>.
- Chen YE, Fischbach MA, Belkaid Y. Skin microbiota-host interactions. *Nature.* 2018;553(7689):427–36. <https://doi.org/10.1038/nature25177>.
- Schleiferi KHK, W. E. Isolation and characterization of staphylococci from human skin I. amended descriptions of *Staphylococcus epidermidis* and *Staphylococcus saprophyticus* and descriptions of three new species: *Staphylococcus cohnii*, *Staphylococcus haemolyticus*, and *Staphylococcus xylosum*. *Int J Syst Evol Microbiol.* 1975;25:50–61.
- Kloss WES, K. H. Isolation and characterization of staphylococci from human skin II. Descriptions of four new species: *Staphylococcus warneri*, *Staphylococcus capitis*, *Staphylococcus hominis*, and *Staphylococcus simulans*. *Int J Syst Bacteriol.* 1975;25(1):62–79. <https://doi.org/10.1099/00207713-25-1-62>.
- Meric G, Mageiros L, Pensar J, Laabei M, Yahara K, Pascoe B, et al. Disease-associated genotypes of the commensal skin bacterium *Staphylococcus epidermidis*. *Nat Commun.* 2018;9(1):5034. <https://doi.org/10.1038/s41467-018-07368-7>.
- Both A, Huang J, Qi M, Lausmann C, Weisselberg S, Buttner H, et al. Distinct clonal lineages and within-host diversification shape invasive *Staphylococcus epidermidis* populations. *PLoS Pathog.* 2021;17(2):e1009304. <https://doi.org/10.1371/journal.ppat.1009304>.

22. Zhou W, Spoto M, Hardy R, Guan C, Fleming E, Larson PJ, et al. Host-specific evolutionary and transmission dynamics shape the functional diversification of *Staphylococcus epidermidis* in human skin. *Cell*. 2020;180(3):454–70 e418. <https://doi.org/10.1016/j.cell.2020.01.006>.
23. Oh J, Byrd AL, Deming C, Conlan S, Program NCS, Kong HH, et al. Biogeography and individuality shape function in the human skin metagenome. *Nature*. 2014;514(7520):59–64. <https://doi.org/10.1038/nature13786>.
24. Conlan S, Mijares LA, Program NCS, Becker J, Blakesley RW, Bouffard GG, et al. *Staphylococcus epidermidis* pan-genome sequence analysis reveals diversity of skin commensal and hospital infection-associated isolates. *Genome Biol*. 2012;13(7):R64. <https://doi.org/10.1186/gb-2012-13-7-r64>.
25. Espadina D, Sobral RG, Mendes CI, Meric G, Sheppard SK, Carrico JA, et al. Distinct phenotypic and genomic signatures underlie contrasting pathogenic potential of *Staphylococcus epidermidis* clonal lineages. *Front Microbiol*. 2019;10:1971. <https://doi.org/10.3389/fmicb.2019.01971>.
26. Meric G, Miragaia M, de Been M, Yahara K, Pascoe B, Mageiros L, et al. Ecological overlap and horizontal gene transfer in *Staphylococcus aureus* and *Staphylococcus epidermidis*. *Genome Biol Evol*. 2015;7(5):1313–28. <https://doi.org/10.1093/gbe/evw066>.
27. Miragaia M, Thomas JC, Couto I, Enright MC, de Lencastre H. Inferring a population structure for *Staphylococcus epidermidis* from multilocus sequence typing data. *J Bacteriol*. 2007;189(6):2540–52. <https://doi.org/10.1128/JB.01484-06>.
28. Kloos WE, Musselwhite MS. Distribution and persistence of *Staphylococcus* and *Micrococcus* species and other aerobic bacteria on human skin. *Appl Microbiol*. 1975;30(3):381–5. <https://doi.org/10.1128/am.30.3.381-395.1975>.
29. Kloos WE, Schleifer KH. Isolation and characterization of staphylococci from human skin. *Int J Syst Bacteriol*. 1975;25(1):62–79. <https://doi.org/10.1099/00207173-25-1-62>.
30. Ward DM, Weller R, Bateson MM. 16S rRNA sequences reveal numerous uncultured microorganisms in a natural community. *Nature*. 1990;345(6270):63–5. <https://doi.org/10.1038/345063a0>.
31. Ghebremedhin B, Layer F, König W, König B. Genetic classification and distinguishing of *Staphylococcus* species based on different partial gap, 16S rRNA, hsp60, rpoB, sodA, and tuf gene sequences. *J Clin Microbiol*. 2008;46(3):1019–25. <https://doi.org/10.1128/JCM.02058-07>.
32. Meisel JS, Hannigan GD, Tyldsley AS, SanMiguel AJ, Hodkinson BP, Zheng Q, et al. Skin microbiome surveys are strongly influenced by experimental design. *J Invest Dermatol*. 2016;136(5):947–56. <https://doi.org/10.1016/j.jid.2016.01.016>.
33. Blaiotta G, Fusco V, Ercolini D, Pepe O, Coppola S. Diversity of *Staphylococcus* species strains based on partial kat (catalase) gene sequences and design of a PCR-restriction fragment length polymorphism assay for identification and differentiation of coagulase-positive species (*S. aureus*, *S. delphini*, *S. hyicus*, *S. intermedius*, *S. pseudintermedius*, and *S. schleiferi* subsp. *coagulans*). *J Clin Microbiol*. 2010;48(1):192–201. <https://doi.org/10.1128/JCM.00542-09>.
34. Yugueros J, Temprano A, Berzal B, Sanchez M, Hernanz C, Luengo JM, et al. Glyceroldehyde-3-phosphate dehydrogenase-encoding gene as a useful taxonomic tool for *Staphylococcus* spp. *J Clin Microbiol*. 2000;38(12):4351–5. <https://doi.org/10.1128/JCM.38.12.4351-4355.2000>.
35. Yugueros J, Temprano A, Sanchez M, Luengo JM, Naharro G. Identification of *Staphylococcus* spp. by PCR-restriction fragment length polymorphism of gap gene. *J Clin Microbiol*. 2001;39(10):3693–5. <https://doi.org/10.1128/JCM.39.10.3693-3695.2001>.
36. Goh SH, Potter S, Wood JO, Hemmingsen SM, Reynolds RP, Chow AW. HSP60 gene sequences as universal targets for microbial species identification: studies with coagulase-negative staphylococci. *J Clin Microbiol*. 1996;34(4):818–23. <https://doi.org/10.1128/jcm.34.4.818-823.1996>.
37. Goh SH, Santucci Z, Kloos WE, Faltyn M, George CG, Driedger D, et al. Identification of *Staphylococcus* species and subspecies by the chaperonin 60 gene identification method and reverse checkerboard hybridization. *J Clin Microbiol*. 1997;35(12):3116–21. <https://doi.org/10.1128/jcm.35.12.3116-3121.1997>.
38. Mollet C, Drancourt M, Raoult D. rpoB sequence analysis as a novel basis for bacterial identification. *Mol Microbiol*. 1997;26(5):1005–11. <https://doi.org/10.1046/j.1365-2958.1997.6382009.x>.
39. Drancourt M, Raoult D. rpoB gene sequence-based identification of *Staphylococcus* species. *J Clin Microbiol*. 2002;40(4):1333–8. <https://doi.org/10.1128/JCM.40.4.1333-1338.2002>.
40. Poyart C, Quesne G, Boumaila C, Trieu-Cuot P. Rapid and accurate species-level identification of coagulase-negative staphylococci by using the sodA gene as a target. *J Clin Microbiol*. 2001;39(12):4296–301. <https://doi.org/10.1128/JCM.39.12.4296-4301.2001>.
41. Martineau F, Picard FJ, Ke D, Paradis S, Roy PH, Ouellette M, et al. Development of a PCR assay for identification of staphylococci at genus and species levels. *J Clin Microbiol*. 2001;39(7):2541–7. <https://doi.org/10.1128/JCM.39.7.2541-2547.2001>.
42. Strube ML, Hansen JE, Rasmussen S, Pedersen K. A detailed investigation of the porcine skin and nose microbiome using universal and *Staphylococcus* specific primers. *Sci Rep*. 2018;8(1):12751. <https://doi.org/10.1038/s41598-018-30689-y>.
43. McMurray CL, Hardy KJ, Calus ST, Loman NJ, Hawkey PM. Staphylococcal species heterogeneity in the nasal microbiome following antibiotic prophylaxis revealed by tuf gene deep sequencing. *Microbiome*. 2016;4(1):63. <https://doi.org/10.1186/s40168-016-0210-1>.
44. Van Reckem E, De Vuyst L, Leroy F, Weckx S. Amplicon-based high-throughput sequencing method capable of species-level identification of coagulase-negative staphylococci in diverse communities. *Microorganisms*. 2020;8.
45. Iversen S, Johannesen TB, Ingham AC, Edslev SM, Tevell S, Mansson E, et al. Alteration of bacterial communities in anterior nares and skin sites of patients undergoing arthroplasty surgery: analysis by 16S rRNA and staphylococcal-specific tuf gene sequencing. *Microorganisms*. 2020;8(12). <https://doi.org/10.3390/microorganisms8121977>.
46. Ederveen THA, Smits JPH, Hajo K, van Schalkwijk S, Kouwenhoven TA, Lukovac S, et al. A generic workflow for single locus sequence typing (SLST) design and subspecies characterization of microbiota. *Sci Rep*. 2019;9(1):19834. <https://doi.org/10.1038/s41598-019-56065-y>.
47. Ahle CM, Stodkilde K, Afshar M, Poehlein A, Ogiilvie LA, Soderquist B, et al. *Staphylococcus saccharolyticus*: an overlooked human skin colonizer. *Microorganisms*. 2020;8(8). <https://doi.org/10.3390/microorganisms8081105>.
48. Stadhouders R, Pas SD, Anber J, Voermans J, Mes TH, Schutten M. The effect of primer-template mismatches on the detection and quantification of nucleic acids using the 5' nuclease assay. *J Mol Diagn*. 2010;12(1):109–17. <https://doi.org/10.2353/jmoldx.2010.090035>.
49. Sipos R, Szekeley AJ, Palatinszky M, Revesz S, Marialigeti K, Nikolauz M. Effect of primer mismatch, annealing temperature and PCR cycle number on 16S rRNA gene-targeting bacterial community analysis. *FEMS Microbiol Ecol*. 2007;50(2):341–50. <https://doi.org/10.1111/j.1574-6941.2007.00283.x>.
50. Zhou H, Shi L, Ren Y, Tan X, Liu W, Liu Z. Applications of human skin microbiota in the cutaneous disorders for ecology-based therapy. *Front Cell Infect Microbiol*. 2020;10:570261. <https://doi.org/10.3389/fcimb.2020.570261>.
51. Rendboe AK, Johannesen TB, Ingham AC, Mansson E, Iversen S, Baig S, et al. The Epidome - a species-specific approach to assess the population structure and heterogeneity of *Staphylococcus epidermidis* colonization and infection. *BMC Microbiol*. 2020;20(1):362. <https://doi.org/10.1186/s12866-020-02041-w>.
52. Bolger AM, Lohse M, Usadel B. Trimmomatic: a flexible trimmer for Illumina sequence data. *Bioinformatics*. 2014;30(15):2114–20. <https://doi.org/10.1093/bioinformatics/btu170>.
53. Bankevich A, Nurk S, Antipov D, Gurevich AA, Dvorkin M, Kulikov AS, et al. SPAdes: a new genome assembly algorithm and its applications to single-cell sequencing. *J Comput Biol*. 2012;19(5):455–77. <https://doi.org/10.1089/cmb.2012.0021>.
54. Garcia-Alcalde F, Okonechnikov K, Carbonell J, Cruz LM, Gotz S, Tarazona S, et al. Qualimap: evaluating next-generation sequencing alignment data. *Bioinformatics*. 2012;28(20):2678–9. <https://doi.org/10.1093/bioinformatics/bts503>.
55. Bolyen E, Rideout JR, Dillon MR, Bokulich NA, Abnet CC, AGhalith GA, et al. Reproducible, interactive, scalable and extensible microbiome data science using QIIME 2. *Nat Biotechnol*. 2019;37(8):852–7. <https://doi.org/10.1038/s41587-019-0209-9>.
56. Wickham H. *ggplot2: Elegant Graphics for Data Analysis*. New York: Springer-Verlag; 2009.
57. Warnes GRB, Bonebakker L, Gentleman R, Huber W, Liaw A, Lumley T, et al. *ggplots: Various R Programming Tools for Plotting Data*; 2020.
58. Oksanen JFGB, Friendly M, Kindt R, Legendre P, McGlenn D, Minchin PR, et al. *vegan: Community Ecology Package*. R package version 2.5–6; 2019.
59. Treangen TJ, Ondov BD, Koren S, Phillippy AM. The harvest suite for rapid core-genome alignment and visualization of thousands of intraspecific microbial genomes. *Genome Biol*. 2014;15(11):S24. <https://doi.org/10.1186/s13059-014-0524-x>.

### Publisher's Note

Springer Nature remains neutral with regard to jurisdictional claims in published maps and institutional affiliations.



### 3 Publication II

## **Staphylococcus saccharolyticus: An Overlooked Human Skin Colonizer**

Charlotte Marie Ahle, Kristian Stødkilde, Mastaneh Afshar, Anja Poehlein, Lesley A. Ogilvie, Bo Söderquist, Jennifer Hüpeden and Holger Brüggemann

**Published in:**

Microorganisms (2020)

**DOI:**

10.3390/microorganisms8081105

**Contributions to the article:**



- Writing of manuscript
- Planning and conducting the study
- Analysis and visualization of amplicon NGS data
- Metagenome database search

---

Associate Prof. Dr. Holger Brüggemann

Article

# *Staphylococcus saccharolyticus*: An Overlooked Human Skin Colonizer

Charlotte M. Ahle <sup>1,2</sup> , Kristian Stødkilde <sup>3</sup>, Mastaneh Afshar <sup>3</sup>, Anja Poehlein <sup>4</sup>, Lesley A. Ogilvie <sup>5</sup>, Bo Söderquist <sup>6</sup>, Jennifer Hüpeden <sup>1</sup> and Holger Brüggemann <sup>3,\*</sup> 

<sup>1</sup> Beiersdorf AG, Research & Development, Front End Innovation, 20245 Hamburg, Germany; charlotte.ahle@beiersdorf.com (C.M.A.); jennifer.huepeden@beiersdorf.com (J.H.)

<sup>2</sup> Department of Microbiology and Biotechnology, University of Hamburg, 22609 Hamburg, Germany

<sup>3</sup> Department of Biomedicine, Aarhus University, 8000 Aarhus, Denmark; kst@biomed.au.dk (K.S.); m.afshar@biomed.au.dk (M.A.)

<sup>4</sup> Department of Genomic and Applied Microbiology, Institute of Microbiology and Genetics, University of Göttingen, 37073 Göttingen, Germany; anja.poehlein@biologie.uni-goettingen.de

<sup>5</sup> Max Planck Institute for Molecular Genetics, 14195 Berlin, Germany; logilvie@molgen.mpg.de

<sup>6</sup> Department of Laboratory Medicine, Clinical Microbiology, Faculty of Medicine and Health, Örebro University, S-701 82 Örebro, Sweden; bo.soderquist@oru.se

\* Correspondence: brueggemann@biomed.au.dk

Received: 7 July 2020; Accepted: 21 July 2020; Published: 23 July 2020



**Abstract:** Coagulase-negative staphylococcal species constitute an important part of the human skin microbiota. In particular, facultative anaerobic species such as *Staphylococcus epidermidis* and *Staphylococcus capitis* can be found on the skin of virtually every human being. Here, we applied a culture-independent amplicon sequencing approach to identify staphylococcal species on the skin of healthy human individuals. While *S. epidermidis* and *S. capitis* were found as primary residents of back skin, surprisingly, the third most abundant member was *Staphylococcus saccharolyticus*, a relatively unstudied species. A search of skin metagenomic datasets detected sequences identical to the genome of *S. saccharolyticus* in diverse skin sites, including the back, forehead, and elbow pit. Although described as a slow-growing anaerobic species, a re-evaluation of its growth behavior showed that *S. saccharolyticus* can grow under oxic conditions, and, in particular, in a CO<sub>2</sub>-rich atmosphere. We argue here that *S. saccharolyticus* was largely overlooked in previous culture-dependent and -independent studies, due to its requirement for fastidious growth conditions and the lack of reference genome sequences, respectively. Future studies are needed to unravel the microbiology and host-interacting properties of *S. saccharolyticus* and its role as a prevalent skin colonizer.

**Keywords:** *Staphylococcus saccharolyticus*; coagulase-negative staphylococci; skin microbiota; skin microbiome; amplicon next generation sequencing

## 1. Introduction

In recent years, new discoveries regarding the composition and functionality of the human skin microbiota have been made, that have enabled a more comprehensive description of this ecosystem [1–3]. Studies highlighted the diversity and uniqueness of the collection of skin microorganisms with essential roles in protection against harmful pathogens, maintaining skin homeostasis, and priming our immune system [3–6].

Coagulase-negative staphylococci (CoNS) constitute an important part of the human skin microbiota. Culture-dependent and -independent studies have highlighted the ubiquity of CoNS, which colonize mostly moist and sebaceous areas of the skin. In this regard, the CoNS species *Staphylococcus epidermidis*, *Staphylococcus capitis*, and *Staphylococcus hominis* occupy many human skin

sites [1,2,6–9]. Other CoNS species, such as *Staphylococcus haemolyticus*, *Staphylococcus lugdunensis*, and *Staphylococcus warneri*, can be found in lower amounts, varying from person to person and from skin site to skin site [1,2,9,10]. Some other CoNS species, such as *Staphylococcus equorum*, are primarily found in food products [11], but are also transient colonizers of human skin.

Culture-dependent approaches have been often applied in the past to isolate major skin residents. Such approaches are often biased, as cultivation results do not reflect the true distribution of the individual members of the microbiota [12,13]. The bias is introduced due to the chosen growth media, as well as the conditions of growth, such as O<sub>2</sub> and CO<sub>2</sub> concentrations, growth temperature, and cultivation time. Fast-growing microorganisms have a growth advantage, and directly or indirectly inhibit the growth of slow-growing microorganisms [6]. Therefore, culture-independent studies employing next generation sequencing (NGS)-based approaches are more frequently used in recent years. Using 16S rRNA gene amplicon-NGS, it was shown that the genus *Staphylococcus* is the third most abundant genus on the skin [14]. In addition, shotgun NGS studies further unraveled the diversity and individuality of staphylococcal species on the skin, and also provided insights into the strain level distribution of these CoNS species [1,2]. Such studies also highlighted the existence of microbial dark matter in the form of unidentified bacterial skin residents. For instance, the study of Oh et al. [1] has identified several uncharacterized genomes (assembled from shotgun NGS data) of unknown species, possibly belonging to the genera *Corynebacterium*, *Cutibacterium*, and *Staphylococcus*. Thus, it can be expected that species exist on the skin that cannot be easily cultivated by standard conditions.

In this context, we have recently described the genomes of seven strains of *Staphylococcus saccharolyticus*, an unusual CoNS species, regarding its growth properties [15]. Unlike almost all other CoNS species known to date, *S. saccharolyticus* largely depends on anaerobic conditions for growth, and requires fastidious growth media and prolonged cultivation time (>3 days). To date, this species has been relatively uncharacterized, with limited reports on its association with implant-associated infections [15] and bacteremia [16]. Interestingly, however, culture-dependent studies have suggested that this species may also be a resident of the skin microbiota [17,18].

Here, we further investigated the composition and relative abundance of staphylococcal species on human skin. For this, we applied an amplicon-NGS approach based on a *Staphylococcus*-specific gene fragment, to survey its presence on human back skin samples from healthy volunteers. We detected an unprecedented high relative abundance of *S. saccharolyticus* in these samples. Supported by investigation of existing skin-derived metagenomic datasets, we posit that *S. saccharolyticus* constitutes a common member of the human skin microbiota.

## 2. Materials and Methods

### 2.1. Study Design and Sampling

Skin swab samples from 19 volunteers (female,  $n = 11$ ; male,  $n = 8$ ) with an age range of 22–43 years were taken from the upper back. None of the volunteers had a history of skin disease; none had undergone treatment with topical medicine or antibiotics during the last six months. Written informed consent was obtained from all volunteers, and the study was approved by International Medical & Dental Ethics Commission GmbH (IMDEC).

An area of 25 cm<sup>2</sup> on the upper back was sampled with a cotton swab pre-moistened in aqueous sampling buffer containing disodium phosphate (12.49 g/L, Merck, Darmstadt, Germany), potassium dihydrogen phosphate (0.63 g/L, Merck, Darmstadt, Germany), and Triton X-100 (1 g/L, Merck, Darmstadt, Germany). After sampling, the swab was transferred into a sterile tube containing 2 mL of sampling buffer; the swab was vigorously shaken in the sampling buffer and then removed. Skin swab material was stored at -20 °C until further processing.

## 2.2. DNA Extraction

DNA from the 2 mL sample was extracted using the DNeasy PowerSoil Kit (QIAGEN, Hilden, Germany) following the manufacturer's protocol, with an additional cell lysis step using lysostaphin (0.05 mg/mL, Merck, Darmstadt, Germany) and lysozyme (9.5 mg/mL, Merck, Darmstadt, Germany) prior to extraction. DNA concentrations were measured using the Qubit dsDNA HS Assay (ThermoFisher Scientific, Waltham, MA, USA) with a Qubit fluorometer following the manufacturer's instructions.

## 2.3. Amplicon PCR

A fragment of the *tuf* gene present in the genomes of all staphylococcal species available in GenBank (as of December 2019) was used for species identification, analogous to a previous study using a different *tuf* gene fragment [19]. The target sequence was amplified using *tuf*-specific primers that contained MiSeq adapter sequences: *tuf*2\_F, 5'-TCGTCGGCAGCGTCAGATGTGTAT AAGAGACAGACAGGCCGTGTGAACGTG-3'; *tuf*2\_R, 5'-GTCTCGTGGGCTCGGAGATGTGT ATAAGAGACAGACAGTACGTCCACCTTCACG-3'.

PCR reaction mixtures were made in a total volume of 25 µl and comprised 5 µl of DNA sample, 2.5 µl AccuPrime PCR Buffer II (Invitrogen, Waltham, MA, USA), 1.5 µl of each primer (10 µM) (DNA Technology, Risskov, Denmark), 0.15 µl AccuPrime Taq DNA Polymerase High Fidelity (Invitrogen, Waltham, MA, USA), and 14.35 µl of PCR grade water. The PCR reaction was performed using the following cycle conditions: an initial denaturation at 94 °C for 2 min, followed by 35 cycles of denaturation at 94 °C for 20 sec, annealing at 55 °C for 30 sec, elongation at 68 °C for 1 min, and a final elongation step at 72 °C for 5 min. PCR products were verified on an agarose gel and purified using the Qiagen Generead™ Size Selection kit (Qiagen, Hilden, Germany). The concentration of the purified PCR products was measured with a NanoDrop 2000 spectrophotometer (ThermoFisher Scientific, Waltham, MA, USA).

## 2.4. Amplicon Next Generation Sequencing

PCR products were used to attach indices and Illumina sequencing adapters using the Nextera XT Index kit (Illumina, San Diego, CA, USA). Index PCR was performed using 5 µl of template PCR product, 2.5 µl of each index primer, 12.5 µl of 2x KAPA HiFi HotStart ReadyMix, and 2.5 µl PCR grade water. The thermal cycling scheme was as follows: 95 °C for 3 min, 8 cycles of 30 sec at 95 °C, 30 sec at 55 °C, and 30 sec at 72 °C, and a final extension at 72 °C for 5 min. Quantification of the products was performed using the Quant-iT dsDNA HS assay kit (ThermoFisher Scientific, Waltham, MA, USA) and a Qubit fluorometer, following the manufacturer's instructions. MagSi-NGS<sup>PREP</sup> Plus Magnetic beads (Steinbrenner Laborsysteme GmbH, Wiesenbach, Germany) were used for purification of the indexed products as recommended by the manufacturer, and normalization was performed using the Janus Automated Workstation from Perkin Elmer (Perkin Elmer, Waltham, MA, USA). Sequencing was conducted using an Illumina MiSeq platform with dual indexing and the MiSeq reagent kit v3 (600 cycles), as recommended by the manufacturer.

## 2.5. Bioinformatics

FASTQ sequences obtained after demultiplexing the reads and trimming the primers were imported into QIIME2 (v. 2019.7) [20]. Sequences with an average quality score lower than 20 or containing unresolved nucleotides were removed from the dataset with the `split_libraries_fastq.py` script from QIIME. The paired-end reads were denoised and chimeras removed with DADA2 via QIIME2, and a feature table was generated [21]. These features were then clustered with VSEARCH at a threshold of 99% identity against an in-house generated *tuf* allele database that contained all *tuf* alleles from all staphylococcal genomes available in GenBank (as of December 2019). Data were normalized, and figures were prepared in R with the packages `ggplot2` and `gplots`.

## 2.6. Metagenome Database Search Strategy

The presence of sequences similar to *S. saccharolyticus* within available metagenomes deposited in the Sequence Read Archive (SRA) was initially assessed using the online tool at [www.searchsra.org](http://www.searchsra.org) to provide a broad overview of datasets with matches. A more detailed investigation of the level of representation of *S. saccharolyticus* in existing human skin and other human-associated metagenomic datasets (identified within the initial search of the SRA) was then conducted by mapping pooled sequencing reads from metagenomic datasets against the *S. saccharolyticus* genome sequence (strain 05B0362; GenBank accession number: QHKH00000000). Sequencing reads were obtained from the SRA and processed using Geneious Prime 2020 to remove low quality reads (Trim using BBDuk; min. 50 bp) and duplicates (Dedupe from BBTools), with default parameters. The resulting collections of high-quality reads were mapped against the genome sequences of *S. saccharolyticus* 05B0362, *Cutibacterium acnes* strain ATCC 6919 (NZ\_CP023676.1) and *Staphylococcus epidermidis* strain ATCC 14990 (NZ\_CP035288.1) using the Geneious Prime 2020 map to reference tool with the following criteria: 100% identity; no gaps or mismatches; maximum ambiguity = 1. For each metagenomic dataset mapped, the total number of reads mapped to each reference genome was normalized by the total size of the dataset, to provide reads mapped per megabase DNA.

A more targeted search strategy was also applied using an *S. saccharolyticus*-specific gene as a query to search metagenomic datasets derived from back skin [1]. The *hya* gene encoding a hyaluronate lyase was chosen (locus tag DMB78\_01130 in the genome of strain 05B0362), due to its low average nucleotide identity with *hya* genes from other staphylococcal species. The search was performed as an SRA nucleotide BLAST. The gene was considered as being present when the coverage exceeded 40%.

## 2.7. *S. Saccharolyticus* Growth

*S. saccharolyticus* (strain DVP5-16-4677) was grown on Fastidious anaerobic agar (FAA) plates (LAB M, Bury, UK) and incubated anaerobically at 37 °C for 4 days. For liquid growth, brain-heart infusion-yeast broth supplemented with 0.05% (w/vol) cysteine (BHCY broth) was used. The following growth conditions were evaluated and performed at 37 °C: anoxic conditions (Oxoid AnaeroGen System; ThermoFisher Scientific, Waltham, MA, USA), and oxic conditions with and without CO<sub>2</sub>-supplementation (Oxoid CO<sub>2</sub> Gen system; ThermoFisher Scientific, Waltham, MA, USA). Optical density (OD) data at 600 nm was determined until the stationary growth phase.

## 3. Results

### 3.1. Amplicon Sequencing of a *tuf* Gene Fragment Identified Staphylococcal Species Diversity on Back Skin Samples

Amplicon sequencing based on a *tuf* gene fragment was applied on swab material derived from the upper back of 19 healthy volunteers, to determine the diversity and relative abundance of staphylococcal species. In total, twelve different staphylococcal species were identified (Figure 1A and Table S1). The majority of samples contained two or more staphylococcal species, with single species found in only two samples (*S. capitis* and *S. epidermidis*, respectively). The four most abundant staphylococcal species identified were *S. epidermidis* (average abundance 34.0%), *S. capitis* (26.6%), *S. saccharolyticus* (20.5%), and *S. hominis* (6.5%) (Figure 1B). *S. saccharolyticus* was identified in 8 out of the 19 samples (42%) tested and, if present, was a dominant species, comprising a minimum of 10.9% and a maximum of 90.4% of the total reads (Figure 1C).

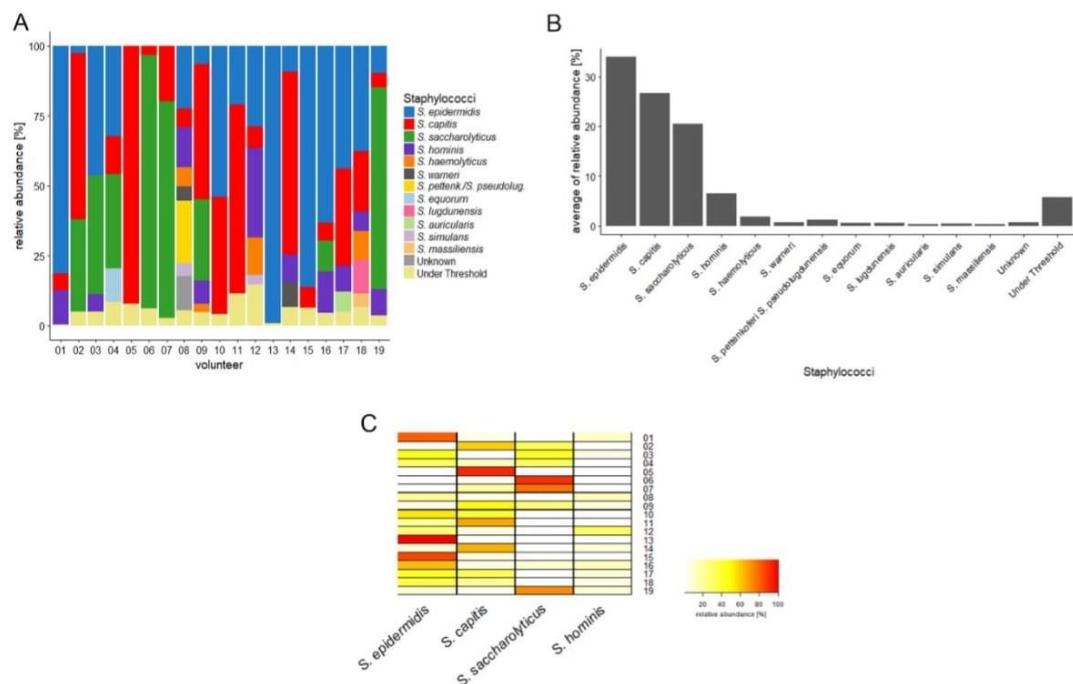


**Figure 1.** Diversity and abundance of staphylococcal species in back skin samples, based on amplicon next generation sequencing (NGS) data. (A) Relative abundance of staphylococcal species for each volunteer ( $n = 19$ ). Twelve staphylococcal species were identified in the cohort using the tuf amplicon-NGS approach. The four most abundant species in the cohort were *Staphylococcus epidermidis* (in blue), *Staphylococcus capitis* (in red), *Staphylococcus saccharolyticus* (in green) and *Staphylococcus hominis* (in purple). (B) The average relative abundance of the identified 12 staphylococcal species is shown; *S. epidermidis* was detected with an average abundance of 34.0%, *S. capitis* with 26.6%, *S. saccharolyticus* with 20.5%, and *S. hominis* with 6.5%. (C) The relative abundance of the four most prevalent staphylococcal species is shown for each back skin sample in a heat map. *S. epidermidis* was detected in four samples with a very high abundance (>60% of all reads); *S. capitis* and *S. saccharolyticus* were detected with such a high abundance in three samples each.

### 3.2. Presence of *S. Saccharolyticus* in Previous Metagenome Studies

Given that *S. saccharolyticus* was detected in 8 out of 19 back skin samples tested, we next decided to determine the prevalence and distribution of sequences with similarity to *S. saccharolyticus* within existing skin metagenomic datasets, using two different search strategies. First, sequencing reads from all skin metagenomes derived from back, forehead, and armpit samples ( $n = 43$ ) [1,2], available within the Sequence Read Archive (SRA), were mapped to the *S. saccharolyticus* genome with high stringency (100% identity; no gaps or mismatches; maximum ambiguity = 1). As a comparison, we also mapped the same reads to the genomes of two bacterial species known to be abundant on human skin, *Cutibacterium acnes* and *S. epidermidis*. Reads mapping to the *S. saccharolyticus* genome were found in all 43 skin metagenomic datasets searched (Figure 2). The percentage of reads mapping to *C. acnes* was significantly higher for all datasets searched, as compared to *S. saccharolyticus* and *S. epidermidis*. To compare relative abundance profiles, we also conducted a survey of a limited set of other human-associated metagenomic datasets (originating from the human gut, tongue dorsum, and supragingival plaque) identified as carrying sequences with similarity to *S. saccharolyticus*, using the SRA metagenomic search tool. Sequencing reads from these human-associated metagenomic datasets were also found to map to all bacterial genomes assessed, but at magnitudes of order lower levels than observed for human skin datasets.

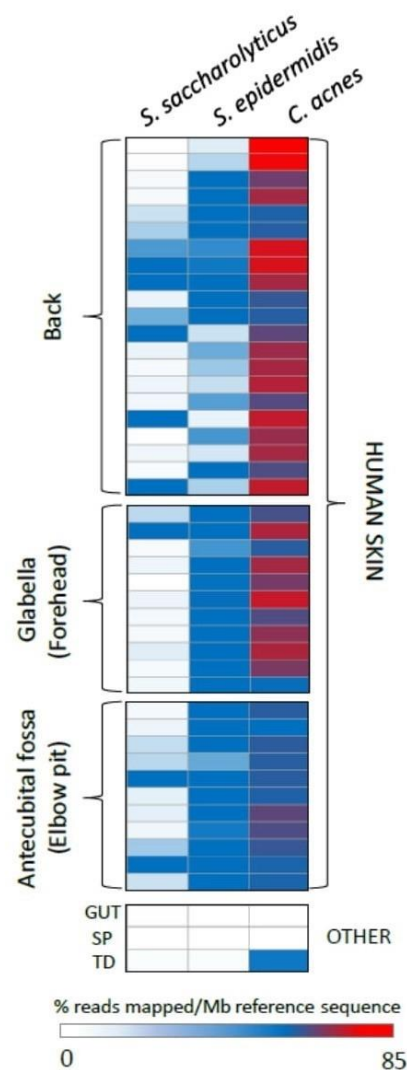


**Figure 2.** Representation of *S. saccharolyticus* in human skin and human-associated metagenomes. Heat map showing relative representation of *S. saccharolyticus* in metagenomes from human skin and other human associated environments. Reads from each reference metagenome were mapped to the genome sequences of *S. saccharolyticus*, *S. epidermidis*, and *Cutibacterium acnes* using high stringency criteria (100% identity; no gaps; max. ambiguity 1). The number of reads mapped was normalized for size of reference datasets (expressed as % of reads mapped/Mb reference sequence). OTHER: non-human skin metagenomes; GUT: human gut; SP: supragingival plaque; TD: tongue dorsum. Details of the metagenomes utilized are provided in Table S3.

To complement the read mapping analyses, we also conducted a more targeted search of the shotgun NGS data derived from back skin samples of Oh et al., 2014 [1] and Oh et al., 2016 [2] (12 volunteers; samples taken at three time points per person), using the hyaluronate lyase gene of *S. saccharolyticus*. Using this approach, we found high-stringency matches (reads with 100% identity) within three of the twelve volunteers at multiple time points (Table S2).

### 3.3. Re-Evaluation of Growth Conditions for *S. Saccharolyticus*

Our data indicate that *S. saccharolyticus* is widespread on human skin, can be detected within diverse skin sites, and may even be more abundant than *S. epidermidis* in some people. However, only a few studies have previously reported the presence of *S. saccharolyticus* on human skin. One possible

reason for the previous lack of recognition is the difficulty of growing *S. saccharolyticus* under standard conditions. The organism cannot be detected on blood agar when incubated under aerobic conditions for 24 to 96 h (data not shown). Instead, it grows on Trypticase soy yeast (TSY) agar plates supplemented with 0.5% Tween-80 or FAA plates when incubated for 72 to 96 h under anaerobic conditions (data not shown). Not much is known about its growth in broth. Thus, we recorded the growth of *S. saccharolyticus* in brain-heart infusion-yeast broth supplemented with 0.05% cysteine (BHCY medium). Different incubation conditions were applied, including anaerobic and aerobic conditions and the supplementation with CO<sub>2</sub> (Figure 3). Results showed that the organism grew almost equally as well under CO<sub>2</sub>-enriched conditions (approx. 6% CO<sub>2</sub> and 15% O<sub>2</sub>), compared to anaerobic conditions. Growth yields were reduced under atmospheric conditions.

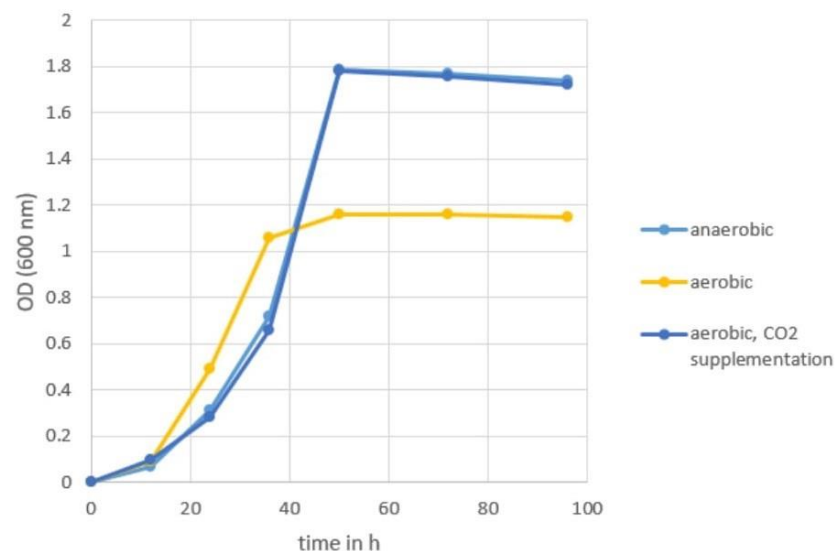


**Figure 3.** Growth of *S. saccharolyticus* in BHCY medium under different conditions. Light blue, anaerobic atmosphere (Oxoid-AnaeroGen system); dark blue, CO<sub>2</sub>-rich atmosphere (Oxoid-CO<sub>2</sub> Gen system; generating ca. 6% CO<sub>2</sub>, ca. 15% O<sub>2</sub>); yellow, aerobic atmosphere. The experiment was replicated twice.

#### 4. Discussion

The skin microbiome affects the health-state of our skin. Understanding the bacterial composition on non-diseased skin is therefore of importance. Here, we focused on the staphylococcal composition of the human back skin. Similar to most previous studies [1,2], *S. epidermidis* was found to be the most abundant staphylococcal species on human back skin, followed by *S. capitis*. Surprisingly, *S. saccharolyticus* ranked third. This species has previously not been reported to be abundant on human skin. However, two studies from 1978 reported the presence of *S. saccharolyticus*, formerly named *Peptococcus saccharolyticus*, in forehead and armpit skin samples [17,18]. In these studies, around 20% of samples were found to be positive for *S. saccharolyticus*. The organism grew on TSY (supplemented with 0.5% Tween-80) agar plates after 4–7 days of incubation, with preference for anaerobic conditions. Identification (and differentiation from other CoNS) was based on cell and colony morphology, anaerobic growth preference, and a weak catalase activity. Biochemically, *S. saccharolyticus* cannot produce lactic acid from glucose (in contrast to other staphylococci); it can ferment glucose, fructose, and glycerol, but not maltose. Interestingly, Evans et al. [17] stated that it was puzzling that the organism was not recognized in past studies “in view of its prevalence”. The authors also suggested that the reason that previous skin studies have overlooked this organism was due to (i) the choice of the culture media, (ii) the need for prolonged incubation time, (iii) the preference for anaerobic culture conditions, and (iv) misidentification. Indeed, 40 years later, not much has changed in this regard. Most culture-dependent skin microbiota studies do overlook this microorganism, possibly due



to inappropriate growth and cultivation conditions, as outlined by Evans et al. [17,18]. In addition, fast-growing species such as *S. epidermidis* might outcompete *S. saccharolyticus* on (standard) agar plates. This could explain why *S. saccharolyticus* was overlooked in culture-dependent studies.

However, this does not explain why *S. saccharolyticus* was previously not detected in culture-independent studies, which are nowadays more frequently conducted. Many culture-independent studies are carried out using 16S rRNA gene amplicon sequencing, which relies on sufficient differences in the 16S rRNA gene to distinguish species. However, the 16S rRNA gene of *S. saccharolyticus* does not carry many single nucleotide polymorphisms (SNPs) that can easily distinguish it from other CoNS, namely *S. capitis* [15]. Thus, depending on the 16S rRNA gene amplification strategy (amplifying the V1, V2, V3, V4, V5, and the V6 region, respectively, or a combination thereof), *S. saccharolyticus* can be indistinguishable from *S. capitis*.

In recent years, shotgun sequencing was employed to identify the skin metagenome [1,2]. However, meaningful analyses of shotgun sequencing data rely on reference genomes of all skin microorganisms. Regarding *S. saccharolyticus*, no such reference genome was available before March 2019. Adding to the confusion, three genomes assigned to *S. saccharolyticus* were publicly available in GenBank before 2019, but these were wrongly classified as *S. saccharolyticus*, and actually belong to *S. capitis*, as previously noted [15]. They were recently correctly reassigned to *S. capitis*. Besides the genomes of seven *S. saccharolyticus* strains that have been sequenced during our previous study [15], the type strain of *S. saccharolyticus* (ATCC 14953/NCTC 11807) has been sequenced by two independent teams (WGS projects UHDZ01 and RXWW01), resulting in nearly identical genome sequences. Taken together, before March 2019 there was no correct reference genome sequence of *S. saccharolyticus* available; this has been now resolved. Thus, current and future shotgun sequencing studies should be able to identify *S. saccharolyticus* correctly.

Here, we employed an amplicon sequencing method that is a modification from an existing method by Strube et al. [19]. The method is based on the amplification of a *tuf* gene fragment, with primers that were designed by Martineau et al. [22]. The *tuf* gene, encoding the elongation factor Tu, is a highly conserved gene in all staphylococcal species. We modified this method by choosing different amplification primers, since we noticed that the reverse primer designed by Martineau et al. [22] has two mismatches with the corresponding *tuf* gene sequence in the genome of *S. saccharolyticus*. It is thus likely that the primers of Martineau et al. [22] do not amplify the *tuf* gene of *S. saccharolyticus*, or only with reduced efficiency.

Previous studies reported that *S. saccharolyticus* has a preference for anaerobic growth conditions [17,18]. Here, we showed that the bacterium can also grow under atmospheric conditions in broth, but with a reduced growth yield compared to anaerobic conditions. However, the growth in a CO<sub>2</sub>-rich atmosphere is comparable to the growth under anaerobic conditions. A mechanistic explanation of the effect of CO<sub>2</sub> on bacterial growth was recently published by Fan et al. [23]. The authors investigated the growth-promoting effect of CO<sub>2</sub> and the CO<sub>2</sub>-dependency of small colony variants of *S. aureus*, whose growth defect can be compensated by increased CO<sub>2</sub>/bicarbonate supplementation. They found that staphylococci employ a CO<sub>2</sub>-concentrating mechanism that enables them to grow at atmospheric CO<sub>2</sub> levels. More specifically, they found that the system MpsAB is crucial for *S. aureus* growth at atmospheric CO<sub>2</sub> levels. From a set of carefully designed experiments, they concluded that the MpsAB system represents a dissolved inorganic carbon transporter, or bicarbonate concentrating system, which creates an elevated concentration of intracellular bicarbonate. Consequently, a staphylococcal species without a functional MpsAB system would only grow poorly at atmospheric CO<sub>2</sub> levels, and would rely on increased CO<sub>2</sub> concentrations for accelerated growth. As we previously noted that the genome of *S. saccharolyticus* contains over 300 frameshift mutations [15], we checked the *mpsAB* genes. Indeed, the *mpsAB* genes in the genome of *S. saccharolyticus* are frameshifted, and thus the MpsAB system is most likely non-functional in *S. saccharolyticus*. In conclusion, the lack of a functional CO<sub>2</sub>-concentrating system in *S. saccharolyticus* is a likely explanation for its insufficient growth under atmospheric conditions. This can be compensated by providing increased CO<sub>2</sub> concentrations.

Many questions remain, e.g., regarding the preferred niche of *S. saccharolyticus* on human skin and its evolutionary history that can be regarded as an example of reductive evolution, indicative of the massive genome decay [15]. Genomic modifications such as genome decay are often a result of a relative recent lifestyle change, e.g., the adaptation to a new host or a new niche within a host, associated with a strict(er) host dependency [24–26]. What could a scenario for the evolutionary history of *S. saccharolyticus* look like? In this regard, an interesting feature of *S. saccharolyticus* is the presence of a hyaluronate lyase (Hya), which is absent in other human-associated skin-resident CoNS. Closest homologs of the *hya* gene of *S. saccharolyticus* are present in two animal-associated staphylococci: *Staphylococcus agnetis* and *Staphylococcus hyicus*. *S. agnetis* is associated with lameness in broiler chickens, and *S. hyicus* causes skin diseases, such as exudative dermatitis in piglets [27,28]. It is tempting to suggest that the (horizontal) acquisition of *hya*, possibly from an animal-associated staphylococcal species, contributed to a lifestyle switch of *S. saccharolyticus*. Hyaluronate lyases degrade hyaluronic acid, a major polysaccharide of the extracellular matrix of tissues [29]. In the epidermis, hyaluronic acid is found in high concentrations, in particular in deeper layers of the epidermis, such as the stratum spinosum [30]. Thus, a hyaluronidase-producing *S. saccharolyticus* is likely better equipped to penetrate and propagate in deeper layers of the epidermis. We further speculate that a strong host association in deeper layers might have been established, where *S. saccharolyticus* would have access to a range of host-derived compounds including amino acids and cofactors. This in turn would render bacterial genes to synthesize such compounds dispensable. As a consequence, genome decay would be accelerated, aiming at a slimmer, less energy-consuming lifestyle that is adapted to an oxygen-depleted niche, i.e., the epidermis below the stratum corneum.

Another open question remains regarding the clinical significance of these findings. At present, only few studies, mainly case reports, have reported the involvement of *S. saccharolyticus* in human disease. The microorganism has been described as the etiologic agent of infective endocarditis, empyema and bone and joint infections such as shoulder synovitis and vertebral osteomyelitis [31–36]. In addition, the bacterium was reported to be responsible for nosocomial bloodstream infections in a German hospital [16]. A few reports have found *S. saccharolyticus* in implant-associated infections, such as prosthetic valve endocarditis [37] and we recently described eight cases of prosthetic joint infections where *S. saccharolyticus* was identified from tissue biopsies [15]. If *S. saccharolyticus* is widespread on human skin, as our study results suggest, one would expect to see more reports regarding the potential disease association of this bacterium, as seen for example for other skin-resident CoNS, such as *S. epidermidis* and *S. capitis*. As outlined above in detail, we hypothesize that mainly due to the fastidious growth conditions, *S. saccharolyticus* was overlooked in numerous disease cases, in particular in implant-associated infections, as such infections are often caused by skin-derived bacteria, including CoNS. In several cases, *S. saccharolyticus* has been identified, but was labeled as contaminant [38]. As also true for other CoNS, assigning an etiological role to *S. saccharolyticus* in disease requires thorough investigations to exclude skin-derived contamination of the biopsy material or contamination during subsequent sample processing steps. Carefully designed and executed future studies are needed to elucidate the etiology and frequency of *S. saccharolyticus* in human disease.

The study has some limitations, most importantly the small sample size ( $n = 19$ ) and the focus on back skin. Moreover, only relatively young participants were investigated in this study. Appropriate skin sampling methods have previously been discussed [39]; due to the here applied sampling method, i.e., skin swabs, we harvested mainly the microbiome of the stratum corneum. Thus, microorganisms that potentially penetrate deeper skin layers of the epidermis might be underrepresented. In future studies, we aim at analyzing more individuals, thereby covering and comparing different age groups and diverse skin health conditions. In addition, different skin sites will be investigated, and different skin sampling methods applied, in order to determine the specific skin tissue location of *S. saccharolyticus*.

In conclusion, here we found that the coagulase-negative species *S. saccharolyticus* is relatively often found in human skin samples, as judged from a culture-independent amplicon sequencing approach. When present, the organism can comprise a major part of the staphylococcal skin population,

and is found in several different skin sites. It has yet to be shown in the future if skin that is primarily colonized with *S. saccharolyticus* has distinguishable features from skin colonized with *S. epidermidis* or *S. capitis*.

**Supplementary Materials:** The following are available online at <http://www.mdpi.com/2076-2607/8/8/1105/s1>, Table S1: Sequence read count matching the *tuf* gene fragment of different staphylococcal species; Table S2: Identification of sequencing reads in back skin metagenomic data that map to the *hya* gene of *S. saccharolyticus* with 100% nucleotide identity; Table S3: List of metagenomic datasets used for read mapping.

**Author Contributions:** Conceptualization: C.M.A., J.H., and H.B.; methodology and experiments: C.M.A., M.A., A.P., and L.A.O.; resources: B.S.; data analysis: C.M.A., K.S., A.P., L.A.O., and H.B.; writing—original draft preparation: C.M.A. and H.B.; writing—review and editing: C.M.A., K.S., M.A., A.P., L.A.O., B.S., J.H., and H.B.; supervision: J.H. and H.B.; project administration: J.H. and H.B.; funding acquisition: H.B. All authors have read and agreed to the published version of the manuscript.

**Funding:** This research was funded by NovoNordisk, grant number NNF18OC0053172.

**Acknowledgments:** We thank Lise Hald Schultz for excellent technical assistance. Data processing was performed on the GenomeDK cluster; we would like to thank GenomeDK and Aarhus University for providing computational resources that contributed to these research results.

**Conflicts of Interest:** C.M.A. and J.H. are employees at Beiersdorf AG. The other authors declare no conflicts of interest. The funders had no role in the design of the study; in the collection, analyses, or interpretation of data; in the writing of the manuscript; or in the decision to publish the results.

## References

1. Oh, J.; Byrd, A.L.; Deming, C.; Conlan, S.; Program, N.C.S.; Kong, H.H.; Segre, J.A. Biogeography and individuality shape function in the human skin metagenome. *Nature* **2014**, *514*, 59–64. [CrossRef] [PubMed]
2. Oh, J.; Byrd, A.L.; Park, M.; Program, N.C.S.; Kong, H.H.; Segre, J.A. Temporal Stability of the Human Skin Microbiome. *Cell* **2016**, *165*, 854–866. [CrossRef] [PubMed]
3. Byrd, A.L.; Belkaid, Y.; Segre, J.A. The human skin microbiome. *Nat. Rev. Microbiol.* **2018**, *16*, 143–155. [CrossRef] [PubMed]
4. Belkaid, Y.; Segre, J.A. Dialogue between skin microbiota and immunity. *Science* **2014**, *346*, 954–959. [CrossRef]
5. Sanford, J.A.; Gallo, R.L. Functions of the skin microbiota in health and disease. *Semin. Immunol.* **2013**, *25*, 370–377. [CrossRef]
6. Otto, M. Staphylococci in the human microbiome: The role of host and interbacterial interactions. *Curr. Opin. Microbiol.* **2020**, *53*, 71–77. [CrossRef]
7. Kloos, W.E.; Musselwhite, M.S. Distribution and persistence of *Staphylococcus* and *Micrococcus* species and other aerobic bacteria on human skin. *Appl. Microbiol.* **1975**, *30*, 381–385. [CrossRef]
8. Schoenfelder, S.M.; Lange, C.; Eckart, M.; Hennig, S.; Kozytska, S.; Ziebuhr, W. Success through diversity—how *Staphylococcus epidermidis* establishes as a nosocomial pathogen. *Int. J. Med. Microbiol.* **2010**, *300*, 380–386. [CrossRef]
9. Heilmann, C.; Ziebuhr, W.; Becker, K. Are coagulase-negative staphylococci virulent? *Clin. Microbiol. Infect.* **2019**, *25*, 1071–1080. [CrossRef]
10. Bieber, L.; Kahlmeter, G. *Staphylococcus lugdunensis* in several niches of the normal skin flora. *Clin. Microbiol. Infect.* **2010**, *16*, 385–388. [CrossRef]
11. Meugnier, H.; Bes, M.; Vernozy-Rozand, C.; Mazuy, C.; Brun, Y.; Freney, J.; Fleurette, J. Identification and ribotyping of *Staphylococcus xylosus* and *Staphylococcus equorum* strains isolated from goat milk and cheese. *Int. J. Food Microbiol.* **1996**, *31*, 325–331. [CrossRef]
12. Ward, D.M.; Weller, R.; Bateson, M.M. 16S rRNA sequences reveal numerous uncultured microorganisms in a natural community. *Nature* **1990**, *345*, 63–65. [CrossRef] [PubMed]
13. Dickson, R.P.; Erb-Downward, J.R.; Prescott, H.C.; Martinez, F.J.; Curtis, J.L.; Lama, V.N.; Huffnagle, G.B. Analysis of culture-dependent versus culture-independent techniques for identification of bacteria in clinically obtained bronchoalveolar lavage fluid. *J. Clin. Microbiol.* **2014**, *52*, 3605–3613. [CrossRef]
14. Grice, E.A.; Kong, H.H.; Conlan, S.; Deming, C.B.; Davis, J.; Young, A.C.; Program, N.C.S.; Bouffard, G.G.; Blakesley, R.W.; Murray, P.R.; et al. Topographical and temporal diversity of the human skin microbiome. *Science* **2009**, *324*, 1190–1192. [CrossRef] [PubMed]

15. Brüggemann, H.; Poehlein, A.; Brzuszkiewicz, E.; Scavenius, C.; Enghild, J.J.; Al-Zeer, M.A.; Brinkmann, V.; Jensen, A.; Söderquist, B. *Staphylococcus saccharolyticus* Isolated from Blood Cultures and Prosthetic Joint Infections Exhibits Excessive Genome Decay. *Front. Microbiol.* **2019**, *10*, 478. [[CrossRef](#)] [[PubMed](#)]
16. Steinbrueckner, B.; Singh, S.; Freney, J.; Kuhnert, P.; Pelz, K.; Aufenanger, J. Facing a mysterious hospital outbreak of bacteraemia due to *Staphylococcus saccharolyticus*. *J. Hosp. Infect.* **2001**, *49*, 305–307. [[CrossRef](#)]
17. Evans, C.A.; Mattern, K.L.; Hallam, S.L. Isolation and identification of *Peptococcus saccharolyticus* from human skin. *J. Clin. Microbiol.* **1978**, *7*, 261–264. [[PubMed](#)]
18. Evans, C.A.; Mattern, K.L. Individual differences in the bacterial flora of the skin of the forehead: *Peptococcus saccharolyticus*. *J. Investig. Dermatol.* **1978**, *71*, 152–153. [[CrossRef](#)]
19. Strube, M.L.; Hansen, J.E.; Rasmussen, S.; Pedersen, K. A detailed investigation of the porcine skin and nose microbiome using universal and *Staphylococcus* specific primers. *Sci. Rep.* **2018**, *8*, 12751. [[CrossRef](#)]
20. Bolyen, E.; Rideout, J.R.; Dillon, M.R.; Bokulich, N.A.; Abnet, C.C.; Al-Ghalith, G.A.; Alexander, H.; Alm, E.J.; Arumugam, M.; Asnicar, F.; et al. Reproducible, interactive, scalable and extensible microbiome data science using QIIME 2. *Nat. Biotechnol.* **2019**, *37*, 852–857. [[CrossRef](#)]
21. Callahan, B.J.; McMurdie, P.J.; Rosen, M.J.; Han, A.W.; Johnson, A.J.; Holmes, S.P. DADA2: High-resolution sample inference from Illumina amplicon data. *Nat. Methods* **2016**, *13*, 581–583. [[CrossRef](#)] [[PubMed](#)]
22. Martineau, F.; Picard, F.J.; Ke, D.; Paradis, S.; Roy, P.H.; Ouellette, M.; Bergeron, M.G. Development of a PCR assay for identification of staphylococci at genus and species levels. *J. Clin. Microbiol.* **2001**, *39*, 2541–2547. [[CrossRef](#)] [[PubMed](#)]
23. Fan, S.H.; Ebner, P.; Reichert, S.; Hertlein, T.; Zabel, S.; Lankapalli, A.K.; Nieselt, K.; Ohlsen, K.; Gotz, F. MpsAB is important for *Staphylococcus aureus* virulence and growth at atmospheric CO<sub>2</sub> levels. *Nat. Commun.* **2019**, *10*, 3627. [[CrossRef](#)] [[PubMed](#)]
24. Pallen, M.J.; Wren, B.W. Bacterial pathogenomics. *Nature* **2007**, *449*, 835–842. [[CrossRef](#)]
25. Argemi, X.; Hansmann, Y.; Prola, K.; Prévost, G. Coagulase-Negative Staphylococci Pathogenomics. *Int. J. Mol. Sci.* **2019**, *20*, 1215. [[CrossRef](#)]
26. Lindsay, J.A. Staphylococci: Evolving Genomes. *Microbiol. Spectr.* **2019**, *7*. [[CrossRef](#)]
27. Hazarika, R.A.; Mahanta, P.N.; Dutta, G.N.; Devriese, L.A. Cutaneous infection associated with *Staphylococcus hyicus* in cattle. *Res. Vet. Sci.* **1991**, *50*, 374–375. [[CrossRef](#)]
28. Foster, A.P. Staphylococcal skin disease in livestock. *Vet. Dermatol.* **2012**, *23*, 342–351, e63. [[CrossRef](#)]
29. Hynes, W.L.; Walton, S.L. Hyaluronidases of Gram-positive bacteria. *FEMS Microbiol. Lett.* **2000**, *183*, 201–207. [[CrossRef](#)]
30. Tammi, R.; Ripellino, J.A.; Margolis, R.U.; Tammi, M. Localization of epidermal hyaluronic acid using the hyaluronate binding region of cartilage proteoglycan as a specific probe. *J. Investig. Dermatol.* **1988**, *90*, 412–414. [[CrossRef](#)]
31. Westblom, T.U.; Gorse, G.J.; Milligan, T.W.; Schindzielorz, A.H. Anaerobic endocarditis caused by *Staphylococcus saccharolyticus*. *J. Clin. Microbiol.* **1990**, *28*, 2818–2819. [[CrossRef](#)] [[PubMed](#)]
32. Godreuil, S.; Jean-Pierre, H.; Morel, J.; Darbas, H.; Jumas-Bilak, E.; Bañuls, A.L.; Marchandin, H. Unusual case of spondylodiscitis due to *Staphylococcus saccharolyticus*. *Joint Bone Spine* **2005**, *72*, 91–93. [[CrossRef](#)] [[PubMed](#)]
33. Mikhael, M.M.; Bach, H.G.; Huddleston, P.M.; Maus, T.P.; Barbari, E.F. Multilevel diskitis and vertebral osteomyelitis after diskography. *Orthopedics* **2009**, *32*, 60. [[CrossRef](#)] [[PubMed](#)]
34. Schneeberger, A.G.; Yian, E.; Steens, W. Injection-induced low-grade infection of the shoulder joint: Preliminary results. *Arch. Orthop. Trauma Surg.* **2012**, *132*, 1387–1392. [[CrossRef](#)]
35. Oberbach, A.; Friedrich, M.; Lehmann, S.; Schlichting, N.; Kullnick, Y.; Gräber, S.; Buschmann, T.; Hagl, C.; Bagaev, E.; CardiOmics group; et al. Bacterial infiltration in structural heart valve disease. *J. Thorac. Cardiovasc. Surg.* **2019**, *S0022-5223*, 30451–30459. [[CrossRef](#)]
36. Wang, P.; Liu, Y.; Xu, Y.; Xu, Z. *Staphylococcus saccharolyticus* infection: Case series with a PRISMA-compliant systemic review. *Med. Baltim.* **2020**, *99*, e20686. [[CrossRef](#)]
37. Krishnan, S.; Haglund, L.; Ashfaq, A.; Leist, P.; Roat, T. Prosthetic valve endocarditis due to *Staphylococcus saccharolyticus*. *Clin. Infect. Dis.* **1996**, *22*, 722–723. [[CrossRef](#)]

38. Hitzenbichler, F.; Simon, M.; Salzberger, B.; Hanses, F. Clinical significance of coagulase-negative staphylococci other than *S. epidermidis* blood stream isolates at a tertiary care hospital. *Infection* **2017**, *45*, 179–186. [[CrossRef](#)]
39. Omer, H.; McDowell, A.; Alexeyev, O.A. Understanding the role of *Propionibacterium acnes* in acne vulgaris: The critical importance of skin sampling methodologies. *Clin. Dermatol.* **2017**, *35*, 118–129. [[CrossRef](#)]



© 2020 by the authors. Licensee MDPI, Basel, Switzerland. This article is an open access article distributed under the terms and conditions of the Creative Commons Attribution (CC BY) license (<http://creativecommons.org/licenses/by/4.0/>).

## 4 Manuscript I

### **Interference and co-existence of staphylococci and *Cutibacterium acnes* within the healthy human skin microbiome**

Charlotte Marie Ahle, Kristian Stødkilde-Jørgensen, Anja Poehlein, Mechthild Bömeke, Cecilie Feidenhansl, Wolfgang R. Streit, Horst Wenck, Jörn Hendrik Reuter, Jennifer Hüpeden, Holger Brüggemann

**Manuscript submitted**

#### **Contributions to the article:**

- Writing of manuscript
- Planning and conducting the study (measuring of skin parameters, taking skin swabs, analysis of CFU count)
- Isolation and species characterisation of staphylococci from skin
- DNA extraction skin swabs and staphylococcal isolates
- Analysis and visualization of amplicon NGS data
- Phylogenomic analysis of *S. epidermidis*
- Establishment and conduction of antagonistic plate assay
- Co-culturing of *S. epidermidis* and *C. acnes*
- Analysis and visualization of RNA-Seq data

---

Associate Prof. Dr. Holger Brüggemann

# Interference and co-existence of staphylococci and *Cutibacterium acnes* within the healthy human skin microbiome

Charlotte Marie Ahle<sup>1,2,\*</sup>, Kristian Stødkilde-Jørgensen<sup>3</sup>, Anja Poehlein<sup>4</sup>, Mechthild Bömeke<sup>4</sup>, Cecilie Feidenhansl<sup>3</sup>, Wolfgang R. Streit<sup>2</sup>, Horst Wenck<sup>1</sup>, Jörn Hendrik Reuter<sup>1</sup>, Jennifer Hüpeden<sup>1</sup>, Holger Brüggemann<sup>3,\*</sup>

<sup>1</sup>Beiersdorf AG, Research & Development, Front End Innovation, 20245 Hamburg, Germany

<sup>2</sup>Department of Microbiology and Biotechnology, University of Hamburg, 22609 Hamburg, Germany

<sup>3</sup>Department of Biomedicine, Aarhus University, 8000 Aarhus, Denmark

<sup>4</sup>Department of Genomic and Applied Microbiology, Institute of Microbiology and Genetics, University of Göttingen, 37073 Göttingen, Germany

Email addresses:

Charlotte Marie Ahle: Charlotte.Marie.Ahle@studium.uni-hamburg.de

Kristian Stødkilde-Jørgensen: kst@biomed.au.dk

Anja Poehlein: apoehle3@gwdg.de

Mechthild Bömeke: mboemek@gwdg.de

Cecilie Feidenhansl: cecilief@biomed.au.dk

Wolfgang R. Streit: wolfgang.streit@uni-hamburg.de

Horst Wenck: Horst.Wenck@Beiersdorf.com

Jörn Hendrik Reuter: JoernHendrikDr.Reuter@Beiersdorf.com

Jennifer Hüpeden: Jennifer.Huepeden@Beiersdorf.com

Holger Brüggemann: brueggemann@biomed.au.dk

\* corresponding authors:

Holger Brüggemann: brueggemann@biomed.au.dk

Charlotte Marie Ahle: Charlotte.Marie.Ahle@studium.uni-hamburg.de

# Abstract

## Background

Human skin is populated by trillions of microbes collectively called the skin microbiome. *Staphylococcus epidermidis* and *Cutibacterium acnes* are among the most abundant members of this ecosystem, with described roles in skin health and disease. Knowledge regarding the exact composition of coexisting populations on healthy skin and the potential interferences of these ubiquitous skin residents is still limited.

## Results

Here, we profiled the staphylococcal and *C. acnes* landscape of 30 individuals across four different skin sites (120 skin samples) using amplicon-based next-generation sequencing. In average, skin sites were colonized with 3.1 and 3.6 different staphylococcal species and *C. acnes* phylotypes, respectively. *S. epidermidis* was found to be the most abundant staphylococcal species across all skin sites, followed by *Staphylococcus capitis* and *Staphylococcus saccharolyticus*. The latter species was not detected by cultivation, likely due to its fastidious growth requirements. Genome-sequencing of 69 *S. epidermidis* strains revealed a large diversity; these healthy skin-associated strains did not overlap with previously identified disease-associated lineages. Regarding the *C. acnes* population, 39 distinct phylotypes differentiated by single-locus sequence typing (SLST) were found, which covered all known 10 SLST classes. Highest relative abundances were determined for A-class *C. acnes* (27.6 %), followed by D-class (20.7%), K-class (19.2%) and H-class (12.2%) *C. acnes*.

Relative abundance profiles indicated the existence of phylotype-specific co-existence and exclusion scenarios. Co-culture experiments with 557 staphylococcal strains identified 30 strains exhibiting anti-*C. acnes* activities. Notably, staphylococcal strains were found to selectively exclude acne-associated *C. acnes* and co-exist with healthy skin-associated phylotypes. Transcriptome sequencing of *S. epidermidis* in the presence of tolerant (D-class) and susceptible (A-class) *C. acnes* strains, respectively, showed that the antimicrobial activity of *S. epidermidis* was



selectively down-regulated in the presence of D-class *C. acnes*. The data suggests that D-class, but not A-class *C. acnes* can interfere with the *agr* quorum sensing system of *S. epidermidis* and suppress the production and activity of antimicrobial peptides.

## Conclusion

Overall, these findings highlight the importance of skin-resident staphylococci and give insight into their phylotype-specific interaction with *C. acnes*. These selective microbial interferences contribute to homeostasis of the microbiome of healthy skin.

**Keywords:** skin microbiome, *Staphylococcus*, coagulase-negative staphylococci, *Staphylococcus epidermidis*, *Cutibacterium acnes*, microbial interference, amplicon-based next-generation sequencing, transcriptome sequencing

## Background

Human skin is colonized by a diverse community of microorganisms, the composition of which is shaped by numerous host-related and external factors, including chemical and physical parameters, skin topography and microbe-microbe interactions [1].

*Staphylococcus* and *Cutibacterium* are known to be the most abundant and ubiquitous genera within the human skin microbiome [2, 3], found across almost all parts of the skin ecosystem, albeit with preferential niches. Some species of staphylococci such as *S. epidermidis* are often located in sites of high humidity, while *C. acnes* is found more often in sebaceous areas [4-6]. Both genera are known to exhibit traits that have been linked to specific health- and disease-related states and are selectively regarded as key skin health sentinels [7-10].

*S. epidermidis* is the most abundant skin colonizing coagulase-negative staphylococci (CoNS). The species is phylogenetically divided into three main clusters (A, B, C) [11-13] and is assigned to different sequence types (ST). Notably,

*S. epidermidis* STs have been linked to nosocomial infections, suggesting relevance for pathogenic potential (e.g. ST2, ST5 and ST23) [14].

*C. acnes* is a polyphyletic species that can be divided into different subspecies and phylotypes, namely, IA<sub>1</sub>, IA<sub>2</sub>, IB, IC, II and III [15, 16]. To enable characterisation of mixed populations of *C. acnes*, a single locus sequence typing (SLST) scheme has been developed that enables the differentiation into ten classes (A to L) [17]. SLST classes A to E correspond to phylotype IA<sub>1</sub> strains, whereas SLST classes F, G, H, K and L correspond to phylotypes IA<sub>2</sub>, IC, IB, II and III, respectively [17]. Recent work has shown that some phylotypes/SLST classes are enriched in individuals with the skin disorder acne vulgaris, whereas others have been identified as markers of healthy skin. Acne-associated phylotypes include SLST classes A and C (both phylotype IA<sub>1</sub>) and F (IA<sub>2</sub>), whereas healthy skin is colonised with more diverse populations with a higher prevalence of strains belonging to the SLST classes H (IB) and K (II) [18-23].

A limited number of studies have indicated that *Staphylococcus* spp. and *Cutibacterium* spp. may be interacting in a strain-dependent manner. For instance, some staphylococcal strains can produce bacteriocins [24, 25] or short-chain fatty acids [26], preventing the colonisation and spread of *C. acnes* and other disease-associated bacteria. However, there is still limited knowledge regarding interactions between the two most abundant genera on human skin.

Here, we used a combination of culture-dependent and -independent approaches to characterise staphylococcal and *C. acnes* populations within the healthy skin microbiome of 30 healthy individuals (four skin sites, 120 samples) and assess their potential for co-existence and mutual exclusion within this ecosystem.

An amplicon-based next-generation sequencing (NGS) method [17, 27, 28] was applied in tandem with *in vitro* antagonistic assays, whole genome sequencing of isolates and gene expression analysis to uncover selective exclusion and co-existence of acne- and healthy skin-associated *C. acnes* lineages, respectively, by staphylococcal strains. Our findings provide new insights into the healthy skin microbiome landscape, revealing a key role of staphylococci in maintaining skin microbiome homeostasis through microbial interference.

## Methods

### Cohort and sample acquisition

Swab samples were collected from 30 volunteers (female, n=14; male, n=16) with an age range of 22-43 years from forehead, cheek, back and forearm skin, as described previously [27]. In brief, an area of 25 cm<sup>2</sup> of forehead, cheek, back skin and 50 cm<sup>2</sup> on forearm skin was swiped with a cotton swap which was pre-moistened in aqueous sampling buffer containing disodium phosphate (12.49 g/L, Merck), potassium dihydrogen phosphate (0.63 g/L, Merck) and 1 % Triton X-100 (Sigma). The swap was vigorously shaken in a tube containing 2 mL of sampling buffer and then removed. The sample was stored at -20°C before DNA extraction. Skin hydration and sebum content were measured with a Corneometer (Courage + Khazaka electronic) and Sebumeter (Courage + Khazaka electronic), respectively. None of the volunteers had a history of skin disease, nor had undergone treatment with topical medicine or antibiotics in the last six months. Written informed consent was obtained from all volunteers and the study was approved by International Medical & Dental Ethics Commission GmbH (IMDEC), Freiburg (Study no. 67885).

### Cultivation of swab sample, CFU count and species identification

The swab samples were diluted (back, cheek, forehead skin sample: 1:10 and 1:1000; forehead skin sample: 1:1 and 1:100) in 0.9 % NaCl solution. Cultivation was done by plating on Columbia agar with 5 % sheep blood; agar plates were incubated at 37°C for 24 h. CFU count was determined with an automatic colony counter (IUL). Up to five colonies that resembled staphylococci based on colony size and color were randomly picked of each plate and pure cultures were obtained by sub-cultivation on the same agar. Each isolate (572 isolates in total) was assigned to species level by MALDI-TOF mass spectrometry (Additional File 1).

### DNA extraction from skin swab samples

Prior to DNA extraction, skin swab samples were centrifuged (8.000 g, 30 min at 4°C), and the supernatant was discarded. The pellets were lysed by using lysostaphin (0.05 mg/mL, Sigma) and lysozyme (9.5 mg/mL, Sigma). DNA was extracted using the DNeasy PowerSoil Kit (QIAGEN), following the manufacturer's

instructions. DNA concentrations were measured with the Qubit dsDNA HS Assay (ThermoFisher Scientific) using a Qubit fluorometer.

### **Amplicon polymerase chain reaction (PCR)**

The *tuf2* amplicon PCR (for staphylococcal population analysis) was performed as described previously [27] using the primers *tuf2\_fw*, 5'-ACAGGCCGTGTTGAACGTG-3' and *tuf2\_rev*, 5'-ACAGTACGTCCACCTTCACG-3'. The SLST amplicon fragment (for *C. acnes* population analysis) was amplified using the primers: 5'-TTGCTCGCAACTGCAAGCA-3' and 5'-CCGGCTGGCAAATGAGGCAT-3'. PCR reaction mixtures were made in a total volume of 25 µl and comprised 5 µl of DNA sample, 2.5 µl AccuPrime PCR Buffer II (Invitrogen, Waltham, MA, USA), 1.5 µl of each primer (10 µM) (DNA Technology, Risskov, Denmark), 0.15 µl AccuPrime Taq DNA Polymerase High Fidelity (Invitrogen, Waltham, MA, USA), and 14.35 µl of PCR grade water. The PCR reaction was performed using the following cycle conditions: initial denaturation at 94°C for 2 min, 35 cycles of denaturation at 94°C for 20 sec, annealing at 55°C for 30 sec, elongation at 68°C for 1 min, final elongation step at 72°C for 5 min. PCR products were verified on an agarose gel and purified using the Qiagen Generead™ Size Selection kit (Qiagen, Hilden, Germany). The concentration of the purified PCR products was measured with a NanoDrop 2000 spectrophotometer (ThermoFisher Scientific, Waltham, MA, USA).

### **Amplicon-based Next-Generation Sequencing**

PCR products were used to attach indices and Illumina sequencing adapters using the Nextera XT Index kit (Illumina, San Diego). Index PCR was performed using 5 µl of template PCR product, 2.5 µl of each index primer, 12.5 µl of 2x KAPA HiFi HotStart ReadyMix and 2.5 µl PCR grade water. Thermal cycling scheme was as follows: 95 °C for 3 min, 8 cycles of 30 s at 95 °C, 30 s at 55 °C and 30 s at 72 °C and a final extension at 72 °C for 5 min. Quantification of the products was performed using the Quant-iT dsDNA HS assay kit and a Qubit fluorometer (Invitrogen GmbH, Karlsruhe, Germany) following the manufacturer's instructions. MagSi-NGS<sup>PREP</sup> Plus Magnetic beads (Steinbrenner Laborsysteme GmbH, Wiesenbach, Germany) were used for purification of the indexed products as recommended by the manufacturer and normalization was performed using the Janus Automated Workstation from

Perkin Elmer (Perkin Elmer, Waltham Massachusetts, USA). Sequencing were conducted using Illumina MiSeq platform using dual indexing and MiSeq reagent kit v3 (600 cycles) as recommended by the manufacturer.

### **Amplicon-based NGS data analysis and visualization**

FASTQ sequences obtained after demultiplexing the reads and trimming the primers were imported into QIIME2 (v. 2019.7) [29]. Sequences with an average quality score lower than 20 or containing unresolved nucleotides were removed from the dataset. The paired-end reads were denoised and chimeras removed with DADA2 via q2-dada2, and a feature table was generated [30]. These features were then clustered with VSEARCH using q2-vsearch at a cut-off of 99 % identity against allele databases. The database for the staphylococcal amplicon scheme contained all *tuf* alleles from all staphylococcal genomes available in GenBank (as of December 2020). The allele database for the *C. acnes* SLST amplicon scheme is available online (<http://medbac.dk/slst/pacnes/>). Data was normalized, low abundant features were filtered with a threshold of 2.5 %, and figures were prepared in R (v. 4.0.1) with the packages phyloseq [31], ggplot2 [32] and gplots [33]. Shannon index was calculated using OUT reads.

### **Whole genome sequencing of *S. epidermidis* isolates**

*S. epidermidis* isolates (n=69) were randomly selected for genome sequencing and cultivated on Columbia agar with 5 % sheep blood for 24 h at 37°C. Bacteria were lysed with lysostaphin (0.05 mg/mL, Sigma) and genomic DNA was extracted using the DNeasy UltraClean Microbial Kit by following manufacturer's instructions. DNA concentration and purity were measured by Nanodrop. DNA integrity was checked with Genomic DNA ScreenTape (Agilent) at the 4200 TapeStation System. Sequencing was done as described previously [28].

### **Phylogenetic and pan-genomic analysis of *S. epidermidis* and *C. acnes***

Genomes of *S. epidermidis* isolates (n=69) of this study and genomes of *S. epidermidis* (n=286) with N50 > 100 kb, taken from the NCBI RefSeq database (status 03.04.2020) were aligned and clustered based on single nucleotide variants (SNVs) in their core genome using Parsnp (v 1.0) [34]. Their ST-type was determined with

CGE Bacterial Analysis Pipeline using the tool MLST (v 1.6) [35]. Visualization of the tree was done with iTOL (v 5.7) [36]. The presence/absence of the genes *icaA* (query locus tag: SEU43366), *mecA* (AHA36637) and IS256 (D9V02\_13220) were determined by blastn. For pan-genomic analyses (69 *S. epidermidis* isolates of this study and 75 *C. acnes* genomes taken from the GenBank database) the Anvi'o [37] tool was used, following Anvi'o workflow for microbial pangenomics (<https://merenlab.org/2016/11/08/pangenomics-v2/>).

### **Antagonistic plate assay**

All 572 CoNS isolates were screened for antimicrobial properties against the indicator strains *S. aureus* DSM799 and *C. acnes* DSM1897. First, bacterial lawn plates were prepared. Liquid cultures of *C. acnes* indicator strains and *S. aureus* were prepared in CASO broth. For staphylococci the liquid culture was adjusted to an optical density of  $OD_{600nm} = 0.002$ ; while for *C. acnes* strain cultures were adjusted to  $OD_{600} = 0.075$ . 6 mL of the adjusted culture was pipetted onto a rectangular Tryptic Soy Agar (TSA) plate and distributed evenly. For round TSA plates 3 mL bacterial suspension was used. After 30 sec excess liquid was removed and the plates were dried for 4 h. The plates were stored up to three weeks at 4°C.

The CoNS isolates were cultivated for 20 h at 37°C shaking in 1 mL CASO broth in 96-Deepwell plates. The 96-Deepwell plate were centrifuged at 2000 rpm for 5 min, 500 µL supernatant was removed and the pellet was re-suspended in the remaining liquid. The concentrated bacterial cultures were transferred into 96-well U-bottom plates. With a replicator stamps bacterial cultures were transferred on rectangular lawn plates. After 4 h of drying, the plates were cultivated with varying conditions (*S. aureus* lawn plates: 24 h, 37°C; *C. acnes* lawn plates: 4-5 days, 37°C, in anaerobic container with AnaeroGen bag (Thermo Scientific)). A visible inhibition zone around a staphylococcal colony was regarded as antimicrobial activity. Staphylococcal strains that showed antimicrobial properties were verified in triplicates. These strains were further tested against eleven different *C. acnes* indicator strains from six different SLST classes. Strain names and accession numbers of all indicator strains are listed in Additional File 2.

### **Co-Cultures of *S. epidermidis* and *C. acnes***

Lawn plates with *C. acnes* DSM1897 and *C. acnes* 30.2.L1 were prepared as described above. A liquid culture of *S. epidermidis* HAF242 was grown to exponential growth phase and diluted 1:10<sup>6</sup> in 0.9 % NaCl solution and plated on the *C. acnes* lawn plates with a spiral plater (Don Whitley Scientific). Plates were incubated for 4 h at 37°C under aerobic conditions and then 72 h in anaerobic conditions (AnaeroGen bag (Thermo Scientific)) at 37°C. The bacteria were harvested using a cell spreader and suspended in 10 mL 0.9 % NaCl solution and immediately frozen at -80°C. Experiments were done in triplicates.

### **RNA extraction and RNA sequencing**

Harvested cells were resuspended in 800 µl RLT buffer (RNeasy Mini Kit, Qiagen) with β-mercaptoethanol (10 µl/ml) and cell lysis was performed using a laboratory ball mill. Subsequently, 400 µl buffer RLT (RNeasy Mini Kit Qiagen) with β-mercaptoethanol (10 µl/ml) and 1200 µl 96 % [v/v] ethanol were added. For RNA isolation, the RNeasy Mini Kit (Qiagen) was used as recommended by the manufacturer, but instead of buffer RW1, the buffer RWT (Qiagen) was used in order to also isolate RNAs smaller 200 nt. To determine the RNA integrity number (RIN) the isolated RNA was run on an Agilent Bioanalyzer 2100 using an Agilent RNA 6000 Nano Kit, as recommended by the manufacturer (Agilent Technologies, Waldbronn, Germany). Remaining genomic DNA was removed by digestion with TURBO DNase (Invitrogen, ThermoFischer Scientific, Paisley, United Kingdom). The Illumina Ribo-Zero plus rRNA Depletion Kit (Illumina Inc., San Diego, CA, USA) was used to reduce the amount of rRNA-derived sequences. For sequencing, strand-specific cDNA libraries were constructed with a NEBNext Ultra II directional RNA library preparation kit for Illumina and the NEBNext Multiplex Oligos for Illumina (New England BioLabs, Frankfurt am Main, Germany). To assess quality and size of the libraries, samples were run on an Agilent Bioanalyzer 2100 using an Agilent High Sensitivity DNA Kit, as recommended by the manufacturer (Agilent Technologies, Waldbronn, Germany). Concentration of the libraries were determined using the Qubit® dsDNA HS Assay Kit, as recommended by the manufacturer (Life Technologies GmbH, Darmstadt, Germany). Sequencing was performed on a

NovaSeq 6000 instrument (Illumina Inc., San Diego, CA, USA) using NovaSeq 6000 SP Reagent Kit v1.5 (100 cycles) and the NovaSeq XP 2-Lane Kit v1.5 for sequencing in the paired-end mode and running 2x 50 cycles. For quality filtering and removing of remaining adaptor sequences, Trimmomatic-0.39 [38] and a cutoff phred-33 score of 15 were used. Mapping against the reference genome was performed with Salmon (v 1.5.2) [39]. As mapping backbone a file that contained all annotated transcripts excluding rRNA genes and the whole genome sequence of the reference as decoy was prepared with a k-mer size of 11. Decoy-aware mapping was done in selective-alignment mode with “-mimicBT2”, “-disableChainingHeuristic”, and “-recoverOrphans” flags as well as sequence and position bias correction. For -fldMean and -fldSD, a value of 325 and 25 was used, respectively. The quant.sf files produced by Salmon were subsequently loaded into R (v 4.0.3) using the tximport package (v 1.18.0) [40]. DeSeq2 (v 1.30.0) [41] was used for normalization of the reads; foldchange-shrinkages were also calculated with DeSeq2 and the apeglm package (v 1.12.0) [42]. Genes with a log<sub>2</sub>-fold change of +2/-2 and a p-adjust value < 0.05 were considered differentially expressed.

### **Statistical analysis**

Statistical analysis was done in R (v. 4.0.1) using the packages ggplot2 (v. 3.3.5), phyloseq (v 1.34.0), gplots (v 3.1.1.), corrplot (v 0.90) [43], ANCOMBC (v 1.0.5) [44] pheatmap (v 1.0.12) [45] and EnhancedVolcano (v 1.8.0) [46]. Unpaired two-sided Wilcoxon was used for comparison of two groups. Correlation analysis was done with Spearman analysis and visualized with ggplot2 and corrplots. Differential abundance with bias correction between was calculated with the ANCOMBC package (100 max. iterations, 0.80 zero cut-off). In case of multiple comparisons *p* values were FDR-adjusted with the Holm method.



## Results

### **Culture-dependent and -independent methods can determine staphylococcal populations with overall high congruency**

Samples for cultivation, amplicon-based NGS analysis and skin parameter measurements (hydration and sebum content) were taken from 30 healthy volunteers across four different skin sites (back, cheek, forearm and forehead; n=120 samples) (Fig. 1a). 572 bacterial isolates were obtained via selective cultivation, of which 557 were identified as staphylococci via MALDI-TOF mass spectrometry (Fig. 1b, Additional File 1). Across all skin sites, the majority of isolates were identified as *S. epidermidis* (n=374, 67.2 %), followed by *Staphylococcus hominis* (n=86, 15.4 %). Forehead, cheek and back skin sites were dominated by strains of *S. epidermidis*, followed by *Staphylococcus capitis* (relative abundance of 74.5% and 11.7 %, respectively), whereas on forearm skin sites, a larger number of strains of *S. hominis* and *Staphylococcus haemolyticus* (relative abundance of 38.7 % and 7.3%, respectively) were isolated (Fig. 1b).

Moisture content (skin hydration) was highest on back and forehead skin as compared to cheek and forearm skin (Fig. 1c). The latter sites exhibited the highest sebum content and numbers of staphylococci per cm<sup>2</sup> (colony forming units/CFU), whereas forearm skin sites were particularly low in sebum and numbers of staphylococci (Fig. 1c).

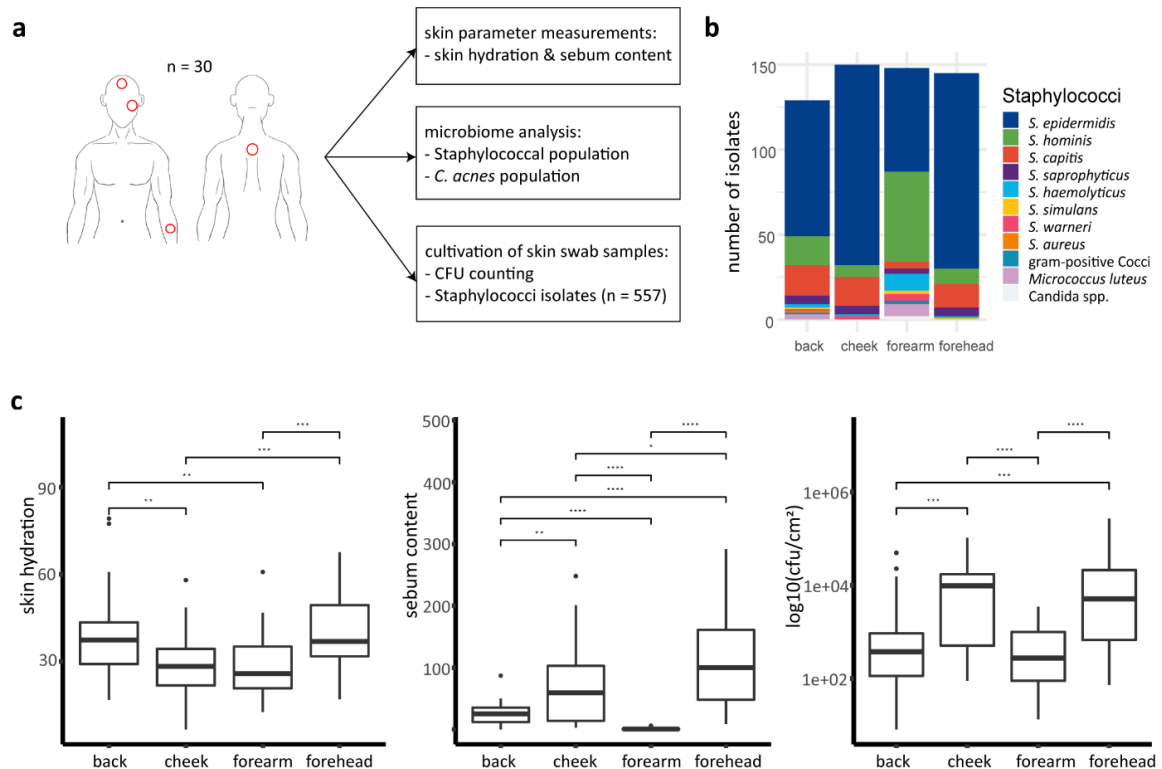


**Figure 1 Skin parameters and distribution of staphylococcal isolates on four different skin sites. a** Study design. **b** Number of isolates of identified staphylococcal species per skin site. **c** Skin hydration, sebum content and CFU per  $\text{cm}^2$  on back, cheek, forearm, and forehead skin (\* $p \leq 0.05$ , \*\* $p \leq 0.01$ , \*\*\* $p \leq 0.001$ , \*\*\*\* $p \leq 0.0001$ . Unpaired Wilcoxon test).

Next, we applied an NGS approach based on the amplification of a specific section of the *tuf* gene [27] to molecularly characterise the resident staphylococcal populations on back, cheek, forearm and forehead skin samples. In total, sixteen different staphylococcal species were identified (Fig. 2a). The majority of skin sites were populated by several different co-existing staphylococcal species (on average 3.1 species) while in nearly one in ten samples (9.7 %) only one staphylococcal species was identified. Across all skin sites tested, *S. epidermidis* was the most abundant species detected (average relative abundance 41.1 %), followed by *S. capitis* (24.7 %), *Staphylococcus saccharolyticus* (10.2 %) and *S. hominis* (9.2 %) (Fig. 2a, 2b).

The relative abundance profiles gained using the NGS-based amplicon approach were found to be in broad agreement with culture-based profiling (*S. epidermidis*, *S. hominis* and *S. capitis* were cultivated most frequently from samples). An exception was *S. saccharolyticus*, which was only detected using the amplicon-based NGS

approach; this is likely due to the fastidious growth requirements of *S. saccharolyticus* [27]. *S. aureus* was only detected in cheek skin samples (relative abundance of 2.5 %), possibly due to the proximity to the nasal cavity, the preferred niche of *S. aureus* [47] (Fig. 2a, 2b).

To test for differential abundance, we performed an Analysis of Compositions of Microbiomes with Bias Correction (ANCOM-BC) between all the four skin sites. The results showed that *S. hominis* was significantly more abundant in forearm skin samples compared to the other skin sites (Additional File 3). Alpha diversity of staphylococcal populations was measured with the Shannon index and compared between the four skin sites. The highest staphylococcal diversity was observed in forearm skin samples, followed by back and cheek skin samples (Fig. 2c). Spearman correlation revealed a significant negative correlation of CFU count and staphylococcal alpha diversity (Fig. 2d). Spearman correlation analysis between staphylococcal species abundance and skin parameters showed that the abundance of *S. hominis* correlated with staphylococcal alpha diversity, and inversely correlated with CFU count and sebum content (Fig. 2e). The correlation analysis was performed for each skin site separately; on back, cheek and forehead skin the positive correlation between *S. hominis* and staphylococcal alpha diversity was observed (Additional File 4).

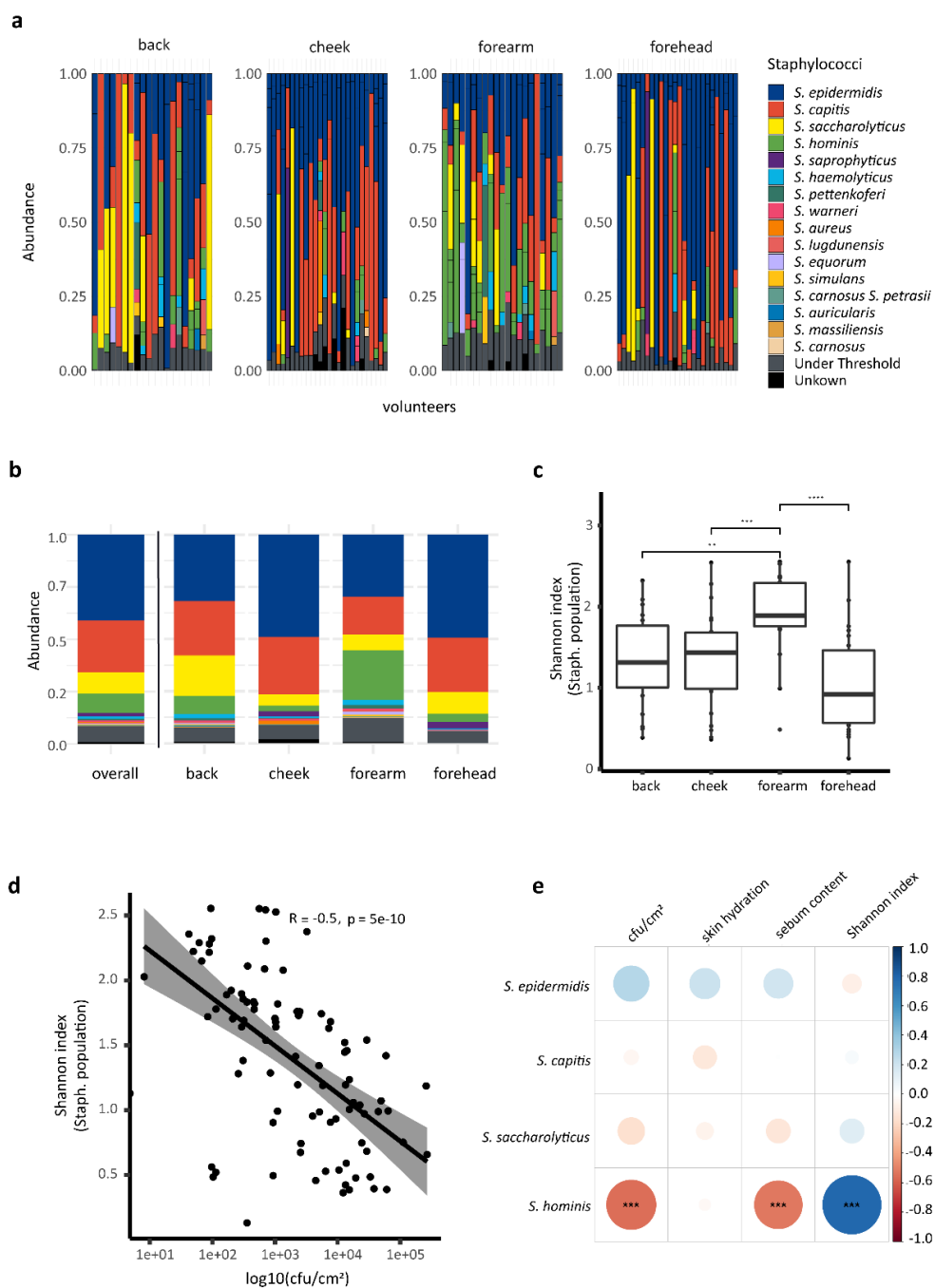


**Figure 2 Staphylococcal populations in 120 skin samples determined by amplicon-based NGS and correlation to skin parameters. a** Relative abundance of staphylococcal species on back, cheek, forearm and forehead skin of 30 volunteers. **b** Stacked bar plot showing mean values of relative abundances of staphylococcal species overall and for the four skin sites. **c** Shannon diversity index of staphylococcal population per skin site (\*\* $p \leq 0.01$ , \*\*\* $p \leq 0.001$ , \*\*\*\* $p \leq 0.0001$ ). Unpaired Wilcoxon test showed highest diversity in forearm skin samples. **d** Spearman correlation between Shannon index of staphylococcal populations and CFU per cm<sup>2</sup>. **e** Spearman correlation between staphylococcal species abundance and skin parameter (FDR-adjusted p-value, \*\*\* $p \leq 0.001$ ).

---

***S. epidermidis* strains from healthy human skin are highly diverse and belong to non-nosocomial-associated phylogenetic lineages**

Given the abundance of *S. epidermidis* across all skin sites, we wanted to further delineate the population structure of the cultured isolates derived from healthy skin. 69 isolates were genome-sequenced and phylogenetically compared to 286 previously published *S. epidermidis* genomes (Fig. 3a). The sequenced *S. epidermidis* strains were highly diverse with distinct strain individuality, as judged by analysis of the pan-genome (Additional File 5). We also found that the accessory genome of *S. epidermidis* is substantially larger than that of *C. acnes* (Additional File 6).

To further delineate the *S. epidermidis* strain diversity, the genomes were assigned to the three clades [11-13], with 42 strains clustering to clade A, four to clade B and 23 to clade C (Fig. 3a). Only four isolates clustered within clade B, a clade that is thought to exhibit reduced pathogenic potential as compared to clades A and C [12]. Interestingly, a high number of isolates were assigned to clade C, which has not previously been associated with staphylococcal isolates from healthy skin. Notably, none of the *S. epidermidis* strains isolated here belonged to known infection-associated STs, namely the described types ST2, ST5 and ST23 [14]. To further ascertain strain-specific traits, we checked for the presence of *mecA*, *icaA* and IS256, genes known to be more prevalent in infection-associated *S. epidermidis* compared to commensal isolates [11, 48]. Out of the 69 *S. epidermidis* genomes sequenced, the *mecA* gene was identified in four and *icaA* in 18. Only one strain was found to have both *mecA* and *icaA*, and IS256 was not identified in any of the genomes analysed (Fig. 3b).

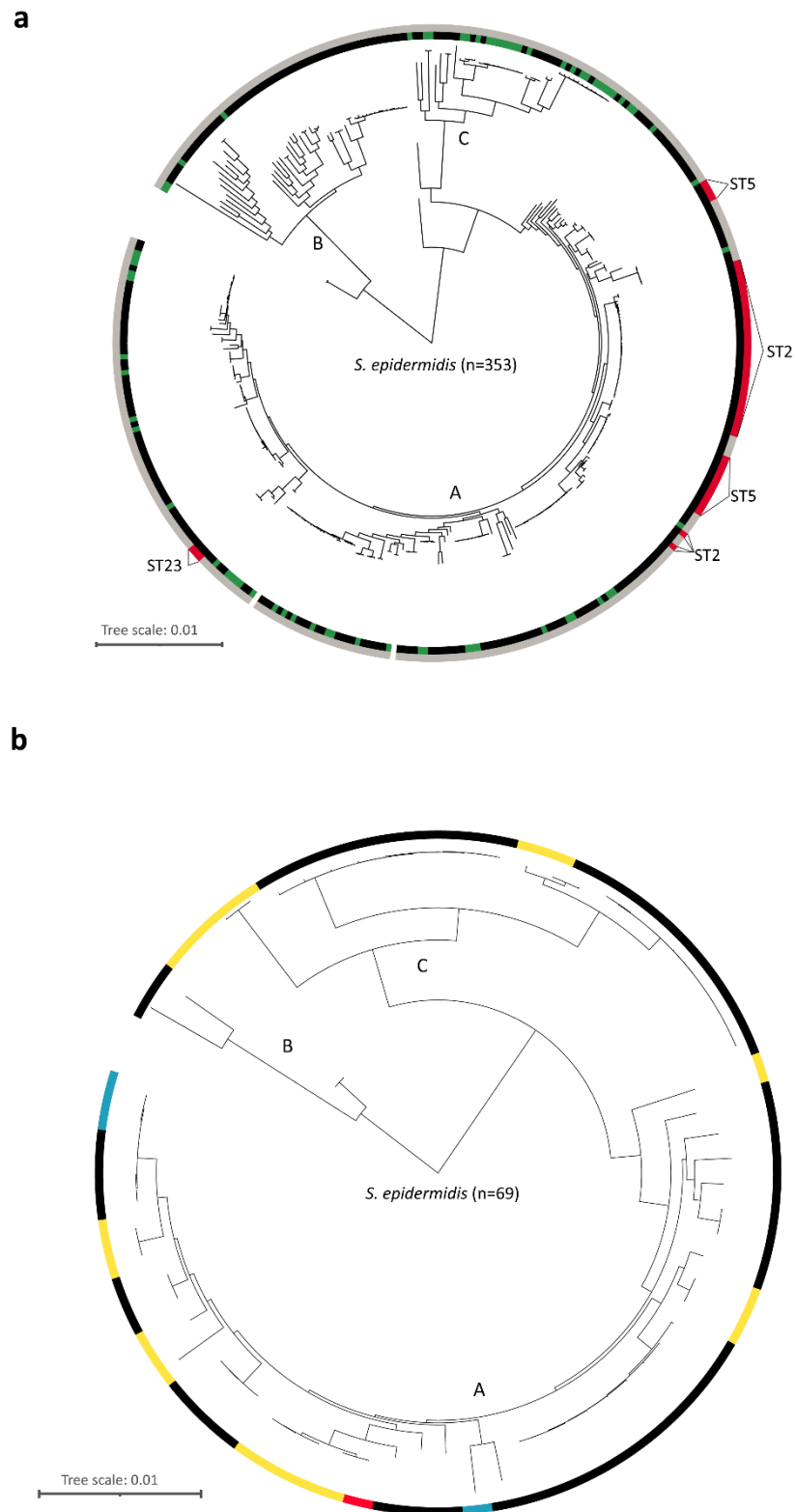


**Figure 3** Phylogeny of *S. epidermidis* strains obtained in this study. Phylogenetic trees are based on single nucleotide variants (SNVs) of the core genomes. **a** 286 *S. epidermidis* strains (genomes taken from RefSeq) (=black) and 69 strains isolated in this study (=green). Nosocomial sequence types (ST2, ST5, ST23) (=red) and non-nosocomial sequence types (=grey) are depicted. **b** 69 *S. epidermidis* strains isolated in this study. Highlighted are strains with *mecA* gene (=blue), *icaA* gene (=yellow) and one strain with *mecA+icaA* gene (=red).

## **Application of an amplicon-based NGS method enables profiling of resident *C. acnes* populations at phylotype resolution**

To gain deeper insight into the landscape of *C. acnes* populations resident on healthy human skin, we next applied a previously developed SLST amplicon-based NGS scheme to the 120 samples [17]. In total, 39 different *C. acnes* SLST types were identified. All of the ten *C. acnes* SLST classes (A to L) were found across the different samples from cheek and forearm skin, whereas the B- and G-class *C. acnes* were absent from forehead and back skin, respectively. On average, 3.6 different *C. acnes* SLST classes were found resident at each skin site.

Across all skin sites, *C. acnes* strains belonging to the IA<sub>1</sub> phylotype were most frequently detected (average 58.1 %) (Fig. 4a). Among the IA<sub>1</sub> phylotype, SLST class A was the most abundant (27.6 %), followed by SLST classes D (20.7 %) and C (5.9 %). The second most abundant *C. acnes* phylotype was II (corresponding to SLST class K) (19.2 %), followed by IB (corresponding to SLST class H) (12.2 %) (Fig. 4a, 4b).

A-class *C. acnes* had a similar average relative abundance across all four skin sites (24.7 % to 30.0 %). A-class *C. acnes* were most abundant on cheek, forearm and forehead skin, whereas on back skin D-class *C. acnes* were dominant (37.3 %) (Fig. 4b). An ANCOM-BC analysis confirmed this observation and showed a significant higher abundance of D-class *C. acnes* in back samples compared to forearm and forehead samples (Additional File 7). As expected, cheek and forehead skin had a more similar *C. acnes* SLST class composition, compared to back and forearm skin (Fig. 4b). L-class *C. acnes* were more abundant on the forearm skin (average of 5.0 %) compared to the other three skin sites (< 0.7 %).

Similar to the observation regarding staphylococcal populations (Fig. 2c), the alpha diversity of *C. acnes* populations from forearm skin samples was higher compared to the other three skin sites (Fig. 4c). Regarding the influence of skin parameters on *C. acnes* populations, it was found that the alpha diversity positively correlated with the abundance of K-class *C. acnes* (Fig. 4d).

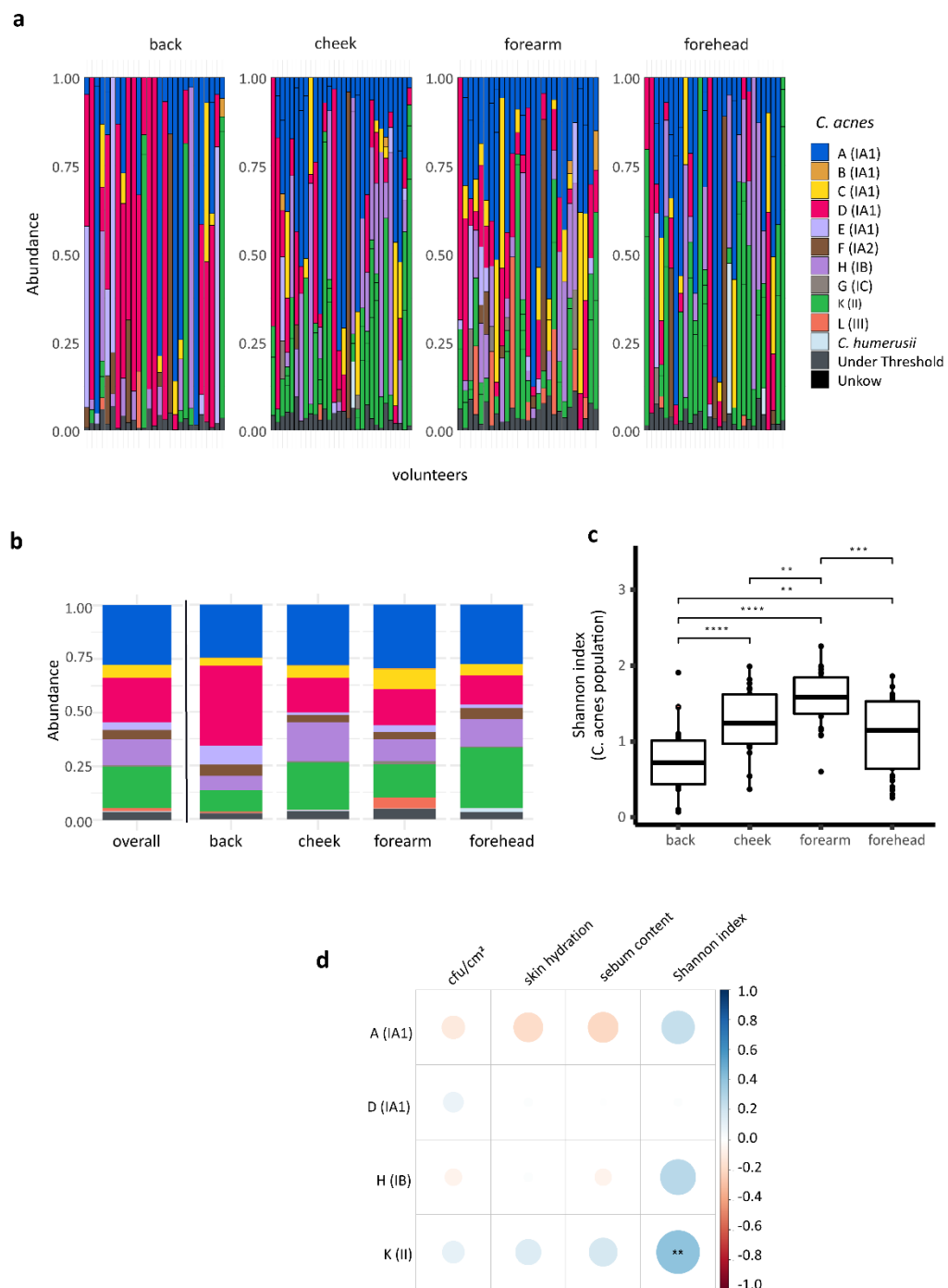


**Figure 4** *C. acnes* populations in 120 skin samples determined by amplicon-based NGS and correlation to skin parameters. **a** Relative abundances of *C. acnes* SLST classes of back, cheek, forearm and forehead skin of 30 volunteers. **b** Stacked bar plot showing mean values of relative abundances of *C. acnes* SLST classes overall and for the four skin sites (for color code see a). **c** Shannon diversity index of *C. acnes* populations per skin site (\*\* $p \leq 0.01$ , \*\*\* $p \leq 0.001$ , \*\*\*\* $p \leq 0.0001$ . Unpaired Wilcoxon test). **d** Spearman correlation between relative abundances of *C. acnes* SLST classes and skin parameters (FDR-adjusted p-value, \* $p \leq 0.05$ ).



## **Staphylococcal isolates exhibit antimicrobial activity against acne- but not healthy skin- associated *C. acnes* phylotypes**

Correlation of the relative abundances of the four most abundant staphylococcal species and *C. acnes* SLST classes revealed a significant positive correlation between *S. epidermidis* and K-class *C. acnes*, as well as an inverse correlation between *S. epidermidis* and A-class *C. acnes*, albeit statistically non-significant (Fig. 5a). We therefore wanted to further understand the potential for microbial interference between staphylococcal and *C. acnes* populations.

First, we conducted in vitro antagonistic assays to ascertain the antimicrobial activity of our isolated CoNS strains. All 572 isolates were screened against a *S. aureus* strain, an A-class and a D-class *C. acnes* strain to identify staphylococcal isolates with bioactivity (Additional File 8). The 30 strains identified with activity against the *C. acnes* strain were then further screened against eleven different *C. acnes* strains covering six different SLST classes (A, C, D, H, K, L) (Table 1), including both acne- and healthy skin-associated types, in order to identify any phylotype-specific bioactivity. In total, 4 % (22/557) of the tested staphylococcal isolates exhibited activity against *S. aureus* and 5 % (30/557) of them against one or more *C. acnes* strains. Of these 30 staphylococcal isolates, 17 were identified as *S. capitis*, six as *S. hominis*, five as *S. epidermidis* and two as *S. warneri*. Strains belonging to different *C. acnes* phylogenetic clades showed a remarkably different susceptibility to the antimicrobial activity of the various staphylococcal isolates. The two A-class *C. acnes* strains, DSM1897 and 12.1.L1, were most susceptible to this bioactivity, being inhibited by the antimicrobial activity and were inhibited by a total of 29 and 15 staphylococcal strains, respectively. In contrast, only one staphylococcal strain (*S. epidermidis* HAC26) was found to exhibit inhibitory bioactivity against D-class and H-class *C. acnes* strains (Table 1).

**Table 1** Antimicrobial activity of staphylococci against *C. acnes* strains from six different SLST classes and *S. aureus* DSM799.

Indicator strains	<i>C. acnes</i> class*						<i>S. aureus</i> DSM799
	A	C	D	H	K	L	
CoNS strain							
<i>S. capitis</i> HAB177	+ +	- - -	- - -	- - -	- - -	- - -	-
<i>S. capitis</i> HAB198	+ +	- - -	- - -	- - -	- - -	- - -	-
<i>S. capitis</i> HAB200	+ +	- - -	- - -	- - -	- - -	- - -	-
<i>S. capitis</i> HAB276	+ +	- - -	- - -	- - -	- - -	- - -	-
<i>S. capitis</i> HAB277	+ +	- - -	- - -	- - -	- - -	- - -	-
<i>S. capitis</i> HAB278	+ +	- - -	- - -	- - -	- - -	- - -	-
<i>S. capitis</i> HAB280	+ +	- - -	- - -	- - -	- - -	- - -	-
<i>S. capitis</i> HAB56	+ +	- - -	- - -	- - -	- - -	- - -	-
<i>S. capitis</i> HAC349	+ -	- - -	- - -	- - -	- - -	- - -	+
<i>S. capitis</i> HAC470	+ -	- - -	- - -	- - -	- - -	- - -	-
<i>S. capitis</i> HAC49	+ +	- - -	- - -	- - -	- - -	- - -	-
<i>S. capitis</i> HAC507	+ -	- - -	- - -	- - -	- - -	- - -	-
<i>S. capitis</i> HAC508	+ -	- - -	- - -	- - -	- - -	- - -	-
<i>S. capitis</i> HAC509	+ -	- - -	- - -	- - -	- - -	- - -	-
<i>S. capitis</i> HAC510	+ -	- - -	- - -	- - -	- - -	- - -	-
<i>S. capitis</i> HAF401	+ -	- - -	- - -	- - -	- - -	- - -	+
<i>S. capitis</i> HAF403	+ -	- - -	- - -	- - -	- - -	- - -	+
<i>S. epidermidis</i> HAC26	+ +	+ + +	- + -	- + -	- + -	- + -	+
<i>S. epidermidis</i> HAC588	+ -	- - -	- - -	- - -	- - -	+ - -	+
<i>S. epidermidis</i> HAC590	+ -	- - -	- - -	- - -	- - -	+ - -	+
<i>S. epidermidis</i> HAF242	+ -	- - -	- - -	- - -	- - -	+ - -	+
<i>S. epidermidis</i> HAF424	+ -	- - -	- - -	- - -	- - -	+ - -	+
<i>S. hominis</i> HAA254	+ -	- - -	- - -	- - -	- - -	+ + -	-
<i>S. hominis</i> HAA272	+ +	+ - -	- - -	- - -	- - -	+ + +	-
<i>S. hominis</i> HAA273	+ +	+ - -	- - -	- - -	- - -	+ + +	-
<i>S. hominis</i> HAA274	+ +	+ - -	- - -	- - -	- - -	+ + +	-
<i>S. hominis</i> HAB257	+ -	- - -	- - -	- - -	- - -	+ + -	-
<i>S. hominis</i> HAC286	- -	- - -	- - -	- - -	- - -	- - +	+
<i>S. warneri</i> HAA333	+ +	+ - -	- - -	- - -	- - -	+ + +	+
<i>S. warneri</i> HAA334	+ +	+ - -	- - -	- - -	- - -	+ + +	+

\*the following *C. acnes* strains were used: A class, DSM1897 and 12.1.L1; C class, 15.1.R1; D class, 30.2.L1 and 09-193; H class, 11-90, KPA171202 and 21.1.L1; K class, 11-49 and 11-79; L class, PMH5.

To provide insight into the in vivo relevance of these observations, we compared the relative abundance profiles of *C. acnes* populations originating from skin samples with and without the presence of antimicrobial active staphylococcal strains. Notably, the relative abundance of A-class *C. acnes* was significantly lower in skin sites that contained a staphylococcal strain exhibiting antimicrobial activity (Fig. 5b and c, Table 1). This inverse correlation of abundance was most pronounced in back skin samples; in samples containing antimicrobial-active staphylococci, there was a

marked increase in the relative abundance of D-class *C. acnes* and a corresponding decrease in A-class *C. acnes* respectively ( $p=0.004$  and  $p=0.0013$ , respectively) (Additional File 9).

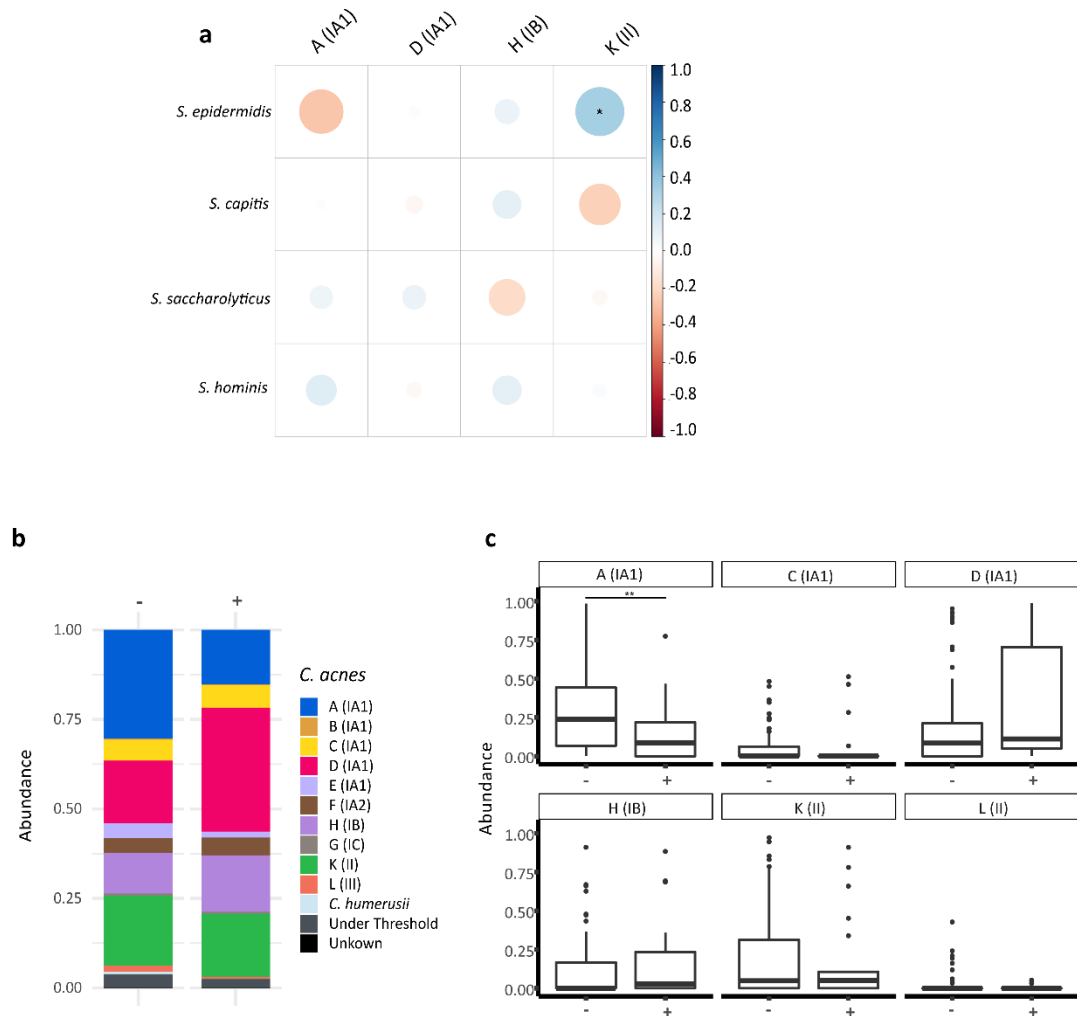


**Figure 5 Staphylococci and *C. acnes* co-existence and inhibition profiles.** **a** A Spearman correlation between four most abundant Staphylococcus species and *C. acnes* SLST classes found on the skin was performed (FDR-adjusted p-value;  $*p \leq 0.05$ ), revealing a correlation between *S. epidermidis* and K-class *C. acnes* and an inverse correlation between *S. epidermidis* and A-class *C. acnes*. **b** The mean relative abundances of *C. acnes* SLST classes on skin sites with (+) and without (-) antimicrobially active staphylococcal strains are depicted. The presence of staphylococcal strains with antimicrobial activity led to a decrease of the relative abundance of A-class *C. acnes*. **c** Boxplots of relative abundances of the six *C. acnes* SLST classes on skin sites with (+) and without (-) antimicrobially active staphylococcal strains are shown (FDR-adjusted p-value,  $**p \leq 0.01$ . Unpaired Wilcoxon test).

## Selective deregulation of the antimicrobial activity of *S. epidermidis* in response to sensitive and tolerant *C. acnes* strains

In an initial effort to gain insight into the mechanisms underlying the selective bioactivity of CoNS strains in response to different *C. acnes* strains (Fig. 5), we undertook genome-wide transcriptional analyses in co-culture experiments.

As a model organism, we chose *S. epidermidis* HAF242, as it was shown to exhibit antimicrobial activity against the A-class *C. acnes* strain DSM1897, but no lethal effects on the D-class *C. acnes* strain 30.2.L1 (Table 1). Genome sequencing of *S. epidermidis* HAF242 revealed the presence of the epidermin biosynthesis cluster (locus tag: LZT96\_12010), which has previously been described as an important antimicrobial determinant [49]. For co-culture experiments, *S. epidermidis* HAF242 was inoculated on a lawn of *C. acnes* DSM1897 and 30.2.L1, respectively. As expected, colonies of *S. epidermidis* HAF242 showed clear inhibition zones on the lawn of *C. acnes* DSM1897, but not on the lawn of *C. acnes* 30.2.L1 (Fig. 6a). Attempts to reproduce this observation in liquid culture failed, indicating that solid surface growth and/or direct contact is a requirement for antimicrobial activity. Plate-grown co-cultures were harvested, subjected to RNA-sequencing and transcriptome analysis was carried out to determine any differential expression of *S. epidermidis* HAF242 genes in the two different co-cultures, representing sensitive and tolerant scenarios, respectively (*S. epidermidis* HAF242/*C. acnes* 30.2.L1 versus *S. epidermidis* HAF242/*C. acnes* DSM1897). Comparison of the transcriptome profiles from the co-culture experiments, revealed 33 significantly differentially expressed *S. epidermidis* genes: six genes were down-regulated, while 27 genes were up-regulated (Fig. 6b, Additional File 10). Notably, when in co-culture with *C. acnes* 30.2.L1, *S. epidermidis* HAF242 exhibited a three-fold downregulation of the quorum-sensing auto-inducing peptide gene (*agrD*) (in comparison to co-culture with *C. acnes* DSM1897). Furthermore, three phenol-soluble modulins (PSM) beta genes (*psm* $\beta$ 1, *psm* $\beta$ 2, *psm* $\beta$ 3) and the precursor peptide gene for epidermin (*epiA*) were also significantly downregulated (Fig. 6b, Additional File 10). To determine whether the differential gene expression profiles observed were due to up-regulation in response to *C. acnes* DSM1897 (sensitive strain) or down-regulation in

response to *C. acnes* 30.2.L1 (tolerant strain), we conducted a comparative transcriptome analysis of *S. epidermidis* in monoculture (hereafter labelled as “control”) (Additional File 11 and 12). The resulting analysis revealed that the three *psm* genes were downregulated 3- to 11-fold in *S. epidermidis* grown in co-culture with *C. acnes* 30.2.L1 (tolerant strain) when compared to the control (Fig. 6c) (Additional File 12). In addition, the *agrD* gene was mildly down-regulated (2-fold), albeit not statistically significant. This indicates that *C. acnes* 30.2.L1, in contrast to *C. acnes* DSM1897, exerts an inhibitory effect on the antimicrobial activity of *S. epidermidis* HAF242 by down-regulating the expression of genes involved in anti-*C. acnes* activity.

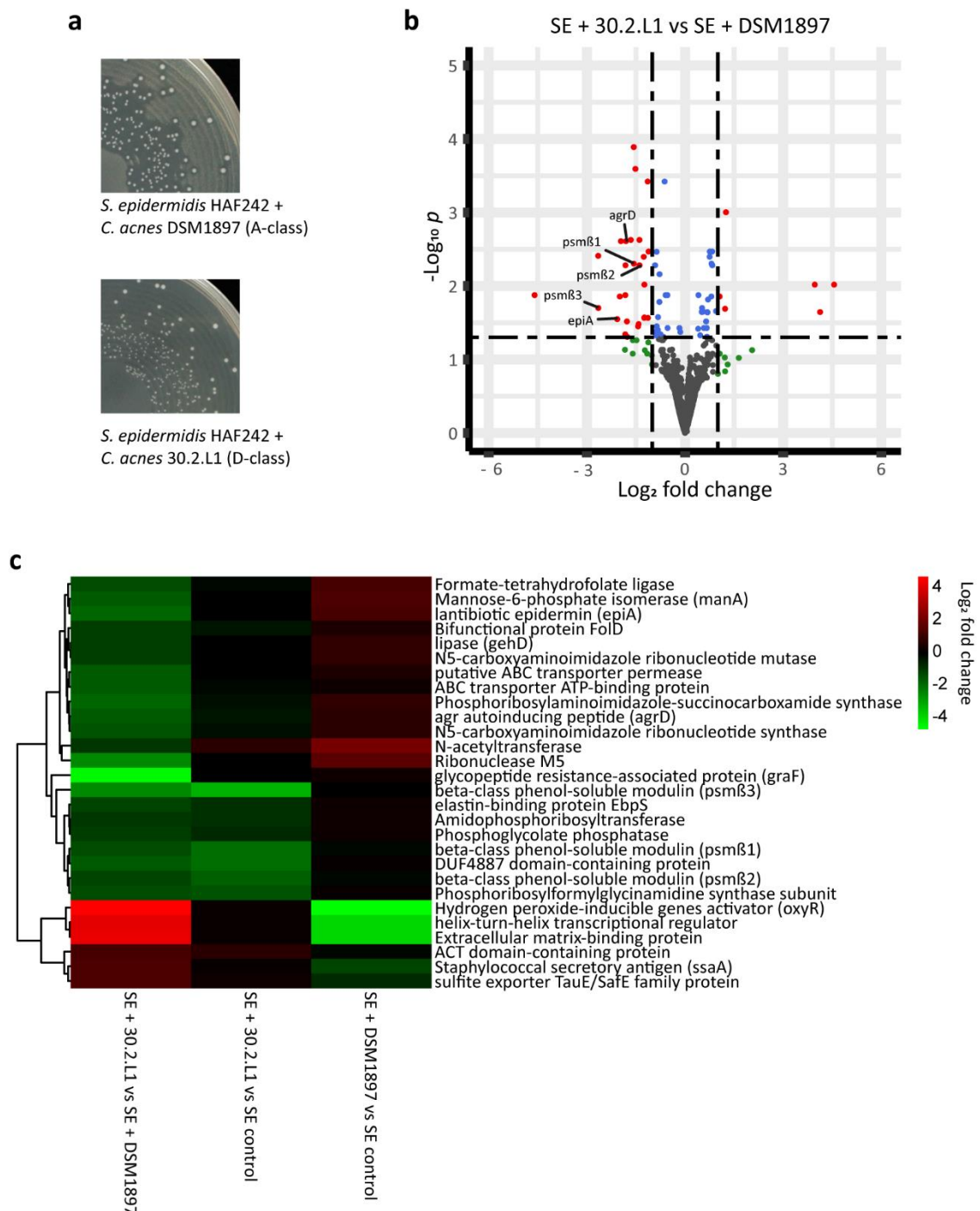


**Figure 6** Differential expression of quorum-sensing regulated genes in *S. epidermidis* HAF242 co-cultured with *C. acnes* 30.2.L1 (D-class) and *C. acnes* DSM1897 (A-class). **a** Colonies of *S. epidermidis* HAF242 exhibit inhibition zones on a lawn of *C. acnes* DSM1897 (A-class) but not on a lawn of *C. acnes* 30.2.L1 (D-class). **b** Differential gene expression of *S. epidermidis* HAF242 (SE) grown in the two co-cultures (co-culture with *C. acnes* 30.2.L1 (D-class) versus co-culture with *C. acnes* DSM1897 (A-class)) (FDR-adjusted p-value, cut off:  $p \leq 0.05$  and fold-change  $>2$  or  $<-2$ ). **c** Heat map of all differentially expressed genes in *S. epidermidis* HAF242 when grown in the two co-cultures (first column; genes encoding hypothetical proteins were excluded). Gene expression was also compared between *S. epidermidis* grown in co-culture (second and third columns) versus *S. epidermidis* grown in monoculture (“SE control”).

## Discussion

Here we highlight the importance of skin-resident staphylococci and the potential role of selective microbial interference for healthy skin homeostasis. Our analysis, encompassing both culture-dependent and -independent methodologies, reveals diverse populations of staphylococci resident on healthy skin with selective microbial interference activity. The tandem application of the amplicon-based NGS methods used within this study enabled a detailed delineation of the diversity of both staphylococci and *C. acnes* populations resident across multiple skin sites to provide species- and phylotype-level resolution, respectively. The resident staphylococci were found to exhibit phylotype-specific antimicrobial activity against acne-associated *C. acnes*, while co-existing with *C. acnes* phlotypes that are more commonly associated with healthy skin.

In agreement with previous studies [2, 3, 50], *S. epidermidis* was found to be the most abundant staphylococcal species detected across all skin sites tested, followed by *S. capitis* and *S. saccharolyticus*. *S. epidermidis* is known both as a skin commensal and an opportunistic pathogen, the latter especially in infections of indwelling devices [51]. Delineation of the *S. epidermidis* strains into clades and STs within the current study revealed that clonal lineages often associated with an elevated pathogenic potential were rarely found on healthy skin: None of the 69 *S. epidermidis* isolates from healthy skin belonged to the three prominent infection-associated sequence types ST2, ST5 and ST23 [14] (clade A). However, only four of the 69 *S. epidermidis* skin isolates were classified here as belonging to the B-clade, which is thought to consist mainly of commensal skin isolates [11, 12]. In addition, many strains were classified as belonging to the C-clade, for which very little knowledge is currently available [12]. The classification of the isolated strains across the range of different clades indicates that the current assignment provides limited information in terms of a strain's particular health-beneficial or -detrimental properties. This assumption supports previous studies that have highlighted the difficulty of using core genome-derived phylogeny to differentiate pathogenic and commensal *S. epidermidis* strains [11, 48], due to the fact that pathogenic traits can be acquired through horizontal gene transfer [13]. Sequences associated with

pathogenicity such as the methicillin-resistance gene *mecA*, the biofilm operon *icaADBC* and the insertion sequence element IS256 are part of the accessory genome, and can thus be present in phylogenetically distinct strains [11, 48]. Of the 69 *S. epidermidis* strains sequenced here, only 5.8 % were positive for *mecA*, 26.1 % for *icaADBC* and none for IS256, aligning with previous studies of commensal *S. epidermidis* (*icaA*: 13.3 % and 33.8 %; IS256: 0 % and 4.2 %; *mecA*: 6.7 % and 15.5 %) [11, 48].

In contrast to *S. epidermidis*, with its open pan-genome and variable genome content, *C. acnes* is more conserved with a relatively limited accessory genome [5] (Additional Files 5 and 6). Core genome-based phylogeny divides *C. acnes* populations into six main phylotypes. In total, 178 different SLST types (medbac.dk/slst/pacnes; status: 15th of January 2022) belonging to ten SLST classes (A-L) have been reported [17]. Here, we identified 39 distinct SLST types that covered all ten SLST classes, within the 120 healthy skin samples profiled. Overall, highest relative abundances were determined for A-class *C. acnes* (27.6 %), followed by D-class (20.7%), K-class (19.2%) and H-class (12.2%) *C. acnes*. All other SLST classes had lower average abundances, ranging between 5.9% and 0.2%.

As yet, the SLST amplicon-based NGS method has not been used for samples from diseased skin, such as acne vulgaris-affected skin. Thus, a direct comparison of our data with samples from diseased skin is not possible at present. However, the SLST scheme has been used in culture-dependent studies, albeit with low patient numbers, highlighting that A- and F-class *C. acnes* strains are primarily associated with acne vulgaris [18, 22]. In addition, previous studies using other schemes for determining the phylogenetic basis of *C. acnes* isolates, such as MLST, have found similar results [15, 21, 52]. These studies have also revealed that healthy skin-associated strains often belong to the SLST classes H and K. In our study, H- and K-class *C. acnes* were also found at high relative abundances. However, the delineation of acne- and healthy skin-associated SLST classes might be oversimplified, as it seems likely that a high diversity of strains belonging to different SLST classes forms the basis of a healthy skin microbiome and thus, the loss of diversity is associated with acne [53]. We also noted a high relative abundance of D-class *C. acnes*,



especially on back skin samples. There is currently very limited information available on this SLST class. Given the dominance of this lineage on back skin sites of multiple healthy individuals, we propose that it could also be health-associated.

The in vitro antagonistic assays conducted here enabled us to identify a range of CoNS strains with antimicrobial activity against A-class *C. acnes*, a class that is overrepresented in acne-affected skin [18-21]. This observation of phylotype-specific activity against disease-associated *C. acnes* strains is in contrast to previous work [24, 25]. Our data indicates that active staphylococcal strains have the potential to modify the composition of resident *C. acnes* populations on skin. Importantly, we noted an inverse relationship between the abundance of staphylococcal strains exhibiting antimicrobial activity and specific phlotypes of *C. acnes*. Skin sites with resident antimicrobial-active staphylococci had a significantly lower abundance of A-class *C. acnes* in comparison to those lacking these active CoNS strains. These observations align with previous work that reported a decreased abundance of staphylococcal strains with antimicrobial activity on atopic dermatitis affected skin compared to healthy controls [54]. Moreover, a low abundance of competitive staphylococcal strains was found to correlate with *S. aureus* colonization [54], a species that is often found on atopic dermatitis lesions [55] and is associated with disease severity [56].

To gain insight into the mechanisms underlying the phylotype-specific microbial interference observed, we conducted co-culture experiments using the antimicrobial-active *S. epidermidis* strain HAF242, and a tolerant D-class strain (30.2.L1) or a sensitive A-class *C. acnes* strain (DSM1897) and analysed the resulting transcriptome profiles. Here, we observed differential expression of genes encoding the lantibiotic epidermin precursor peptide EpiA and the phenol soluble modulins PSM $\beta$ . The activity of epidermin against *C. acnes* has been previously reported [57], but the role of PSM $\beta$  is still not understood. Interestingly, a *S. capitis* strain was recently identified that secretes four PSMs, which act synergistically as antimicrobials against *C. acnes* [24], opening up the possibility that PSM $\beta$ s might contribute together with epidermin to the antimicrobial activity of *S. epidermidis* HAF242.

The transcriptome analyses also highlighted a potential role for *agrD*, which is part of the *agr* quorum sensing (QS) system that encodes an autoinducing peptide (AIP) belonging to type I AIPs. It is detected by the histidine kinase AgrC, which in turn activates the response regulator AgrA. AgrA directly binds to the promoter region of target genes such as the *psm* locus and activates their expression [58, 59]. In our experiments, co-culture with the D-class *C. acnes* strain led to down-regulation of the expression of *agrD*, *epiA* and *psmβ* in *S. epidermidis*. Thus, we hypothesize that D-class *C. acnes* can interfere with the QS system of *S. epidermidis* and suppresses the production and activity of antimicrobial peptides. This interference with the *agr* QS system has been observed previously: inter- and intraspecies interference of staphylococci through their *agr* quorum sensing system (“quorum quenching”) can alter the expression of various target genes related to virulence and biofilm formation [6, 60-62]. While these interactions occur mainly between staphylococcal species [6, 60-62], one study found that *Candida albicans* can interfere with the alpha toxin production of *S. aureus* via the *agr* system [63]. It needs to be proven in future studies if *C. acnes*, in a phylotype-specific manner, can interfere with the *agr* QS system of staphylococci. This interference might not only have a benefit for *C. acnes*, i.e. guaranteeing its survival, but also for the staphylococcal strain exhibiting antimicrobial activity. It was shown that the production of antimicrobial peptides negatively affects the growth rate of the producing *S. epidermidis* strain [64]. Therefore, the suppression of antimicrobial peptide production could also be beneficial for the staphylococcal strain.

The insights gained within this study are of course framed within the confines of relatively small sample size (30 individuals) and the semi-quantitative nature of the data generated by the amplicon-based NGS methods applied here (relative abundance). We also use two distinct NGS methods for profiling the CoNS and *C. acnes* populations, with differing analytical scope: The SLST scheme used for *C. acnes* populations provides phylotype resolution, whereas the *tuf2* scheme used to dissect CoNS populations offers species level identification. Further work is required to dissect the CoNS population with strain level resolution.

## Conclusions

Overall, however, our results provide further insight into the importance of commensal staphylococci on healthy human skin and their crucial role for *C. acnes* population homeostasis. The knowledge and insights gained regarding the potential of CoNS strains to exclude and co-exist with disease- and healthy skin-associated *C. acnes* phylotypes has potential relevance for skin health maintenance and customized bacteriotherapy; for instance, applied to skin disorders that are associated with dysbiosis of *C. acnes* populations such as acne vulgaris.

## List of Abbreviations

AIP: Autoinducing peptide

ANCOM-BC: Analysis of Compositions of Microbiomes with Bias Correction

CFU: Colony forming units

IMDEC: International Medical & Dental Ethics Commission GmbH

NGS: Next-generation sequencing

QS: Quorum sensing

RIN: RNA integrity number

SLST: Single locus sequence typing

SNV: Single nucleotide variant

ST: Sequence types

TSA: Tryptic soy agar

## Additional Files

Additional Files of this manuscript are in the appendix of this thesis.

## Declarations

### Ethics approval and consent to participate

The study was approved by International Medical & Dental Ethics Commission GmbH (IMDEC), Freiburg, Germany (Study no. 67885). Written informed consent was obtained from all volunteers.

### Consent for publication

Not applicable.

### Availability of data and material

Whole genome sequence data (69 *S. epidermidis* genomes) generated for this study is deposited in GenBank with the bioproject number PRJNA793831 and can be accessed here: <https://www.ncbi.nlm.nih.gov/bioproject/PRJNA793831>. The closed whole genome sequence of *S. epidermidis* HAF242 is deposited in GenBank with the accession numbers CP090941 (chromosome) and CP090942-CP090944 (plasmids). The amplicon-based NGS data is stored at SRA with the bioproject number PRJNA795320 and can be accessed here: <https://www.ncbi.nlm.nih.gov/bioproject/PRJNA795320>.

(temporary reviewer link:

<https://dataview.ncbi.nlm.nih.gov/object/PRJNA795320?reviewer=m9f5c5gqrt4te0stufpod4kflo>)

The transcriptome sequencing data (*S. epidermidis* HAF242 in mono- and co-cultures) is stored at SRA with the bioproject number PRJNA801462 and can be accessed here:

<https://www.ncbi.nlm.nih.gov/bioproject/PRJNA801462>.

(temporary reviewer link:

<https://dataview.ncbi.nlm.nih.gov/object/PRJNA801462?reviewer=u2unj2ut1ca3btelpiin679md>)

## Competing interests

CMA, HW, JHR and JH are employees at Beiersdorf AG. The other authors declare no conflict of interest.

## Funding

This work was supported by grants from the NovoNordisk Foundation (grant no. NNF18OC0053172) to HB and the Leo Foundation (LF-OC-21-000826) to HB.

## Authors' contributions

CMA, WRS, HW, JHR, JH and HB contributed to the conception and design of the study. CMA performed wet lab benchwork and analyzed data. AP, MB and CF contributed to sequence data generation and CMA, KSJ, AP and HB analysed sequence data. CMA and HB wrote the manuscript and all authors contributed to manuscript revision and read and approved the submitted version.

## Acknowledgments

We thank Lise Hald Schultz for excellent technical assistance, and Lesley Ann Ogilvie for carefully reading the manuscript. Data processing was performed on the GenomeDK cluster; we would like to thank GenomeDK and Aarhus University for providing computational resources.

## Corresponding authors

Correspondence to Charlotte Marie Ahle and Holger Brüggemann.

## References

1. Grice EA, Segre JA: **The skin microbiome.** *Nat Rev Microbiol* 2011, **9**:244-253.
2. Kloos WE, Schleiferi KH: **Isolation and Characterization of Staphylococci from Human skin.** *International Journal of Systematic Bacteriology* 1975, **25**:62-79.
3. Kloos WE, Musselwhite MS: **Distribution and persistence of Staphylococcus and Micrococcus species and other aerobic bacteria on human skin.** *Appl Microbiol* 1975, **30**:381-385.
4. Oh J, Byrd AL, Deming C, Conlan S, Program NCS, Kong HH, Segre JA: **Biogeography and individuality shape function in the human skin metagenome.** *Nature* 2014, **514**:59-64.

5. Oh J, Byrd AL, Park M, Program NCS, Kong HH, Segre JA: **Temporal Stability of the Human Skin Microbiome.** *Cell* 2016, **165**:854-866.
6. Zhou W, Spoto M, Hardy R, Guan C, Fleming E, Larson PJ, Brown JS, Oh J: **Host-Specific Evolutionary and Transmission Dynamics Shape the Functional Diversification of Staphylococcus epidermidis in Human Skin.** *Cell* 2020, **180**:454-470 e418.
7. Bruggemann H, Salar-Vidal L, Gollnick HPM, Lood R: **A Janus-Faced Bacterium: Host-Beneficial and -Detrimental Roles of Cutibacterium acnes.** *Front Microbiol* 2021, **12**:673845.
8. Paetzold B, Willis JR, Pereira de Lima J, Knodlseder N, Bruggemann H, Quist SR, Gabaldon T, Guell M: **Skin microbiome modulation induced by probiotic solutions.** *Microbiome* 2019, **7**:95.
9. Stacy A, Belkaid Y: **Microbial guardians of skin health.** *Science* 2019, **363**:227-228.
10. Brown MM, Horswill AR: **Staphylococcus epidermidis-Skin friend or foe?** *PLoS Pathog* 2020, **16**:e1009026.
11. Conlan S, Mijares LA, Program NCS, Becker J, Blakesley RW, Bouffard GG, Brooks S, Coleman H, Gupta J, Gurson N, et al: **Staphylococcus epidermidis pan-genome sequence analysis reveals diversity of skin commensal and hospital infection-associated isolates.** *Genome Biol* 2012, **13**:R64.
12. Espadinha D, Sobral RG, Mendes CI, MERIC G, Sheppard SK, Carrico JA, de Lencastre H, Miragaia M: **Distinct Phenotypic and Genomic Signatures Underlie Contrasting Pathogenic Potential of Staphylococcus epidermidis Clonal Lineages.** *Front Microbiol* 2019, **10**:1971.
13. MERIC G, Miragaia M, de Been M, Yahara K, Pascoe B, Mageiros L, Mikhail J, Harris LG, Wilkinson TS, Rolo J, et al: **Ecological Overlap and Horizontal Gene Transfer in Staphylococcus aureus and Staphylococcus epidermidis.** *Genome Biol Evol* 2015, **7**:1313-1328.
14. Lee JYH, Monk IR, Goncalves da Silva A, Seemann T, Chua KYL, Kearns A, Hill R, Woodford N, Bartels MD, Strommenger B, et al: **Global spread of three multidrug-resistant lineages of Staphylococcus epidermidis.** *Nat Microbiol* 2018, **3**:1175-1185.
15. Lomholt HB, Kilian M: **Population genetic analysis of Propionibacterium acnes identifies a subpopulation and epidemic clones associated with acne.** *PLoS One* 2010, **5**:e12277.
16. McDowell A, Nagy I, Magyari M, Barnard E, Patrick S: **The opportunistic pathogen Propionibacterium acnes: insights into typing, human disease, clonal diversification and CAMP factor evolution.** *PLoS One* 2013, **8**:e70897.
17. Scholz CF, Jensen A, Lomholt HB, Bruggemann H, Kilian M: **A novel high-resolution single locus sequence typing scheme for mixed populations of Propionibacterium acnes in vivo.** *PLoS One* 2014, **9**:e104199.
18. Dagnelie MA, Corvec S, Saint-Jean M, Bourdes V, Nguyen JM, Khammari A, Dreno B: **Decrease in Diversity of Propionibacterium acnes Phylotypes in Patients with Severe Acne on the Back.** *Acta Derm Venereol* 2018, **98**:262-267.

19. Lomholt HB, Scholz CFP, Bruggemann H, Tettelin H, Kilian M: **A comparative study of Cutibacterium (Propionibacterium) acnes clones from acne patients and healthy controls.** *Anaerobe* 2017, **47**:57-63.
20. McDowell A, Barnard E, Nagy I, Gao A, Tomida S, Li H, Eady A, Cove J, Nord CE, Patrick S: **An expanded multilocus sequence typing scheme for propionibacterium acnes: investigation of 'pathogenic', 'commensal' and antibiotic resistant strains.** *PLoS One* 2012, **7**:e41480.
21. McDowell A, Gao A, Barnard E, Fink C, Murray PI, Dowson CG, Nagy I, Lambert PA, Patrick S: **A novel multilocus sequence typing scheme for the opportunistic pathogen Propionibacterium acnes and characterization of type I cell surface-associated antigens.** *Microbiology (Reading)* 2011, **157**:1990-2003.
22. Nakase K, Hayashi N, Akiyama Y, Aoki S, Noguchi N: **Antimicrobial susceptibility and phylogenetic analysis of Propionibacterium acnes isolated from acne patients in Japan between 2013 and 2015.** *J Dermatol* 2017, **44**:1248-1254.
23. Nakase K, Aoki S, Sei S, Fukumoto S, Horiuchi Y, Yasuda T, Tanioka M, Sugai J, Huh WW, Kakuta M, et al: **Characterization of acne patients carrying clindamycin-resistant Cutibacterium acnes: A Japanese multicenter study.** *J Dermatol* 2020, **47**:863-869.
24. O'Neill AM, Nakatsuji T, Hayachi A, Williams MR, Mills RH, Gonzalez DJ, Gallo RL: **Identification of a human skin commensal bacterium that selectively kills Cutibacterium acnes.** *J Invest Dermatol* 2020.
25. Christensen GJ, Scholz CF, Enghild J, Rohde H, Kilian M, Thurmer A, Brzuszkiewicz E, Lomholt HB, Bruggemann H: **Antagonism between Staphylococcus epidermidis and Propionibacterium acnes and its genomic basis.** *BMC Genomics* 2016, **17**:152.
26. Wang Y, Kuo S, Shu M, Yu J, Huang S, Dai A, Two A, Gallo RL, Huang CM: **Staphylococcus epidermidis in the human skin microbiome mediates fermentation to inhibit the growth of Propionibacterium acnes: implications of probiotics in acne vulgaris.** *Appl Microbiol Biotechnol* 2014, **98**:411-424.
27. Ahle CM, Stodkilde K, Afshar M, Poehlein A, Ogilvie LA, Soderquist B, Hupeden J, Bruggemann H: **Staphylococcus saccharolyticus: An Overlooked Human Skin Colonizer.** *Microorganisms* 2020, **8**.
28. Ahle CM, Stodkilde-Jorgensen K, Poehlein A, Streit WR, Hupeden J, Bruggemann H: **Comparison of three amplicon sequencing approaches to determine staphylococcal populations on human skin.** *BMC Microbiol* 2021, **21**:221.
29. Bolyen E, Rideout JR, Dillon MR, Bokulich NA, Abnet CC, Al-Ghalith GA, Alexander H, Alm EJ, Arumugam M, Asnicar F, et al: **Reproducible, interactive, scalable and extensible microbiome data science using QIIME 2.** *Nat Biotechnol* 2019, **37**:852-857.
30. Callahan BJ, McMurdie PJ, Rosen MJ, Han AW, Johnson AJ, Holmes SP: **DADA2: High-resolution sample inference from Illumina amplicon data.** *Nat Methods* 2016, **13**:581-583.

31. McMurdie PJ, Holmes S: **phyloseq: an R package for reproducible interactive analysis and graphics of microbiome census data.** *PLoS One* 2013, **8**:e61217.
32. Wickham H: **ggplot2: Elegant Graphics for Data Analysis.** *Springer-Verlag New York* 2009.
33. Warnes GRB, B.; Bonebakker, L.; Gentleman, R.; Huber, W.; Liaw, A.; Lumley, T.; Maechler, M.; Magnusson, A.; Moeller, S.; Schwartz, M.; Venables, B.: **gplots: Various R Programming Tools for Plotting Data.** 2020.
34. Treangen TJ, Ondov BD, Koren S, Phillippy AM: **The Harvest suite for rapid core-genome alignment and visualization of thousands of intraspecific microbial genomes.** *Genome Biol* 2014, **15**:524.
35. Thomsen MC, Ahrenfeldt J, Cisneros JL, Jurtz V, Larsen MV, Hasman H, Aarestrup FM, Lund O: **A Bacterial Analysis Platform: An Integrated System for Analysing Bacterial Whole Genome Sequencing Data for Clinical Diagnostics and Surveillance.** *PLoS One* 2016, **11**:e0157718.
36. Letunic I, Bork P: **Interactive Tree Of Life (iTOL) v5: an online tool for phylogenetic tree display and annotation.** *Nucleic Acids Res* 2021, **49**:W293-W296.
37. Eren AM, Kiefl E, Shaiber A, Veseli I, Miller SE, Schechter MS, Fink I, Pan JN, Yousef M, Fogarty EC, et al: **Community-led, integrated, reproducible multi-omics with anvi'o.** *Nat Microbiol* 2021, **6**:3-6.
38. Bolger AM, Lohse M, Usadel B: **Trimmomatic: a flexible trimmer for illumina sequence data.** *Bioinformatics* 2014, **30**:2114-2120.
39. Patro R, Duggal G, Love MI, Irizarry RA, Kingsford C: **Salmon provides fast and bias-aware quantification of transcript expression.** *Nat Methods* 2017, **14**:417-419.
40. Sonesson C, Love MI, Robinson MD: **Differential analyses for RNA-seq: transcript-level estimates improve gene-level inferences.** *F1000Res* 2015, **4**:1521.
41. Love MI, Huber W, Anders S: **Moderated estimation of fold change and dispersion for RNA-seq data with DESeq2.** *Genome Biol* 2014, **15**:550.
42. Zhu A, Ibrahim JG, Love MI: **Heavy-tailed prior distributions for sequence count data: removing the noise and preserving large differences.** *Bioinformatics* 2019, **35**:2084-2092.
43. Wei T, Simko V: **R package 'corrplot': Visualization of a Correlation Matrix. version 0.90.** 2021.
44. Lin H, Peddada SD: **Analysis of compositions of microbiomes with bias correction.** *Nat Commun* 2020, **11**:3514.
45. Kolde R: **pheatmap: Pretty Heatmaps. version 1.0.12.** 2019.
46. Blighe K, Rana S, Lewis M: **EnhancedVolcano: publication-ready volcano plots with enhanced colouring and labeling. version 1.8.0.** 2020.
47. Hanssen AM, Kindlund B, Stenklev NC, Furberg AS, Fismen S, Olsen RS, Johannessen M, Sollid JU: **Localization of Staphylococcus aureus in tissue from the nasal vestibule in healthy carriers.** *BMC Microbiol* 2017, **17**:89.
48. Rohde H, Kalitzky M, Kroger N, Scherpe S, Horstkotte MA, Knobloch JK, Zander AR, Mack D: **Detection of virulence-associated genes not useful for discriminating between invasive and commensal Staphylococcus**



- epidermidis strains from a bone marrow transplant unit. *J Clin Microbiol* 2004, **42**:5614-5619.**
49. Gotz F, Perconti S, Popella P, Werner R, Schlag M: **Epidermin and gallidermin: Staphylococcal lantibiotics.** *Int J Med Microbiol* 2014, **304**:63-71.
50. Byrd AL, Belkaid Y, Segre JA: **The human skin microbiome.** *Nat Rev Microbiol* 2018, **16**:143-155.
51. Otto M: **Staphylococcus epidermidis--the 'accidental' pathogen.** *Nat Rev Microbiol* 2009, **7**:555-567.
52. McLaughlin J, Watterson S, Layton AM, Bjourson AJ, Barnard E, McDowell A: **Propionibacterium acnes and Acne Vulgaris: New Insights from the Integration of Population Genetic, Multi-Omic, Biochemical and Host-Microbe Studies.** *Microorganisms* 2019, **7**.
53. Dagnelie MA, Corvec S, Saint-Jean M, Nguyen JM, Khammari A, Dreno B: **Cutibacterium acnes phylotypes diversity loss: a trigger for skin inflammatory process.** *J Eur Acad Dermatol Venereol* 2019, **33**:2340-2348.
54. Nakatsuji T, Chen TH, Narala S, Chun KA, Two AM, Yun T, Shafiq F, Kotol PF, Bouslimani A, Melnik AV, et al: **Antimicrobials from human skin commensal bacteria protect against Staphylococcus aureus and are deficient in atopic dermatitis.** *Sci Transl Med* 2017, **9**.
55. Leyden JJ, Marples RR, Kligman AM: **Staphylococcus aureus in the lesions of atopic dermatitis.** *Br J Dermatol* 1974, **90**:525-530.
56. Tauber M, Balica S, Hsu CY, Jean-Decoster C, Lauze C, Redoules D, Viode C, Schmitt AM, Serre G, Simon M, Paul CF: **Staphylococcus aureus density on lesional and nonlesional skin is strongly associated with disease severity in atopic dermatitis.** *J Allergy Clin Immunol* 2016, **137**:1272-1274 e1273.
57. Kellner R, Jung G, Horner T, Zahner H, Schnell N, Entian KD, Gotz F: **Gallidermin: a new lanthionine-containing polypeptide antibiotic.** *Eur J Biochem* 1988, **177**:53-59.
58. Vuong C, Durr M, Carmody AB, Peschel A, Klebanoff SJ, Otto M: **Regulated expression of pathogen-associated molecular pattern molecules in Staphylococcus epidermidis: quorum-sensing determines pro-inflammatory capacity and production of phenol-soluble modulins.** *Cell Microbiol* 2004, **6**:753-759.
59. Queck SY, Jameson-Lee M, Villaruz AE, Bach TH, Khan BA, Sturdevant DE, Ricklefs SM, Li M, Otto M: **RNAIII-independent target gene control by the agr quorum-sensing system: insight into the evolution of virulence regulation in Staphylococcus aureus.** *Mol Cell* 2008, **32**:150-158.
60. Olson ME, Todd DA, Schaeffer CR, Paharik AE, Van Dyke MJ, Buttner H, Dunman PM, Rohde H, Cech NB, Fey PD, Horswill AR: **Staphylococcus epidermidis agr quorum-sensing system: signal identification, cross talk, and importance in colonization.** *J Bacteriol* 2014, **196**:3482-3493.
61. Peng P, Baldry M, Gless BH, Bojer MS, Espinosa-Gongora C, Baig SJ, Andersen PS, Olsen CA, Ingmer H: **Effect of Co-inhabiting Coagulase Negative Staphylococci on S. aureus agr Quorum Sensing, Host Factor Binding, and Biofilm Formation.** *Front Microbiol* 2019, **10**:2212.

- 
62. Williams MR, Costa SK, Zaramela LS, Khalil S, Todd DA, Winter HL, Sanford JA, O'Neill AM, Liggins MC, Nakatsuji T, et al: **Quorum sensing between bacterial species on the skin protects against epidermal injury in atopic dermatitis.** *Sci Transl Med* 2019, **11**.
  63. Todd OA, Fidel PL, Jr., Harro JM, Hilliard JJ, Tkaczyk C, Sellman BR, Noverr MC, Peters BM: **Candida albicans Augments Staphylococcus aureus Virulence by Engaging the Staphylococcal agr Quorum Sensing System.** *mBio* 2019, **10**.
  64. Ebner P, Reichert S, Luqman A, Krismer B, Popella P, Gotz F: **Lantibiotic production is a burden for the producing staphylococci.** *Sci Rep* 2018, **8**:7471.

## 5 Discussion

The skin microbiome is composed of a multitude of different microbial species and strains. Besides *Cutibacterium*, *Staphylococcus* is the second most abundant bacterial genus on skin at most skin sites and their diverse populations play an important role in skin microbiome homeostasis (Dagnelie, Corvec, Timon-David, Khammari, & Dreno, 2021; Zhou et al., 2020). This study analyzed composition, abundances, geno- and phenotypic properties of commensal staphylococci on healthy human skin and their interaction with other skin microbiota. An amplicon-based NGS scheme was established to characterise the staphylococcal populations in a culture-independent manner and compared it with two other previously published NGS schemes (publication I). The results showed an unexpected occurrence of *S. saccharolyticus*, an abundant staphylococcal species on the skin (publication II). Furthermore, staphylococcal strains from healthy skin were isolated and characterised with regard to their antagonistic properties against *S. aureus* and *C. acnes*. Surprisingly, acne-associated A-class *C. acnes* strains were more susceptible to the antimicrobial activity of CoNS than non-acne-associated D- and H-class *C. acnes* (manuscript I).

### 5.1 Establishment of a novel amplicon-based NGS approach for the characterisation of staphylococcal populations

The staphylococcal populations on the skin make up a big part of the human skin microbiome. Staphylococci are of importance for the microbiome of healthy skin, as well as playing a role in skin diseases, e.g. atopic dermatitis (Leyden et al., 1974). NGS sequencing made it possible to get extensive insights into skin microbiota populations. A common approach for the characterisation of mixed bacterial communities is targeting fragments of the 16S rRNA gene. However, this amplicon-based approach, is not capable of distinguishing staphylococci beyond the genus level (Ghebremedhin, Layer, Konig, & Konig, 2008; Meisel et al., 2016).

To be able to determine staphylococcal populations accurately down to the species level, a novel scheme was developed in this study. It relies on the amplification of a *tuf* gene fragment, which codes for the elongation factor Tu (Ef-Tu) (publication II). Two previously published amplicon-based NGS schemes (designated ‘tuf1’ and ‘rpsk’) were compared to the novel NGS scheme, designated the tuf2 scheme (publication I). The tuf1 scheme was first established by Martineau et al. (2001) and targets the *tuf* gene as well. The tuf1 and tuf2 schemes have overlapping target sequences. However, the tuf2 scheme is generating a longer amplicon than the tuf1 scheme (467 bp and 366 bp, respectively). The rpsk scheme was established by Ederveen et al. (2019) and targets a 381 bp long sequence of the *rpsk* gene (Fig. 4).

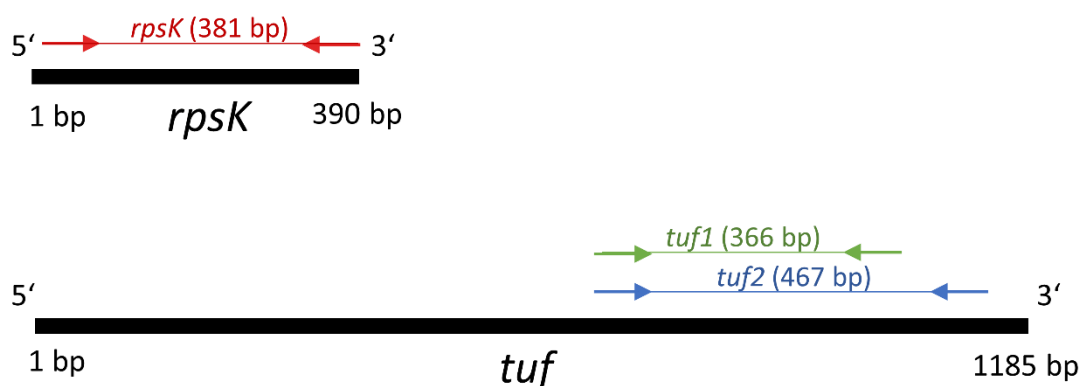


**Figure 4** Target gene regions and amplicon lengths of the three amplicon-based NGS schemes (rpsk = red, tuf1 = green, tuf2 = blue) (reprinted from publication I, figure 1).

First, different mock communities and skin swab samples were analysed by using the three schemes. All three NGS schemes performed comparatively well in capturing the staphylococcal populations. However, the tuf1 and rpsk schemes showed difficulties in detecting *S. saccharolyticus*. Furthermore, the tuf1 scheme did not properly capture the *S. epidermidis* abundance within the mock communities. This could be attributed to primer sequence mismatches, which can lead to no or a reduced PCR amplification (Sipos et al., 2007; Stadhouders et al., 2010). The primers used for the tuf1 and rpsk schemes have a mismatch with the sequence of *S. saccharolyticus* strains DVP4-17-2404 and 13T0028. Additionally, the tuf1

scheme reverse primer has a mismatch to the genomes of the four *S. epidermidis* strains included in the mock community. One human individual's skin is not only colonized by different CoNS species, but also different strains of one species from different phylogenetic backgrounds (Oh et al., 2016; Zhou et al., 2020). Of all CoNS, the population structure of *S. epidermidis*, which can be divided into three main clades (A, B and C), is best researched (Conlan et al., 2012; Espadinha et al., 2019). That is why the three amplicon-dependent schemes were compared *in situ* in their ability to distinguish the three phylogenetic clades of *S. epidermidis*. Therefore, a phylogenetic tree of *S. epidermidis* was constructed and the ability of the three schemes to depict the population structure was analysed. The *tuf2* scheme could distinguish the three phylogenetic clades of *S. epidermidis* best. This is most likely due to the longer amplicon sequence of the *tuf2* scheme, which could lead to the higher resolution power.

While all three schemes were able to characterise the staphylococcal populations, the *tuf2* scheme could differentiate between the phylogenetic clades of *S. epidermidis* and was superior in detecting *S. saccharolyticus* and *S. epidermidis* (publication I). Therefore, the *tuf2* scheme was chosen for all following amplicon-based analyses of staphylococcal populations.

## 5.2 Staphylococcal populations on healthy skin determined with culture-dependent and amplicon-based NGS approaches

The staphylococcal populations of forehead, cheek, back and forearm skin of 30 volunteers with healthy skin was determined with the amplicon-based *tuf2* scheme (Fig. 5a). The most abundant staphylococcal species identified, was *S. epidermidis* (in average 41.1 %), followed by *S. capitis*. Surprisingly, *S. saccharolyticus* was the third most abundant staphylococcal species detected (manuscript I), and particular abundant on the back (publication II). While *S. saccharolyticus* was previously found on human skin via culture-based studies (Evans & Mattern, 1978; Evans, Mattern, & Hallam, 1978), the species was not described in metagenomic studies of the skin before. Many NGS-based studies of skin relied on the 16S rRNA gene or fragments

thereof. These are highly conserved in staphylococci, and therefore most microbiome studies based on 16S rRNA gene-based amplicon sequencing approaches, were unable to differentiate *S. saccharolyticus* from other CoNS species (Ghebremedhin et al., 2008; Meisel et al., 2016). Recently, shotgun metagenomic approaches were used to study the skin microbiome, which rely on reference genomes for taxonomic assignment (Oh et al., 2014; Oh et al., 2016). All publicly available genomes of *S. saccharolyticus* before 2019 were wrongly assigned to this species and actually belonged to *S. capitis* (Bruggemann et al., 2019). Therefore, no reference genome of *S. saccharolyticus* was available, which made shotgun metagenomic analyzes before 2019 unable to detect this species. Recently, correctly assigned genomes of *S. saccharolyticus* have been deposited (Bruggemann et al., 2019), which should enable future shotgun metagenomic studies to detect *S. saccharolyticus*.

In addition to the amplicon-based *tuf2* scheme, the staphylococcal populations were characterised by a culture-dependent approach. An advantage of this approach is the ability to acquire bacterial isolates, which can be further characterised phenotypically. Of 572 bacterial isolates, the vast majority (n=557, 97.3 %) belonged to a staphylococcal species (manuscript I) (Fig. 5b). Similar to the NGS scheme, the culture dependent approach identified *S. epidermidis* as the most abundant staphylococcal species (n=374, 67.2 %). Furthermore, *S. hominis* (n=86) and *S. capitis* (n=53) were isolated frequently. Both, the NGS scheme and the culture-dependent approach, found a high abundance of *S. hominis* on the forearm, compared to the other three skin sites. Future experiments assessing the phenotypic features of *S. hominis* isolates, could help clarify whether *S. hominis* is particularly adapted to the harsh conditions found on the skin of forearms. In contrast to the NGS scheme, *S. saccharolyticus* was not detected via the culture-dependent approach (Fig. 5). This can be attributed to the fastidious growth conditions of *S. saccharolyticus* (publication II). Previous studies showed the preference of *S. saccharolyticus* for anaerobic growth conditions (Evans & Mattern, 1978; Evans et al., 1978). Similar growth is observed when culturing *S. saccharolyticus* under aerobic CO<sub>2</sub>-rich conditions, while atmospheric conditions (aerobic, low CO<sub>2</sub> concentration) resulted in a reduced growth (publication II). The accelerated

growth under increased CO<sub>2</sub> concentrations is most likely attributed to a nonfunctional MpsAB system (publication II). The MpsAB system is a dissolved inorganic carbon transporter and essential for the uptake of bicarbonate. Bicarbonate is essential for carboxylase reactions. Mutations of the MpsAB system in *S. aureus* leads to a growth defect caused by a bicarbonate deficiency, which can be compensated by increased CO<sub>2</sub> levels (Fan et al., 2019). These fastidious growth requirements differ vastly from that of other common skin staphylococci species (Kloss, 1975). This led to an underrepresentation of *S. saccharolyticus*, not only in metagenomic studies, but also in culture-dependent studies.

Interestingly, the diversity of the staphylococcal populations determined with the NGS scheme is higher compared to the culture-based analysis. Several other staphylococcal species besides *S. saccharolyticus* were only detected with the culture-independent NGS approach, such as *Staphylococcus pettenkoferi*, *S. lugdunensis*, *S. equorum* and *Staphylococcus carnosus* (Fig. 5). Some of the identified staphylococcal species are not commonly found on human skin and are rather associated with the colonization of animals or food products. For example, *S. equorum* is commonly found on pig skin (Strube et al., 2018), while *S. carnosus* is used in the fermentation of sausage (Schleifer & Fischer, 1982). The culture-dependent approach could have missed these species because of their low abundance. For each skin sites, five isolates were randomly selected, when possible. This leads to an incomplete picture of the staphylococcal populations, with the most abundant species being overrepresented (Fig. 5b).

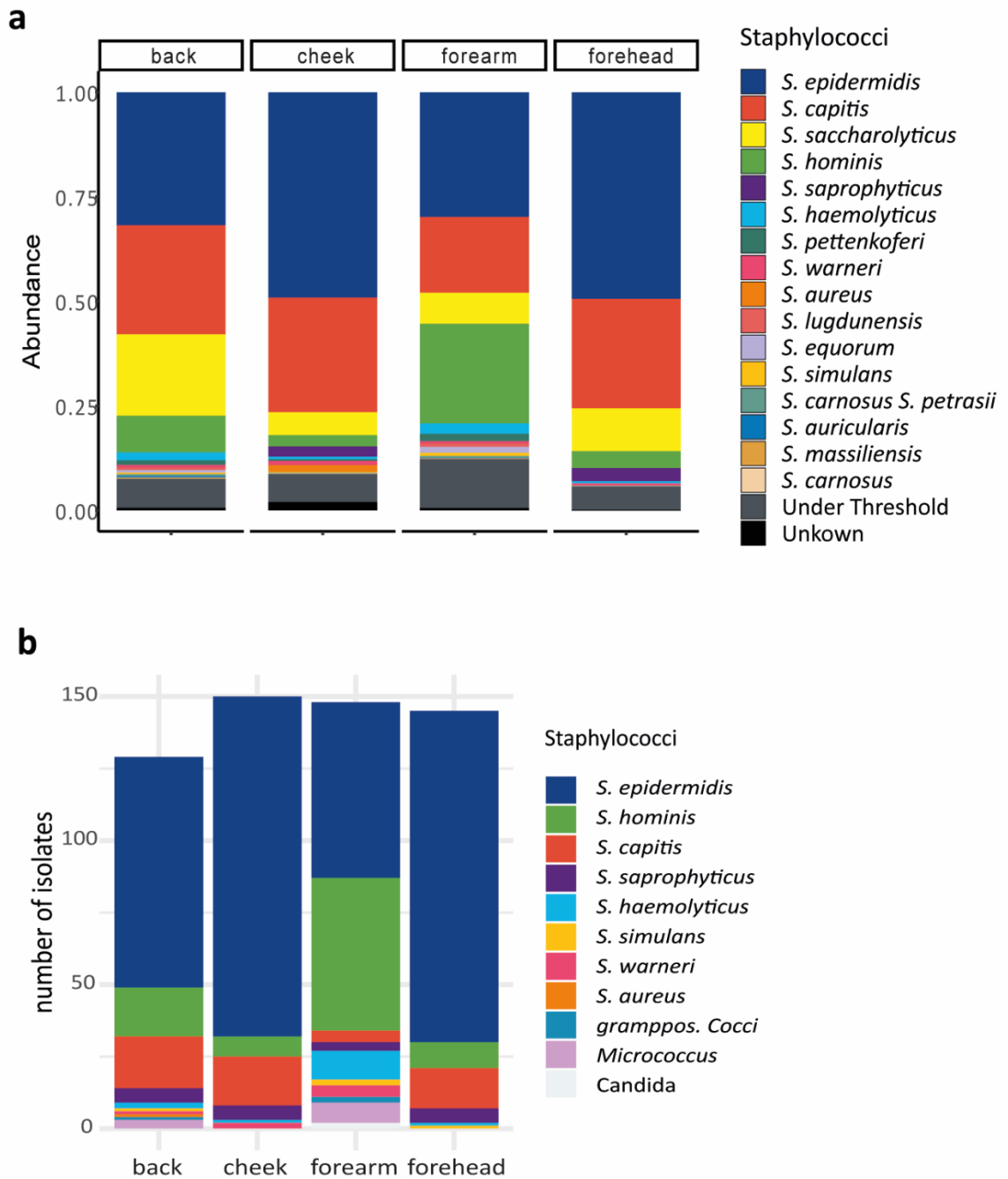


**Figure 5 Staphylococcal populations on back, cheek, forearm and forehead from volunteers (n=30) with healthy skin. a** Staphylococcal abundance analysed with amplicon-based tuf2 scheme (reprinted from manuscript I, Figure 2b). **b** Bacterial isolates gained after a culture-dependent approach (reprinted from manuscript I, Figure 1b).



One disadvantage of the NGS amplicon-based scheme: it cannot distinguish between DNA of live and dead staphylococcal cells. Thus, it cannot be ruled out that these staphylococcal species found in low abundances are dead bacterial contaminants aggregated on skin derived, e.g. from pet animals. An approach using benzonase to pre-digest dead bacterial DNA before amplicon-based sequencing, could enable the differentiation between living and dead bacteria within the microbiome (Amar et al., 2021). This approach could be used in future studies to get a more realistic picture of the microbiome and the staphylococcal populations therein. Furthermore, it would be of interest to sample the same volunteers at different time points. This way, the staphylococcal species of the core microbiome could be distinguished from transient colonizers.

CoNS are not only commensal skin colonizers but can also be opportunistic pathogens in nosocomial infections (reviewed in: Becker, Heilmann, and Peters (2014)). Exemplary, the role of *S. epidermidis* on skin and in infections is discussed in the next section.

### 5.3 *S. epidermidis* – skin guardian or infection-causing pathogen?

*S. epidermidis* was the most frequently detected staphylococcal species obtained with a culture-dependent and independent approaches in this study (manuscript I). Recent studies indicate that *S. epidermidis* may have a beneficial role in maintaining the skin microbiome homeostasis. Several *S. epidermidis* strains are able to secrete antimicrobial peptides such as epidermin, that inhibit the growth of *S. aureus* and *C. acnes* (Kellner et al., 1988), which are implicated in atopic dermatitis and acne, respectively. In this study, *S. epidermidis* isolates (n=374) were screened for their antimicrobial activity. The screen resulted in 5.6 % (21 of 374) of the isolates showing antagonistic activity against *S. aureus* and/or *C. acnes* (manuscript I). *S. epidermidis* can inhibit *S. aureus* biofilm formation through the secretion of protease Esp (Iwase et al., 2010) and *S. aureus* toxin production through quorum quenching (Williams et al., 2019). Both biofilm and toxin production of *S. aureus* are disease-promoting factors in atopic dermatitis (Allen et al., 2014; Brauweiler et al., 2014; Travers, 2014). Furthermore, strains of *S. epidermidis* have been shown to

allegedly inhibit skin cancer cells through the secretion of 6-N-hydroxyaminopurine (6-HAP) (Nakatsuji et al., 2018) and in addition, certain strains showed beneficial effects in wound repair (Leonel et al., 2019) and UV-B induced damage (Balasubramaniam et al., 2020). Previous studies applied live cells of *S. epidermidis* or closely related CoNS species to harness their health-beneficial properties. In the study of Nodake et al. (2015), *S. epidermidis* was isolated from the skin of volunteers, cultivated and then re-applied on the same volunteer (autologous transplantation). Transplantation of *S. epidermidis* resulted in increased lipid and water content as well as decreased water evaporation. No adverse reactions were reported. In Nakatsuji et al. (2017) antimicrobially active CoNS strains from patients with atopic dermatitis were isolated and then autologously transplanted on skin lesions. This approach resulted in a significant reduction of *S. aureus* numbers. However, no statement was made whether the disease severity improved. In the same study, a *S. hominis* strain with proven anti-*S. aureus* activity through the secretion of two lantibiotics (named *Sh*-lantibiotic- $\alpha$  and *Sh*-lantibiotic- $\beta$ ), was found. The *S. hominis* strain was applied on the skin of atopic dermatitis patients. It turned out that *S. aureus* was significantly reduced on the treated skin of atopic dermatitis patients compared to healthy controls. However, no significant changes in the atopic dermatitis severity score was observed (Nakatsuji et al., 2021). These contradictory results made in the few public available studies indicate that the application of live bacterial cells on the skin may have the potential to treat skin diseases. However, realizing these approaches is difficult and reports on the success are still lacking.

Despite being a common colonizer of skin, *S. epidermidis* can be the cause of infections – especially with regard to indwelling devices and infections in immunocompromised patients (Otto, 2009). *S. epidermidis* is able to form biofilms on these indwelling devices, causing disruption of their function and bacteremia, which can lead to blood stream infection (Mishra et al., 2015; Otto, 2017). *S. epidermidis* is mostly the cause of subacute or chronic infections (Otto, 2009).

But what differentiates a commensal skin-colonizing strain with health-beneficial properties from a pathogenic infection-causing *S. epidermidis* strain? To explore

these differences, *S. epidermidis* isolates (n = 69) from healthy skin were genome-sequenced and compared to genomes from public databases (manuscript I). None of the isolates from skin belonged to ST types most frequently involved in infections, such as ST2, ST23 and ST5 (manuscript I). The phylogenetic tree of *S. epidermidis* is divided into three clades (A, B and C). Previous studies showed that the B-clade harbored mostly commensal *S. epidermidis* strains (Conlan et al., 2012; Espadinha et al., 2019). In contrast, the 69 *S. epidermidis* strains analysed in this study, mostly belonged to the A- or C-clade. Only four isolates clustered within the B-clade. The novel *tuf2* NGS amplicon-based scheme is able to differentiate between all three phylogenetic clades of *S. epidermidis* (publication I). Therefore, the *tuf2* scheme could be used in future studies to analyse *S. epidermidis* populations on skin down to a sub-species level. Furthermore, the *S. epidermidis* isolates from skin were checked for the presence of virulence markers, such as *mecA* (methicillin-resistance gene), *icaADBC* (biofilm operon) and IS256 (insertion sequence) (manuscript I). Only 5.8 % were positive for *mecA*, 26.1 % for *icaADBC*, and none for IS256. This is in line with previous studies of Rohde et al. (2004) and Conlan et al. (2012) where *S. epidermidis* derived from skin and infection were compared. A similar proportion of commensal skin isolates harbored these sequences, while a higher rate of *S. epidermidis* isolates from infections were found positive for these markers (*icaA*: 63.0 % and 93.8 %, *mecA*: 80.4 % and 87.5 %, IS256: 47.8 % and 93.8 %) (Conlan et al., 2012; Rohde et al., 2004). A genome wide association study compared *S. epidermidis* isolates from infection to commensal colonizers. The authors found k-mers containing sequences associated to infection isolates such as the staphylococcal cassette chromosome *mec* (SCC*mec*). In contrast to other studies, they did not find differences between infection and commensal *S. epidermidis* isolates when looking at their phylogenetic background based on the core genome (such as ST type or phylogenetic clades) (Meric et al., 2018).

There is no clear-cut marker that differentiates pathogenic from commensal *S. epidermidis* strains. A multitude of different factors might play a role, such as ST type assignment and the absence/presence of virulence marker sequences (such as *mecA*, *icaA*, IS256). To harness the health-beneficial properties of *S. epidermidis* the absence of all so far identified factors implicated in infections has to be assured.

#### 5.4 *C. acnes* populations on healthy skin

Besides staphylococcal species, *C. acnes* is one of the major bacterial species found in the human skin microbiome. To understand the differences between the microbiome of healthy skin and acne-affected skin, the determination of the *C. acnes* populations is important. Therefore, the *C. acnes* populations was analysed on the forehead, cheek, forearm and back of 30 volunteers as part of this study (manuscript I). An NGS amplicon-based approach was used to differentiate between the SLST classes of *C. acnes* in skin samples (Scholz et al., 2014).

The phylogeny of *C. acnes* distinguishes six main phylotypes (IA<sub>1</sub>, IA<sub>2</sub>, IB, IC, II, III) (Lomholt & Kilian, 2010; McDowell et al., 2013), which are subdivided into ten SLST classes (A-L) (Scholz et al., 2014). A-, C- and F-class *C. acnes* are found in high abundances on acne-affected skin, while K- and H-class *C. acnes* are more abundant on healthy skin. Furthermore, the overall *C. acnes* strain diversity is lower on acne-affected skin (Dagnelie et al., 2018; Lomholt et al., 2017; McDowell et al., 2012; McDowell et al., 2011; Nakase et al., 2020; Nakase et al., 2017). On the skin sites of volunteers with healthy skin, all ten SLST classes were represented. The most abundant SLST class identified was A-class *C. acnes* with a relative abundance of 27.6 %, followed by D-class with 20.7 %, K-class with 19.2 % and H-class with 12.2 %. Even though a high abundance of acne-associated A-class *C. acnes* was identified, the abundance was lower than described for acne-affected skin (~50-90 %) (Dagnelie et al., 2018). In particular on the back, D-class *C. acnes* were highly abundant with 37.3 %. In general, it was the most abundant *C. acnes* SLST class on that skin site (manuscript I). A recent culture-dependent study showed the dominance of A-type *C. acnes* on acne-affected skin on the back (Dagnelie et al., 2018). Hence, D-class *C. acnes* could be associated with healthy skin, despite being closely related to the acne-associated A-class *C. acnes*. Interestingly, a positive correlation of K-class *C. acnes* with alpha diversity was observed in this study, indicating a preference of this *C. acnes* class to skin with high bacterial diversity (manuscript I).

This study shows few limitations due to sampling technics and study design. Sebaceous glands are the main habitat of *C. acnes* on skin (Kearney et al., 1984). The

swab sampling method used in manuscript I is not suitable to draw a conclusion regarding the *C. acnes* populations in the sebaceous glands. Therefore, the analysis of *C. acnes* populations done in this study, is only an overall average of all *C. acnes* from the skin surface. A study of Nakase et al. (2017) on Japanese acne patients, showed a strong association of F-class *C. acnes* to acne; in contrast, European studies have identified A- or C-class *C. acnes* as acne-associated strains. This indicates a strong influence of ethnicity or geographic location on the *C. acnes* populations on skin. Therefore, the *C. acnes* populations of healthy skin in this study are only representative for the European area.

### 5.5 Interaction of CoNS and *C. acnes* on the skin

Even though staphylococci mainly colonize the skin surface and *C. acnes* the sebaceous glands (Kearney et al., 1984), several mechanisms of interactions are described for these members of the skin microbiome. For staphylococci various antagonistic properties against *C. acnes* are described. Staphylococci can inhibit *C. acnes* by producing antimicrobial peptides, short-chain fatty acids or by activating the host immune system (Kellner et al., 1988; O'Neill et al., 2020; O'Sullivan et al., 2020; Y. Wang et al., 2014; Xia et al., 2016). So far, only a few antagonistic properties are reported, which are emanated from *C. acnes* against staphylococci. Some H-class *C. acnes* strains can produce cutimycin, which can inhibit the growth of *S. epidermidis* in hair follicles (Claesen et al., 2020). Furthermore, *C. acnes* can reduce *S. epidermidis* biofilm formation through the production of short-chain fatty acids (K. Nakamura et al., 2020).

To characterise the antagonistic properties of the staphylococcal isolates (n=557) obtained in this study, isolates were screened for their antimicrobial activity against a *C. acnes* indicator strain (manuscript I). Staphylococcal isolates that exhibited antimicrobial activity were subsequently tested against eleven different *C. acnes* strains from six different SLST classes. Overall, the two acne-associated A-class *C. acnes* strains were much more susceptible than other *C. acnes* SLST classes to the antimicrobial activity of the staphylococcal strains. In contrast, the non-acne-associated D- and H-class-*C. acnes* strains were highly tolerant towards the

antimicrobial activity (manuscript I). This contradicts previous studies, where no specificity against acne-associated *C. acnes* classes was found (Christensen et al., 2016; O'Neill et al., 2020).

To gain insights into the underlying mechanisms of the interaction between CoNS with antimicrobial activity and acne-/non-acne-associated *C. acnes* strains, co-culture experiments were conducted (manuscript I). *S. epidermidis* HAF242, whose genome encodes an epidermin operon, was cultivated with A-class *C. acnes* strain DSM1897 and with D-class *C. acnes* strain 30.2.L1, respectively. Furthermore, as a reference, *S. epidermidis* HAF242 was grown as a monoculture. As expected, the *S. epidermidis* HAF242 inhibited the growth of A-class *C. acnes*, while the D-class *C. acnes* was not affected (manuscript I). The transcriptome of *S. epidermidis* HAF242 in each set-up was analysed subsequently. Surprisingly, *S. epidermidis* in co-culture with D-class compared to A-class *C. acnes*, showed a reduced expression of the phenol-soluble modulins operon (*psm* $\beta$ 1-3), epidermin precursor gene (*epiA*) and autoinducing peptide (AIP) precursor gene (*agrD*) (manuscript I, Fig. 6b). Epidermin is described as inhibiting *C. acnes* even in low concentrations (MIC = 0.25  $\mu$ g/mL); it is even more effective against *C. acnes* than against *S. aureus* (MIC = 8  $\mu$ g/mL) (Kellner et al., 1988). Previous studies found that only PSM $\beta$ 1 and PSM $\beta$ 2 are produced by *S. epidermidis*, while a secreted PSM $\beta$ 3 peptide was so far not detected (Queck et al., 2009; Vuong, Kocianova, Yao, Carmody, & Otto, 2004). Antimicrobial properties for PSM $\beta$ s of *S. epidermidis* are not reported yet. However, PSM $\gamma$  of *S. epidermidis* was shown to be active against *S. aureus* and Group A *Streptococcus* (Cogen, Yamasaki, Muto, et al., 2010). Furthermore, a *S. capitis* strain was found which secretes four different PSM $\beta$ s that act against *C. acnes* (O'Neill et al., 2020). PSMs often act in synergy with other AMPs and amplify their activity (Cogen, Yamasaki, Sanchez, et al., 2010; O'Neill et al., 2020). Therefore, the antimicrobial effect of *S. epidermidis* HAF242 through the secretion of epidermin could potentially be reinforced by the production of PSM $\beta$ s. Additionally, the downregulation of *agrD* in *S. epidermidis* in co-culture with D-class *C. acnes* was observed in the transcriptomic dataset. The AIP precursor encoded by *agrD*, displays a central part of the *agr* quorum sensing system in staphylococci. The *agr* system is directly involved in the expression and activation of AMPs in

staphylococci. AIP activates the histidine kinase AgrC, which in turn activates the response regulator AgrA. AgrA directly activates the expression of the *psm $\beta$*  operon in *S. epidermidis* (Queck et al., 2008; Vuong, Durr, et al., 2004). Furthermore, the *agr* system regulates the activation of the epidermin precursor through the protease EpiP (Kies et al., 2003). Therefore, it is hypothesized that D-class *C. acnes* can interfere with the *agr* system of *S. epidermidis* through an unknown mechanism. This may lead to the suppression of expression and activation of AMPs in *S. epidermidis* (Fig. 6).

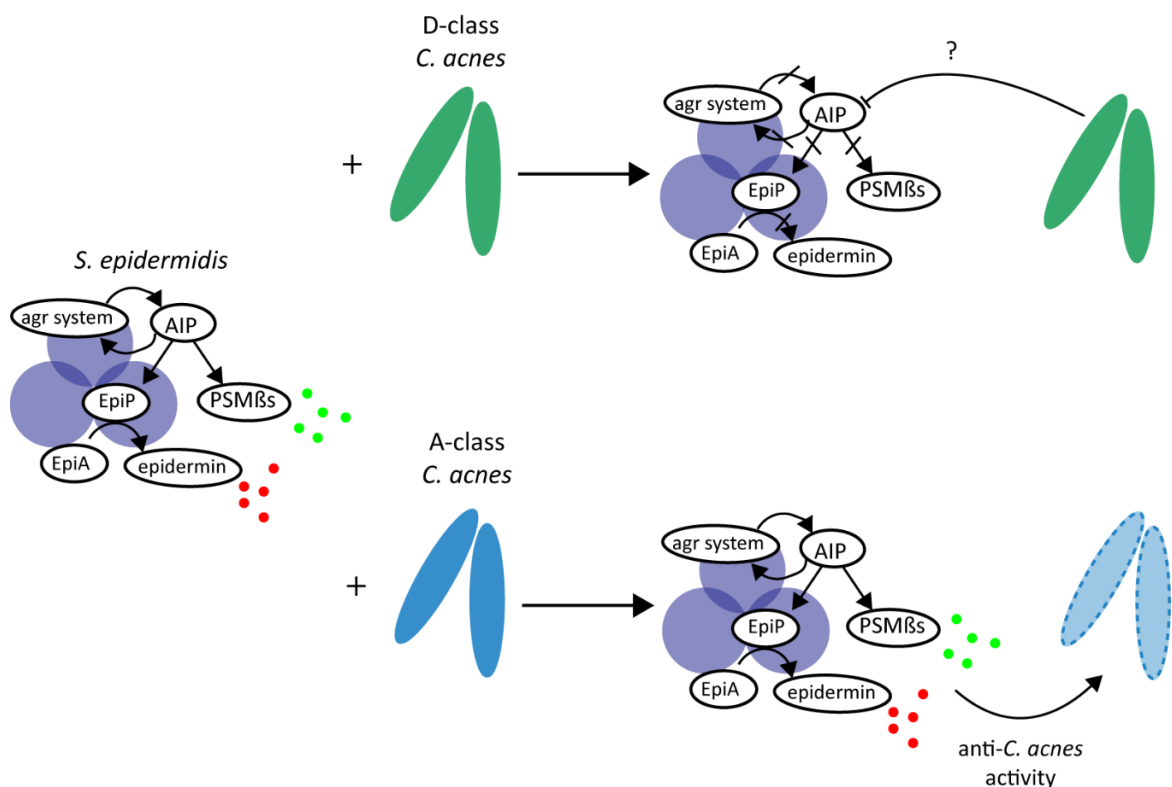


**Figure 6 Schematic model of the interaction between epidermin-producing *S. epidermidis* and A- and D-class *C. acnes*, respectively.** *S. epidermidis* can produce epidermin and phenol-soluble modulins (i.e. PSM $\beta$ s) that are antimicrobially active against *C. acnes*. The *agr* system controls the expression of PSM $\beta$  and EpiP. EpiP is a protease, which converts the precursor EpiA into the active epidermin. D-class *C. acnes* inhibits the *agr* system by an unknown mechanism, probably by targeting the production of the autoinducing peptide (AIP). Through the inhibition of the *agr* system, both epidermin and PSM $\beta$ s are not secreted in the presence of tolerant D-class *C. acnes*. A-class *C. acnes* does not inhibit the *agr* system of *S. epidermidis* and is killed by epidermin and PSM $\beta$ s.

The suppression of AMP expression in *S. epidermidis* may not only be of benefit for D-class *C. acnes*. It could also achieve a beneficial effect for *S. epidermidis* itself, since the production of epidermin reduces the growth rate in *S. epidermidis* and thus, can be a burden for the producing strain (Ebner et al., 2018).

The results obtained in this study provide a small insight into the extensive interaction network of bacterial members of the skin microbiome. Because of the high strain and species variety, there is still much to learn about occurring interferences between skin microbiome members. A next interesting step could be to analyse the influence of *S. epidermidis* on the transcriptomic profile of different *C. acnes* strains. It was previously shown that transcriptional changes in the vitamin B12 metabolism pathway of *C. acnes* could be implicated in acne pathogenesis (Kang, Shi, Erfe, Craft, & Li, 2015). Therefore, it would be of interest to see if *S. epidermidis* may have an influence on these genes in *C. acnes*.

To explore if the CoNS strains influence the population structure of *C. acnes in vivo*, the *C. acnes* populations of skin sites with and without antimicrobially active CoNS were compared (manuscript I). Interestingly, skin sites colonized with antimicrobial active CoNS strains showed a reduced abundance of acne-associated A-type *C. acnes*. This is a first indication that these CoNS strains can shape the *C. acnes* populations on the skin *in vivo* and that they may have a crucial role in the prevention of skin microbiome dysbiosis in acne.



## References

- Allen, H. B., Vaze, N. D., Choi, C., Hailu, T., Tulbert, B. H., Cusack, C. A., & Joshi, S. G. (2014). The presence and impact of biofilm-producing staphylococci in atopic dermatitis. *JAMA Dermatol*, *150*(3), 260-265. doi:10.1001/jamadermatol.2013.8627
- Alouf, J. E., Dufourcq, J., Siffert, O., Thiaudiere, E., & Geoffroy, C. (1989). Interaction of staphylococcal delta-toxin and synthetic analogues with erythrocytes and phospholipid vesicles. Biological and physical properties of the amphipathic peptides. *Eur J Biochem*, *183*(2), 381-390. doi:10.1111/j.1432-1033.1989.tb14939.x
- Amar, Y., Lagkouvardos, I., Silva, R. L., Ishola, O. A., Foesel, B. U., Kublik, S., . . . Koberle, M. (2021). Pre-digest of unprotected DNA by Benzonase improves the representation of living skin bacteria and efficiently depletes host DNA. *Microbiome*, *9*(1), 123. doi:10.1186/s40168-021-01067-0
- Balasubramaniam, A., Adi, P., Do Thi, T. M., Yang, J. H., Labibah, A. S., & Huang, C. M. (2020). Skin Bacteria Mediate Glycerol Fermentation to Produce Electricity and Resist UV-B. *Microorganisms*, *8*(7). doi:10.3390/microorganisms8071092
- Becker, K., Heilmann, C., & Peters, G. (2014). Coagulase-negative staphylococci. *Clin Microbiol Rev*, *27*(4), 870-926. doi:10.1128/CMR.00109-13
- Belkaid, Y., & Hand, T. W. (2014). Role of the microbiota in immunity and inflammation. *Cell*, *157*(1), 121-141. doi:10.1016/j.cell.2014.03.011
- Bierbaum, G., & Sahl, H. G. (2009). Lantibiotics: mode of action, biosynthesis and bioengineering. *Curr Pharm Biotechnol*, *10*(1), 2-18. doi:10.2174/138920109787048616
- Bitschar, K., Sauer, B., Focken, J., Dehmer, H., Moos, S., Konnerth, M., . . . Schitteck, B. (2019). Lugdunin amplifies innate immune responses in the skin in synergy with host- and microbiota-derived factors. *Nat Commun*, *10*(1), 2730. doi:10.1038/s41467-019-10646-7
- Boden, M. K., & Flock, J. I. (1989). Fibrinogen-binding protein/clumping factor from *Staphylococcus aureus*. *Infect Immun*, *57*(8), 2358-2363. doi:10.1128/iai.57.8.2358-2363.1989
- Brauweiler, A. M., Goleva, E., & Leung, D. Y. M. (2014). Th2 cytokines increase *Staphylococcus aureus* alpha toxin-induced keratinocyte death through the signal transducer and activator of transcription 6 (STAT6). *J Invest Dermatol*, *134*(8), 2114-2121. doi:10.1038/jid.2014.43
- Brown, M. M., Kwiecinski, J. M., Cruz, L. M., Shahbandi, A., Todd, D. A., Cech, N. B., & Horswill, A. R. (2020). Novel Peptide from Commensal *Staphylococcus simulans* Blocks Methicillin-Resistant *Staphylococcus aureus* Quorum Sensing and Protects Host Skin from Damage. *Antimicrob Agents Chemother*, *64*(6). doi:10.1128/AAC.00172-20
- Bruggemann, H., Poehlein, A., Brzuszkiewicz, E., Scavenius, C., Enghild, J. J., Al-Zeer, M. A., . . . Soderquist, B. (2019). *Staphylococcus saccharolyticus* Isolated From Blood Cultures and Prosthetic Joint Infections Exhibits Excessive Genome Decay. *Front Microbiol*, *10*, 478. doi:10.3389/fmicb.2019.00478

- Byrd, A. L., Belkaid, Y., & Segre, J. A. (2018). The human skin microbiome. *Nat Rev Microbiol*, *16*(3), 143-155. doi:10.1038/nrmicro.2017.157
- Campoccia, D., Montanaro, L., & Arciola, C. R. (2006). The significance of infection related to orthopedic devices and issues of antibiotic resistance. *Biomaterials*, *27*(11), 2331-2339. doi:10.1016/j.biomaterials.2005.11.044
- Cheung, G. Y., Rigby, K., Wang, R., Queck, S. Y., Braughton, K. R., Whitney, A. R., . . . Otto, M. (2010). Staphylococcus epidermidis strategies to avoid killing by human neutrophils. *PLoS Pathog*, *6*(10), e1001133. doi:10.1371/journal.ppat.1001133
- Christensen, G. J., Scholz, C. F., Enghild, J., Rohde, H., Kilian, M., Thurmer, A., . . . Bruggemann, H. (2016). Antagonism between Staphylococcus epidermidis and Propionibacterium acnes and its genomic basis. *BMC Genomics*, *17*, 152. doi:10.1186/s12864-016-2489-5
- Claesen, J., Spagnolo, J. B., Ramos, S. F., Kurita, K. L., Byrd, A. L., Aksenov, A. A., . . . Lemon, K. P. (2020). A Cutibacterium acnes antibiotic modulates human skin microbiota composition in hair follicles. *Sci Transl Med*, *12*(570). doi:10.1126/scitranslmed.aay5445
- Cogen, A. L., Yamasaki, K., Muto, J., Sanchez, K. M., Crotty Alexander, L., Tanios, J., . . . Gallo, R. L. (2010). Staphylococcus epidermidis antimicrobial delta-toxin (phenol-soluble modulins-gamma) cooperates with host antimicrobial peptides to kill group A Streptococcus. *PLoS One*, *5*(1), e8557. doi:10.1371/journal.pone.0008557
- Cogen, A. L., Yamasaki, K., Sanchez, K. M., Dorschner, R. A., Lai, Y., MacLeod, D. T., . . . Gallo, R. L. (2010). Selective antimicrobial action is provided by phenol-soluble modulins derived from Staphylococcus epidermidis, a normal resident of the skin. *J Invest Dermatol*, *130*(1), 192-200. doi:10.1038/jid.2009.243
- Conlan, S., Mijares, L. A., Program, N. C. S., Becker, J., Blakesley, R. W., Bouffard, G. G., . . . Segre, J. A. (2012). Staphylococcus epidermidis pan-genome sequence analysis reveals diversity of skin commensal and hospital infection-associated isolates. *Genome Biol*, *13*(7), R64. doi:10.1186/gb-2012-13-7-r64
- Costello, E. K., Lauber, C. L., Hamady, M., Fierer, N., Gordon, J. I., & Knight, R. (2009). Bacterial community variation in human body habitats across space and time. *Science*, *326*(5960), 1694-1697. doi:10.1126/science.1177486
- Dagnelie, M. A., Corvec, S., Saint-Jean, M., Bourdes, V., Nguyen, J. M., Khammari, A., & Dreno, B. (2018). Decrease in Diversity of Propionibacterium acnes Phylotypes in Patients with Severe Acne on the Back. *Acta Derm Venereol*, *98*(2), 262-267. doi:10.2340/00015555-2847
- Dagnelie, M. A., Corvec, S., Saint-Jean, M., Nguyen, J. M., Khammari, A., & Dreno, B. (2019). Cutibacterium acnes phylotypes diversity loss: a trigger for skin inflammatory process. *J Eur Acad Dermatol Venereol*, *33*(12), 2340-2348. doi:10.1111/jdv.15795
- Dagnelie, M. A., Corvec, S., Timon-David, E., Khammari, A., & Dreno, B. (2021). Cutibacterium acnes and Staphylococcus epidermidis: the unmissable modulators of skin inflammatory response. *Exp Dermatol*. doi:10.1111/exd.14467
- Draper, L. A., Cotter, P. D., Hill, C., & Ross, R. P. (2015). Lantibiotic resistance. *Microbiol Mol Biol Rev*, *79*(2), 171-191. doi:10.1128/MMBR.00051-14

- Ebner, P., Reichert, S., Luqman, A., Krismer, B., Popella, P., & Gotz, F. (2018). Lantibiotic production is a burden for the producing staphylococci. *Sci Rep*, 8(1), 7471. doi:10.1038/s41598-018-25935-2
- Ederveen, T. H. A., Smits, J. P. H., Hajo, K., van Schalkwijk, S., Kouwenhoven, T. A., Lukovac, S., . . . van Hijum, S. (2019). A generic workflow for Single Locus Sequence Typing (SLST) design and subspecies characterization of microbiota. *Sci Rep*, 9(1), 19834. doi:10.1038/s41598-019-56065-y
- Espadinha, D., Sobral, R. G., Mendes, C. I., Meric, G., Sheppard, S. K., Carrico, J. A., . . . Miragaia, M. (2019). Distinct Phenotypic and Genomic Signatures Underlie Contrasting Pathogenic Potential of *Staphylococcus epidermidis* Clonal Lineages. *Front Microbiol*, 10, 1971. doi:10.3389/fmicb.2019.01971
- Evans, C. A., & Mattern, K. L. (1978). Individual differences in the bacterial flora of the skin of the forehead: *Peptococcus saccharolyticus*. *J Invest Dermatol*, 71(2), 152-153. doi:10.1111/1523-1747.ep12546913
- Evans, C. A., Mattern, K. L., & Hallam, S. L. (1978). Isolation and identification of *Peptococcus saccharolyticus* from human skin. *J Clin Microbiol*, 7(3), 261-264.
- Fan, S. H., Ebner, P., Reichert, S., Hertlein, T., Zabel, S., Lankapalli, A. K., . . . Gotz, F. (2019). MpsAB is important for *Staphylococcus aureus* virulence and growth at atmospheric CO<sub>2</sub> levels. *Nat Commun*, 10(1), 3627. doi:10.1038/s41467-019-11547-5
- Gallo, R. L. (2017). Human Skin Is the Largest Epithelial Surface for Interaction with Microbes. *J Invest Dermatol*, 137(6), 1213-1214. doi:10.1016/j.jid.2016.11.045
- Ghebremedhin, B., Layer, F., Konig, W., & Konig, B. (2008). Genetic classification and distinguishing of *Staphylococcus* species based on different partial gap, 16S rRNA, hsp60, rpoB, sodA, and tuf gene sequences. *J Clin Microbiol*, 46(3), 1019-1025. doi:10.1128/JCM.02058-07
- Grice, E. A., Kong, H. H., Conlan, S., Deming, C. B., Davis, J., Young, A. C., . . . Segre, J. A. (2009). Topographical and temporal diversity of the human skin microbiome. *Science*, 324(5931), 1190-1192. doi:10.1126/science.1171700
- Heidrich, C., Pag, U., Josten, M., Metzger, J., Jack, R. W., Bierbaum, G., . . . Sahl, H. G. (1998). Isolation, characterization, and heterologous expression of the novel lantibiotic epicidin 280 and analysis of its biosynthetic gene cluster. *Appl Environ Microbiol*, 64(9), 3140-3146.
- Iwase, T., Uehara, Y., Shinji, H., Tajima, A., Seo, H., Takada, K., . . . Mizunoe, Y. (2010). *Staphylococcus epidermidis* Esp inhibits *Staphylococcus aureus* biofilm formation and nasal colonization. *Nature*, 465(7296), 346-349. doi:10.1038/nature09074
- Janzon, L., Lofdahl, S., & Arvidson, S. (1989). Identification and nucleotide sequence of the delta-lysin gene, hld, adjacent to the accessory gene regulator (agr) of *Staphylococcus aureus*. *Mol Gen Genet*, 219(3), 480-485. doi:10.1007/BF00259623
- Ji, G., Beavis, R., & Novick, R. P. (1997). Bacterial interference caused by autoinducing peptide variants. *Science*, 276(5321), 2027-2030. doi:10.1126/science.276.5321.2027
- Johnson, J. G., Wang, B., Debelouchina, G. T., Novick, R. P., & Muir, T. W. (2015). Increasing AIP Macrocycle Size Reveals Key Features of agr Activation in

- Staphylococcus aureus. *Chembiochem*, 16(7), 1093-1100. doi:10.1002/cbic.201500006
- Johnson, T., Kang, D., Barnard, E., & Li, H. (2016). Strain-Level Differences in Porphyrin Production and Regulation in Propionibacterium acnes Elucidate Disease Associations. *mSphere*, 1(1). doi:10.1128/mSphere.00023-15
- Kaletta, C., Entian, K. D., Kellner, R., Jung, G., Reis, M., & Sahl, H. G. (1989). Pep5, a new lantibiotic: structural gene isolation and prepeptide sequence. *Arch Microbiol*, 152(1), 16-19. doi:10.1007/bf00447005
- Kang, D., Shi, B., Erfe, M. C., Craft, N., & Li, H. (2015). Vitamin B12 modulates the transcriptome of the skin microbiota in acne pathogenesis. *Sci Transl Med*, 7(293), 293ra103. doi:10.1126/scitranslmed.aab2009
- Kearney, J. N., Harnby, D., Gowland, G., & Holland, K. T. (1984). The follicular distribution and abundance of resident bacteria on human skin. *J Gen Microbiol*, 130(4), 797-801. doi:10.1099/00221287-130-4-797
- Kellner, R., Jung, G., Horner, T., Zahner, H., Schnell, N., Entian, K. D., & Gotz, F. (1988). Gallidermin: a new lanthionine-containing polypeptide antibiotic. *Eur J Biochem*, 177(1), 53-59. doi:10.1111/j.1432-1033.1988.tb14344.x
- Kennedy, E. A., Connolly, J., Hourihane, J. O., Fallon, P. G., McLean, W. H. I., Murray, D., . . . Irvine, A. D. (2017). Skin microbiome before development of atopic dermatitis: Early colonization with commensal staphylococci at 2 months is associated with a lower risk of atopic dermatitis at 1 year. *J Allergy Clin Immunol*, 139(1), 166-172. doi:10.1016/j.jaci.2016.07.029
- Kies, S., Vuong, C., Hille, M., Peschel, A., Meyer, C., Gotz, F., & Otto, M. (2003). Control of antimicrobial peptide synthesis by the agr quorum sensing system in Staphylococcus epidermidis: activity of the lantibiotic epidermin is regulated at the level of precursor peptide processing. *Peptides*, 24(3), 329-338. doi:10.1016/s0196-9781(03)00046-9
- Kloos, W. E., & Musselwhite, M. S. (1975). Distribution and persistence of Staphylococcus and Micrococcus species and other aerobic bacteria on human skin. *Appl Microbiol*, 30(3), 381-385.
- Kloss, W. E. S., K. H. (1975). Isolation and Characterization of Staphylococci from Human Skin II. Descriptions of Four New Species: Staphylococcus warneri, Staphylococcus capitis, Staphylococcus hominis, and Staphylococcus simulans. *Int J Syst Bacteriol*, 25(1), 62-79. doi:/10.1099/00207713-25-1-62
- Lai, Y., Cogen, A. L., Radek, K. A., Park, H. J., Macleod, D. T., Leichtle, A., . . . Gallo, R. L. (2010). Activation of TLR2 by a small molecule produced by Staphylococcus epidermidis increases antimicrobial defense against bacterial skin infections. *J Invest Dermatol*, 130(9), 2211-2221. doi:10.1038/jid.2010.123
- Lai, Y., Di Nardo, A., Nakatsuji, T., Leichtle, A., Yang, Y., Cogen, A. L., . . . Gallo, R. L. (2009). Commensal bacteria regulate Toll-like receptor 3-dependent inflammation after skin injury. *Nat Med*, 15(12), 1377-1382. doi:10.1038/nm.2062
- Lane, D. J., Pace, B., Olsen, G. J., Stahl, D. A., Sogin, M. L., & Pace, N. R. (1985). Rapid determination of 16S ribosomal RNA sequences for phylogenetic analyses. *Proc Natl Acad Sci U S A*, 82(20), 6955-6959. doi:10.1073/pnas.82.20.6955
- Laughter, D., Istvan, J. A., Tofte, S. J., & Hanifin, J. M. (2000). The prevalence of atopic dermatitis in Oregon schoolchildren. *J Am Acad Dermatol*, 43(4), 649-655. doi:10.1067/mjd.2000.107773

- Lee, J. Y. H., Monk, I. R., Goncalves da Silva, A., Seemann, T., Chua, K. Y. L., Kearns, A., . . . Howden, B. P. (2018). Global spread of three multidrug-resistant lineages of *Staphylococcus epidermidis*. *Nat Microbiol*, *3*(10), 1175-1185. doi:10.1038/s41564-018-0230-7
- Leonel, C., Sena, I. F. G., Silva, W. N., Prazeres, P., Fernandes, G. R., Mancha Agresti, P., . . . Birbrair, A. (2019). *Staphylococcus epidermidis* role in the skin microenvironment. *J Cell Mol Med*, *23*(9), 5949-5955. doi:10.1111/jcmm.14415
- Leyden, J. J., Marples, R. R., & Kligman, A. M. (1974). *Staphylococcus aureus* in the lesions of atopic dermatitis. *Br J Dermatol*, *90*(5), 525-530. doi:10.1111/j.1365-2133.1974.tb06447.x
- Lomholt, H. B., & Kilian, M. (2010). Population genetic analysis of *Propionibacterium acnes* identifies a subpopulation and epidemic clones associated with acne. *PLoS One*, *5*(8), e12277. doi:10.1371/journal.pone.0012277
- Lomholt, H. B., Scholz, C. F. P., Bruggemann, H., Tettelin, H., & Kilian, M. (2017). A comparative study of *Cutibacterium* (*Propionibacterium*) *acnes* clones from acne patients and healthy controls. *Anaerobe*, *47*, 57-63. doi:10.1016/j.anaerobe.2017.04.006
- Mack, D., Rohde, H., Harris, L. G., Davies, A. P., Horstkotte, M. A., & Knobloch, J. K. (2006). Biofilm formation in medical device-related infection. *Int J Artif Organs*, *29*(4), 343-359. doi:10.1177/039139880602900404
- Martineau, F., Picard, F. J., Ke, D., Paradis, S., Roy, P. H., Ouellette, M., & Bergeron, M. G. (2001). Development of a PCR assay for identification of staphylococci at genus and species levels. *J Clin Microbiol*, *39*(7), 2541-2547. doi:10.1128/JCM.39.7.2541-2547.2001
- McDevitt, D., Vaudaux, P., & Foster, T. J. (1992). Genetic evidence that bound coagulase of *Staphylococcus aureus* is not clumping factor. *Infect Immun*, *60*(4), 1514-1523. doi:10.1128/iai.60.4.1514-1523.1992
- McDowell, A., Barnard, E., Nagy, I., Gao, A., Tomida, S., Li, H., . . . Patrick, S. (2012). An expanded multilocus sequence typing scheme for *propionibacterium acnes*: investigation of 'pathogenic', 'commensal' and antibiotic resistant strains. *PLoS One*, *7*(7), e41480. doi:10.1371/journal.pone.0041480
- McDowell, A., Gao, A., Barnard, E., Fink, C., Murray, P. I., Dowson, C. G., . . . Patrick, S. (2011). A novel multilocus sequence typing scheme for the opportunistic pathogen *Propionibacterium acnes* and characterization of type I cell surface-associated antigens. *Microbiology (Reading)*, *157*(Pt 7), 1990-2003. doi:10.1099/mic.0.049676-0
- McDowell, A., Nagy, I., Magyari, M., Barnard, E., & Patrick, S. (2013). The opportunistic pathogen *Propionibacterium acnes*: insights into typing, human disease, clonal diversification and CAMP factor evolution. *PLoS One*, *8*(9), e70897. doi:10.1371/journal.pone.0070897
- Mehlin, C., Headley, C. M., & Klebanoff, S. J. (1999). An inflammatory polypeptide complex from *Staphylococcus epidermidis*: isolation and characterization. *J Exp Med*, *189*(6), 907-918. doi:10.1084/jem.189.6.907
- Meisel, J. S., Hannigan, G. D., Tyldsley, A. S., SanMiguel, A. J., Hodkinson, B. P., Zheng, Q., & Grice, E. A. (2016). Skin Microbiome Surveys Are Strongly Influenced by Experimental Design. *J Invest Dermatol*, *136*(5), 947-956. doi:10.1016/j.jid.2016.01.016

- Meric, G., Mageiros, L., Pensar, J., Laabei, M., Yahara, K., Pascoe, B., . . . Sheppard, S. K. (2018). Disease-associated genotypes of the commensal skin bacterium *Staphylococcus epidermidis*. *Nat Commun*, *9*(1), 5034. doi:10.1038/s41467-018-07368-7
- Meyer, K., Pappas, A., Dunn, K., Cula, G. O., Seo, I., Ruvolo, E., & Batchvarova, N. (2015). Evaluation of Seasonal Changes in Facial Skin With and Without Acne. *J Drugs Dermatol*, *14*(6), 593-601.
- Mishra, S. K., Basukala, P., Basukala, O., Parajuli, K., Pokhrel, B. M., & Rijal, B. P. (2015). Detection of biofilm production and antibiotic resistance pattern in clinical isolates from indwelling medical devices. *Curr Microbiol*, *70*(1), 128-134. doi:10.1007/s00284-014-0694-5
- Naik, S., Bouladoux, N., Linehan, J. L., Han, S. J., Harrison, O. J., Wilhelm, C., . . . Belkaid, Y. (2015). Commensal-dendritic-cell interaction specifies a unique protective skin immune signature. *Nature*, *520*(7545), 104-108. doi:10.1038/nature14052
- Nakagawa, S., Matsumoto, M., Katayama, Y., Oguma, R., Wakabayashi, S., Nygaard, T., . . . Nakamura, Y. (2017). *Staphylococcus aureus* Virulent PSMalpha Peptides Induce Keratinocyte Alarmin Release to Orchestrate IL-17-Dependent Skin Inflammation. *Cell Host Microbe*, *22*(5), 667-677 e665. doi:10.1016/j.chom.2017.10.008
- Nakamura, K., O'Neill, A. M., Williams, M. R., Cau, L., Nakatsuji, T., Horswill, A. R., & Gallo, R. L. (2020). Short chain fatty acids produced by *Cutibacterium acnes* inhibit biofilm formation by *Staphylococcus epidermidis*. *Sci Rep*, *10*(1), 21237. doi:10.1038/s41598-020-77790-9
- Nakamura, Y., Oscherwitz, J., Cease, K. B., Chan, S. M., Munoz-Planillo, R., Hasegawa, M., . . . Nunez, G. (2013). *Staphylococcus delta-toxin* induces allergic skin disease by activating mast cells. *Nature*, *503*(7476), 397-401. doi:10.1038/nature12655
- Nakamura, Y., Takahashi, H., Takaya, A., Inoue, Y., Katayama, Y., Kusuya, Y., . . . Shimojo, N. (2020). *Staphylococcus Agr* virulence is critical for epidermal colonization and associates with atopic dermatitis development. *Sci Transl Med*, *12*(551). doi:10.1126/scitranslmed.aay4068
- Nakase, K., Aoki, S., Sei, S., Fukumoto, S., Horiuchi, Y., Yasuda, T., . . . Noguchi, N. (2020). Characterization of acne patients carrying clindamycin-resistant *Cutibacterium acnes*: A Japanese multicenter study. *J Dermatol*, *47*(8), 863-869. doi:10.1111/1346-8138.15397
- Nakase, K., Hayashi, N., Akiyama, Y., Aoki, S., & Noguchi, N. (2017). Antimicrobial susceptibility and phylogenetic analysis of *Propionibacterium acnes* isolated from acne patients in Japan between 2013 and 2015. *J Dermatol*, *44*(11), 1248-1254. doi:10.1111/1346-8138.13913
- Nakatsuji, T., Chen, T. H., Butcher, A. M., Trzoss, L. L., Nam, S. J., Shirakawa, K. T., . . . Gallo, R. L. (2018). A commensal strain of *Staphylococcus epidermidis* protects against skin neoplasia. *Sci Adv*, *4*(2), eaao4502. doi:10.1126/sciadv.aao4502
- Nakatsuji, T., Chen, T. H., Narala, S., Chun, K. A., Two, A. M., Yun, T., . . . Gallo, R. L. (2017). Antimicrobials from human skin commensal bacteria protect against *Staphylococcus aureus* and are deficient in atopic dermatitis. *Sci Transl Med*, *9*(378). doi:10.1126/scitranslmed.aah4680

- Nakatsuji, T., Chen, T. H., Two, A. M., Chun, K. A., Narala, S., Geha, R. S., . . . Gallo, R. L. (2016). Staphylococcus aureus Exploits Epidermal Barrier Defects in Atopic Dermatitis to Trigger Cytokine Expression. *J Invest Dermatol*, *136*(11), 2192-2200. doi:10.1016/j.jid.2016.05.127
- Nakatsuji, T., Hata, T. R., Tong, Y., Cheng, J. Y., Shafiq, F., Butcher, A. M., . . . Gallo, R. L. (2021). Development of a human skin commensal microbe for bacteriotherapy of atopic dermatitis and use in a phase 1 randomized clinical trial. *Nat Med*. doi:10.1038/s41591-021-01256-2
- Nodake, Y., Matsumoto, S., Miura, R., Honda, H., Ishibashi, G., Matsumoto, S., . . . Sakakibara, R. (2015). Pilot study on novel skin care method by augmentation with Staphylococcus epidermidis, an autologous skin microbe--A blinded randomized clinical trial. *J Dermatol Sci*, *79*(2), 119-126. doi:10.1016/j.jdermsci.2015.05.001
- O'Neill, A. M., Nakatsuji, T., Hayachi, A., Williams, M. R., Mills, R. H., Gonzalez, D. J., & Gallo, R. L. (2020). Identification of a human skin commensal bacterium that selectively kills Cutibacterium acnes. *J Invest Dermatol*. doi:10.1016/j.jid.2019.12.026
- O'Sullivan, J. N., O'Connor, P. M., Rea, M. C., O'Sullivan, O., Walsh, C. J., Healy, B., . . . Ross, R. P. (2020). Nisin J, a Novel Natural Nisin Variant, Is Produced by Staphylococcus capitis Sourced from the Human Skin Microbiota. *J Bacteriol*, *202*(3). doi:10.1128/JB.00639-19
- Oh, J., Byrd, A. L., Deming, C., Conlan, S., Program, N. C. S., Kong, H. H., & Segre, J. A. (2014). Biogeography and individuality shape function in the human skin metagenome. *Nature*, *514*(7520), 59-64. doi:10.1038/nature13786
- Oh, J., Byrd, A. L., Park, M., Program, N. C. S., Kong, H. H., & Segre, J. A. (2016). Temporal Stability of the Human Skin Microbiome. *Cell*, *165*(4), 854-866. doi:10.1016/j.cell.2016.04.008
- Otto, M. (2009). Staphylococcus epidermidis--the 'accidental' pathogen. *Nat Rev Microbiol*, *7*(8), 555-567. doi:10.1038/nrmicro2182
- Otto, M. (2017). Staphylococcus epidermidis: a major player in bacterial sepsis? *Future Microbiol*, *12*, 1031-1033. doi:10.2217/fmb-2017-0143
- Otto, M., Echner, H., Voelter, W., & Gotz, F. (2001). Pheromone cross-inhibition between Staphylococcus aureus and Staphylococcus epidermidis. *Infect Immun*, *69*(3), 1957-1960. doi:10.1128/IAI.69.3.1957-1960.2001
- Otto, M., Sussmuth, R., Vuong, C., Jung, G., & Gotz, F. (1999). Inhibition of virulence factor expression in Staphylococcus aureus by the Staphylococcus epidermidis agr pheromone and derivatives. *FEBS Lett*, *450*(3), 257-262. doi:10.1016/s0014-5793(99)00514-1
- Paharik, A. E., Parlet, C. P., Chung, N., Todd, D. A., Rodriguez, E. I., Van Dyke, M. J., . . . Horswill, A. R. (2017). Coagulase-Negative Staphylococcal Strain Prevents Staphylococcus aureus Colonization and Skin Infection by Blocking Quorum Sensing. *Cell Host Microbe*, *22*(6), 746-756 e745. doi:10.1016/j.chom.2017.11.001
- Pastar, I., O'Neill, K., Padula, L., Head, C. R., Burgess, J. L., Chen, V., . . . Strbo, N. (2020). Staphylococcus epidermidis Boosts Innate Immune Response by Activation of Gamma Delta T Cells and Induction of Perforin-2 in Human Skin. *Front Immunol*, *11*, 550946. doi:10.3389/fimmu.2020.550946

- Peng, P., Baldry, M., Gless, B. H., Bojer, M. S., Espinosa-Gongora, C., Baig, S. J., . . . Ingmer, H. (2019). Effect of Co-inhabiting Coagulase Negative Staphylococci on *S. aureus* agr Quorum Sensing, Host Factor Binding, and Biofilm Formation. *Front Microbiol*, *10*, 2212. doi:10.3389/fmicb.2019.02212
- Peschel, A., Jack, R. W., Otto, M., Collins, L. V., Staubitz, P., Nicholson, G., . . . van Strijp, J. A. (2001). Staphylococcus aureus resistance to human defensins and evasion of neutrophil killing via the novel virulence factor MprF is based on modification of membrane lipids with l-lysine. *J Exp Med*, *193*(9), 1067-1076. doi:10.1084/jem.193.9.1067
- Queck, S. Y., Jameson-Lee, M., Villaruz, A. E., Bach, T. H., Khan, B. A., Sturdevant, D. E., . . . Otto, M. (2008). RNAIII-independent target gene control by the agr quorum-sensing system: insight into the evolution of virulence regulation in Staphylococcus aureus. *Mol Cell*, *32*(1), 150-158. doi:10.1016/j.molcel.2008.08.005
- Queck, S. Y., Khan, B. A., Wang, R., Bach, T. H., Kretschmer, D., Chen, L., . . . Otto, M. (2009). Mobile genetic element-encoded cytolysin connects virulence to methicillin resistance in MRSA. *PLoS Pathog*, *5*(7), e1000533. doi:10.1371/journal.ppat.1000533
- Rogers, K. L., Fey, P. D., & Rupp, M. E. (2009). Coagulase-negative staphylococcal infections. *Infect Dis Clin North Am*, *23*(1), 73-98. doi:10.1016/j.idc.2008.10.001
- Rohde, H., Kalitzky, M., Kroger, N., Scherpe, S., Horstkotte, M. A., Knobloch, J. K., . . . Mack, D. (2004). Detection of virulence-associated genes not useful for discriminating between invasive and commensal Staphylococcus epidermidis strains from a bone marrow transplant unit. *J Clin Microbiol*, *42*(12), 5614-5619. doi:10.1128/JCM.42.12.5614-5619.2004
- Sandiford, S., & Upton, M. (2012). Identification, characterization, and recombinant expression of epidermicin NI01, a novel unmodified bacteriocin produced by Staphylococcus epidermidis that displays potent activity against Staphylococci. *Antimicrob Agents Chemother*, *56*(3), 1539-1547. doi:10.1128/AAC.05397-11
- Schaller, M., Loewenstein, M., Borelli, C., Jacob, K., Vogeser, M., Burgdorf, W. H., & Plewig, G. (2005). Induction of a chemoattractive proinflammatory cytokine response after stimulation of keratinocytes with Propionibacterium acnes and coproporphyrin III. *Br J Dermatol*, *153*(1), 66-71. doi:10.1111/j.1365-2133.2005.06530.x
- Schleiferi, & Fischer, U. (1982). Description of a New Species of the Genus Staphylococcus: Staphylococcus carnosus. *Int J Syst Evol Microbiol*, *32*(2). doi:doi:10.1099
- Schleiferi, K. H. K., W. E. (1975). Isolation and Characterization of Staphylococci from Human Skin I. Amended Descriptions of Staphylococcus epidermidis and Staphylococcus saprophyticus and Descriptions of Three New Species: Staphylococcus cohnii, Staphylococcus haemolyticus, and Staphylococcus xylosus. *INT J SYST EVOL MICR*, *25*(1), 50-61.
- Schnell, N., Entian, K. D., Schneider, U., Gotz, F., Zahner, H., Kellner, R., & Jung, G. (1988). Prepeptide sequence of epidermin, a ribosomally synthesized antibiotic with four sulphide-rings. *Nature*, *333*(6170), 276-278. doi:10.1038/333276a0



- Schoch, C. L., Ciuffo, S., Domrachev, M., Hotton, C. L., Kannan, S., Khovanskaya, R., . . . Karsch-Mizrachi, I. (2020). NCBI Taxonomy: a comprehensive update on curation, resources and tools. *Database (Oxford)*, 2020. doi:10.1093/database/baaa062
- Scholz, C. F., Jensen, A., Lomholt, H. B., Bruggemann, H., & Kilian, M. (2014). A novel high-resolution single locus sequence typing scheme for mixed populations of *Propionibacterium acnes* in vivo. *PLoS One*, 9(8), e104199. doi:10.1371/journal.pone.0104199
- Schultz Larsen, F., Diepgen, T., & Svensson, A. (1996). The occurrence of atopic dermatitis in north Europe: an international questionnaire study. *J Am Acad Dermatol*, 34(5 Pt 1), 760-764. doi:10.1016/s0190-9622(96)90009-2
- Sipos, R., Szekely, A. J., Palatinszky, M., Revesz, S., Marialigeti, K., & Nikolausz, M. (2007). Effect of primer mismatch, annealing temperature and PCR cycle number on 16S rRNA gene-targeting bacterial community analysis. *FEMS Microbiol Ecol*, 60(2), 341-350. doi:10.1111/j.1574-6941.2007.00283.x
- Spergel, J. M., & Paller, A. S. (2003). Atopic dermatitis and the atopic march. *J Allergy Clin Immunol*, 112(6 Suppl), S118-127. doi:10.1016/j.jaci.2003.09.033
- Stadhouders, R., Pas, S. D., Anber, J., Voermans, J., Mes, T. H., & Schutten, M. (2010). The effect of primer-template mismatches on the detection and quantification of nucleic acids using the 5' nuclease assay. *J Mol Diagn*, 12(1), 109-117. doi:10.2353/jmoldx.2010.090035
- Strube, M. L., Hansen, J. E., Rasmussen, S., & Pedersen, K. (2018). A detailed investigation of the porcine skin and nose microbiome using universal and *Staphylococcus* specific primers. *Sci Rep*, 8(1), 12751. doi:10.1038/s41598-018-30689-y
- Sugiura, H., Umemoto, N., Deguchi, H., Murata, Y., Tanaka, K., Sawai, T., . . . Uehara, M. (1998). Prevalence of childhood and adolescent atopic dermatitis in a Japanese population: comparison with the disease frequency examined 20 years ago. *Acta Derm Venereol*, 78(4), 293-294. doi:10.1080/000155598441891
- Tauber, M., Balica, S., Hsu, C. Y., Jean-Decoster, C., Lauze, C., Redoules, D., . . . Paul, C. F. (2016). *Staphylococcus aureus* density on lesional and nonlesional skin is strongly associated with disease severity in atopic dermatitis. *J Allergy Clin Immunol*, 137(4), 1272-1274 e1273. doi:10.1016/j.jaci.2015.07.052
- Thoendel, M., Kavanaugh, J. S., Flack, C. E., & Horswill, A. R. (2011). Peptide signaling in the staphylococci. *Chem Rev*, 111(1), 117-151. doi:10.1021/cr100370n
- Tomida, S., Nguyen, L., Chiu, B. H., Liu, J., Sodergren, E., Weinstock, G. M., & Li, H. (2013). Pan-genome and comparative genome analyses of *propionibacterium acnes* reveal its genomic diversity in the healthy and diseased human skin microbiome. *mBio*, 4(3), e00003-00013. doi:10.1128/mBio.00003-13
- Travers, J. B. (2014). Toxic interaction between Th2 cytokines and *Staphylococcus aureus* in atopic dermatitis. *J Invest Dermatol*, 134(8), 2069-2071. doi:10.1038/jid.2014.122
- van de Kamp, M., Horstink, L. M., van den Hooven, H. W., Konings, R. N., Hilbers, C. W., Frey, A., . . . van de Ven, F. J. (1995). Sequence analysis by NMR spectroscopy of the peptide lantibiotic epilancin K7 from *Staphylococcus*

- epidermidis K7. *Eur J Biochem*, 227(3), 757-771. doi:10.1111/j.1432-1033.1995.tb20199.x
- Verdier-Metz, I., Gagne, G., Bornes, S., Monsallier, F., Veisseire, P., Delbes-Paus, C., & Montel, M. C. (2012). Cow teat skin, a potential source of diverse microbial populations for cheese production. *Appl Environ Microbiol*, 78(2), 326-333. doi:10.1128/AEM.06229-11
- Vuong, C., Durr, M., Carmody, A. B., Peschel, A., Klebanoff, S. J., & Otto, M. (2004). Regulated expression of pathogen-associated molecular pattern molecules in *Staphylococcus epidermidis*: quorum-sensing determines pro-inflammatory capacity and production of phenol-soluble modulins. *Cell Microbiol*, 6(8), 753-759. doi:10.1111/j.1462-5822.2004.00401.x
- Vuong, C., Kocianova, S., Yao, Y., Carmody, A. B., & Otto, M. (2004). Increased colonization of indwelling medical devices by quorum-sensing mutants of *Staphylococcus epidermidis* in vivo. *J Infect Dis*, 190(8), 1498-1505. doi:10.1086/424487
- Wang, R., Khan, B. A., Cheung, G. Y., Bach, T. H., Jameson-Lee, M., Kong, K. F., . . . Otto, M. (2011). *Staphylococcus epidermidis* surfactant peptides promote biofilm maturation and dissemination of biofilm-associated infection in mice. *J Clin Invest*, 121(1), 238-248. doi:10.1172/JCI42520
- Wang, Y., Kuo, S., Shu, M., Yu, J., Huang, S., Dai, A., . . . Huang, C. M. (2014). *Staphylococcus epidermidis* in the human skin microbiome mediates fermentation to inhibit the growth of *Propionibacterium acnes*: implications of probiotics in acne vulgaris. *Appl Microbiol Biotechnol*, 98(1), 411-424. doi:10.1007/s00253-013-5394-8
- White, G. M. (1998). Recent findings in the epidemiologic evidence, classification, and subtypes of acne vulgaris. *J Am Acad Dermatol*, 39(2 Pt 3), S34-37. doi:10.1016/s0190-9622(98)70442-6
- Williams, M. R., Costa, S. K., Zaramela, L. S., Khalil, S., Todd, D. A., Winter, H. L., . . . Gallo, R. L. (2019). Quorum sensing between bacterial species on the skin protects against epidermal injury in atopic dermatitis. *Sci Transl Med*, 11(490). doi:10.1126/scitranslmed.aat8329
- Williams, M. R., Nakatsuji, T., Sanford, J. A., Vrbanc, A. F., & Gallo, R. L. (2017). *Staphylococcus aureus* Induces Increased Serine Protease Activity in Keratinocytes. *J Invest Dermatol*, 137(2), 377-384. doi:10.1016/j.jid.2016.10.008
- Xia, X., Li, Z., Liu, K., Wu, Y., Jiang, D., & Lai, Y. (2016). Staphylococcal LTA-Induced miR-143 Inhibits *Propionibacterium acnes*-Mediated Inflammatory Response in Skin. *J Invest Dermatol*, 136(3), 621-630. doi:10.1016/j.jid.2015.12.024
- Yao, Y., Sturdevant, D. E., & Otto, M. (2005). Genomewide analysis of gene expression in *Staphylococcus epidermidis* biofilms: insights into the pathophysiology of *S. epidermidis* biofilms and the role of phenol-soluble modulins in formation of biofilms. *J Infect Dis*, 191(2), 289-298. doi:10.1086/426945
- Yarwood, J. M., & Schlievert, P. M. (2003). Quorum sensing in *Staphylococcus* infections. *J Clin Invest*, 112(11), 1620-1625. doi:10.1172/JCI20442
- Yoshida, A. (1963). Staphylococcal delta-hemolysin. I. Purification and chemical properties. *Biochim Biophys Acta*, 71, 544-553. doi:10.1016/0006-3002(63)91126-0

- Zheng, Y., Hunt, R. L., Villaruz, A. E., Fisher, E. L., Liu, R., Liu, Q., . . . Otto, M. (2022). Commensal *Staphylococcus epidermidis* contributes to skin barrier homeostasis by generating protective ceramides. *Cell Host Microbe*. doi:10.1016/j.chom.2022.01.004
- Zhou, W., Spoto, M., Hardy, R., Guan, C., Fleming, E., Larson, P. J., . . . Oh, J. (2020). Host-Specific Evolutionary and Transmission Dynamics Shape the Functional Diversification of *Staphylococcus epidermidis* in Human Skin. *Cell*, 180(3), 454-470 e418. doi:10.1016/j.cell.2020.01.006
- Zipperer, A., Konnerth, M. C., Laux, C., Berscheid, A., Janek, D., Weidenmaier, C., . . . Krismer, B. (2016). Human commensals producing a novel antibiotic impair pathogen colonization. *Nature*, 535(7613), 511-516. doi:10.1038/nature18634

## Appendix

The appendix includes relevant additional files from the manuscript I.

**Additional File 1: Origin and strain name of bacterial isolates (n=572) obtained in this study.**

test person	skin area	species	strain
1	Forehead	<i>S. epidermidis</i>	HAF1
1	Forehead	<i>S. haemolyticus</i>	HAF3
1	Forehead	<i>S. epidermidis</i>	HAF4
1	Forehead	<i>S. epidermidis</i>	HAF5
1	Cheek	<i>S. epidermidis</i>	HAC6
1	Cheek	<i>S. epidermidis</i>	HAC7
1	Cheek	<i>S. epidermidis</i>	HAC8
1	Cheek	<i>S. epidermidis</i>	HAC9
1	Cheek	<i>S. epidermidis</i>	HAC10
1	Forearm	<i>S. haemolyticus</i>	HAA11
1	Forearm	<i>S. epidermidis</i>	HAA12
1	Forearm	<i>S. epidermidis</i>	HAA13
1	Forearm	<i>S. epidermidis</i>	HAA14
1	Forearm	<i>S. epidermidis</i>	HAA15
1	Back	<i>S. epidermidis</i>	HAB16
1	Back	<i>S. epidermidis</i>	HAB17
1	Back	<i>S. epidermidis</i>	HAB18
1	Back	<i>S. epidermidis</i>	HAB19
1	Back	<i>S. epidermidis</i>	HAB20
2	Forehead	<i>S. epidermidis</i>	HAF21
2	Forehead	<i>S. capitis</i>	HAF22
2	Forehead	<i>S. epidermidis</i>	HAF23
2	Forehead	<i>S. epidermidis</i>	HAF24
2	Forehead	<i>S. epidermidis</i>	HAF25
2	Cheek	<i>S. epidermidis</i>	HAC26
2	Cheek	<i>S. epidermidis</i>	HAC27
2	Cheek	<i>S. epidermidis</i>	HAC28
2	Cheek	<i>S. epidermidis</i>	HAC29
2	Cheek	<i>S. epidermidis</i>	HAC30
2	Forearm	<i>S. hominis</i>	HAA31
2	Forearm	<i>S. capitis</i>	HAA32

2	Forearm	<i>S. capitis</i>	HAA33
2	Forearm	<i>S. hominis</i>	HAA34
2	Forearm	<i>S. hominis</i>	HAA35
2	Back	<i>S. epidermidis</i>	HAB36
2	Back	<i>S. epidermidis</i>	HAB37
2	Back	<i>S. hominis</i>	HAB38
2	Back	<i>S. epidermidis</i>	HAB39
2	Back	<i>S. epidermidis</i>	HAB40
3	Forehead	<i>S. epidermidis</i>	HAF41
3	Forehead	<i>S. epidermidis</i>	HAF42
3	Forehead	<i>S. epidermidis</i>	HAF43
3	Forehead	<i>S. epidermidis</i>	HAF44
3	Forehead	<i>S. epidermidis</i>	HAF45
3	Cheek	<i>S. epidermidis</i>	HAC46
3	Cheek	<i>S. capitis</i>	HAC47
3	Cheek	<i>S. epidermidis</i>	HAC48
3	Cheek	<i>S. capitis</i>	HAC49
3	Cheek	<i>S. epidermidis</i>	HAC50
3	Forearm	<i>S. epidermidis</i>	HAA51
3	Forearm	<i>M. luteus</i>	HAA52
3	Forearm	<i>S. hominis</i>	HAA53
3	Forearm	<i>S. hominis</i>	HAA54
3	Forearm	<i>S. epidermidis</i>	HAA55
3	Back	<i>S. capitis</i>	HAB56
3	Back	<i>S. capitis</i>	HAB57
3	Back	<i>M. luteus</i>	HAB58
3	Back	<i>S. aureus</i>	HAB59
3	Back	<i>S. epidermidis</i>	HAB60
4	Forehead	<i>S. epidermidis</i>	HAF61
4	Forehead	<i>S. epidermidis</i>	HAF62
4	Forehead	<i>S. capitis</i>	HAF63
4	Cheek	<i>S. epidermidis</i>	HAC66
4	Cheek	<i>S. epidermidis</i>	HAC67
4	Cheek	<i>S. epidermidis</i>	HAC68
4	Cheek	<i>S. epidermidis</i>	HAC69
4	Cheek	<i>S. epidermidis</i>	HAC70
4	Forearm	<i>S. hominis</i>	HAA71

4	Forearm	<i>S. epidermidis</i>	HAA72
4	Forearm	<i>S. hominis</i>	HAA73
4	Forearm	<i>S. hominis</i>	HAA74
4	Forearm	<i>M. luteus</i>	HAA75
4	Back	<i>S. epidermidis</i>	HAB76
4	Back	<i>S. epidermidis</i>	HAB77
4	Back	grampositive cocci	HAB78
5	Forehead	<i>S. epidermidis</i>	HAF81
5	Forehead	<i>S. epidermidis</i>	HAF82
5	Forehead	<i>S. epidermidis</i>	HAF83
5	Forehead	<i>S. epidermidis</i>	HAF84
5	Forehead	<i>S. epidermidis</i>	HAF85
5	Cheek	<i>S. epidermidis</i>	HAC86
5	Cheek	<i>S. epidermidis</i>	HAC87
5	Cheek	<i>S. epidermidis</i>	HAC88
5	Cheek	<i>S. epidermidis</i>	HAC89
5	Cheek	<i>S. epidermidis</i>	HAC90
5	Forearm	<i>S. epidermidis</i>	HAA91
5	Forearm	<i>S. hominis</i>	HAA92
5	Forearm	<i>S. epidermidis</i>	HAA93
5	Forearm	<i>S. epidermidis</i>	HAA94
5	Forearm	<i>S. hominis</i>	HAA95
5	Back	<i>S. epidermidis</i>	HAB96
5	Back	<i>S. epidermidis</i>	HAB97
5	Back	<i>S. epidermidis</i>	HAB98
5	Back	<i>S. epidermidis</i>	HAB99
5	Back	<i>S. epidermidis</i>	HAB100
6	Forehead	<i>S. epidermidis</i>	HAF101
6	Forehead	<i>S. epidermidis</i>	HAF102
6	Forehead	<i>S. simulans</i>	HAF103
6	Forehead	<i>S. epidermidis</i>	HAF104
6	Forehead	<i>S. epidermidis</i>	HAF105
6	Cheek	<i>S. epidermidis</i>	HAC106
6	Cheek	<i>S. epidermidis</i>	HAC107
6	Cheek	<i>S. epidermidis</i>	HAC108
6	Cheek	<i>S. epidermidis</i>	HAC109
6	Cheek	<i>S. epidermidis</i>	HAC110

6	Forearm	<i>S. hominis</i>	HAA111
6	Forearm	<i>Candida sp.</i>	HAA112
6	Forearm	<i>Candida sp.</i>	HAA113
6	Forearm	grampositive cocci	HAA114
6	Forearm	grampositive cocci	HAA115
6	Back	<i>S. hominis</i>	HAB116
7	Forehead	<i>S. saprophyticus</i>	HAF121
7	Forehead	<i>S. saprophyticus</i>	HAF122
7	Forehead	<i>S. saprophyticus</i>	HAF123
7	Forehead	<i>S. saprophyticus</i>	HAF124
7	Forehead	<i>S. saprophyticus</i>	HAF125
7	Cheek	<i>S. saprophyticus</i>	HAC126
7	Cheek	<i>S. saprophyticus</i>	HAC127
7	Cheek	<i>S. saprophyticus</i>	HAC128
7	Cheek	<i>S. saprophyticus</i>	HAC129
7	Cheek	<i>S. saprophyticus</i>	HAC130
7	Forearm	<i>S. saprophyticus</i>	HAA131
7	Forearm	<i>S. saprophyticus</i>	HAA132
7	Forearm	<i>S. saprophyticus</i>	HAA133
7	Forearm	<i>S. hominis</i>	HAA134
7	Forearm	<i>S. hominis</i>	HAA135
7	Back	<i>S. saprophyticus</i>	HAB136
7	Back	<i>S. saprophyticus</i>	HAB137
7	Back	<i>S. saprophyticus</i>	HAB138
7	Back	<i>S. saprophyticus</i>	HAB139
7	Back	<i>S. saprophyticus</i>	HAB140
8	Forehead	<i>S. epidermidis</i>	HAF141
8	Forehead	<i>S. epidermidis</i>	HAF142
8	Forehead	<i>S. epidermidis</i>	HAF143
8	Forehead	<i>S. epidermidis</i>	HAF144
8	Forehead	<i>S. epidermidis</i>	HAF145
8	Cheek	<i>S. epidermidis</i>	HAC146
8	Cheek	<i>S. epidermidis</i>	HAC147
8	Cheek	<i>S. epidermidis</i>	HAC148
8	Cheek	<i>S. epidermidis</i>	HAC149
8	Cheek	<i>S. epidermidis</i>	HAC150
8	Forearm	<i>S. hominis</i>	HAA151

8	Forearm	<i>S. epidermidis</i>	HAA152
8	Forearm	<i>S. hominis</i>	HAA153
8	Forearm	<i>S. hominis</i>	HAA154
8	Back	<i>S. hominis</i>	HAB156
8	Back	<i>S. epidermidis</i>	HAB157
8	Back	<i>S. epidermidis</i>	HAB158
8	Back	<i>S. epidermidis</i>	HAB159
8	Back	<i>S. capitis</i>	HAB160
9	Forehead	<i>S. epidermidis</i>	HAF161
9	Forehead	<i>S. epidermidis</i>	HAF162
9	Forehead	<i>S. epidermidis</i>	HAF163
9	Forehead	<i>S. epidermidis</i>	HAF164
9	Forehead	<i>S. epidermidis</i>	HAF165
9	Cheek	<i>S. epidermidis</i>	HAC166
9	Cheek	<i>S. epidermidis</i>	HAC167
9	Cheek	<i>S. epidermidis</i>	HAC168
9	Cheek	<i>S. epidermidis</i>	HAC169
9	Cheek	<i>S. epidermidis</i>	HAC170
9	Forearm	<i>S. epidermidis</i>	HAA171
9	Forearm	<i>S. epidermidis</i>	HAA172
9	Forearm	<i>S. epidermidis</i>	HAA173
9	Forearm	<i>S. epidermidis</i>	HAA174
9	Forearm	<i>S. epidermidis</i>	HAA175
9	Back	<i>S. epidermidis</i>	HAB176
9	Back	<i>S. capitis</i>	HAB177
9	Back	<i>S. epidermidis</i>	HAB178
9	Back	<i>S. epidermidis</i>	HAB179
9	Back	<i>S. capitis</i>	HAB180
10	Forehead	<i>S. capitis</i>	HAF181
10	Forehead	<i>S. capitis</i>	HAF182
10	Forehead	<i>S. epidermidis</i>	HAF183
10	Forehead	<i>S. epidermidis</i>	HAF184
10	Forehead	<i>S. epidermidis</i>	HAF185
10	Cheek	<i>S. capitis</i>	HAC186
10	Cheek	<i>S. epidermidis</i>	HAC187
10	Cheek	<i>S. epidermidis</i>	HAC188
10	Cheek	<i>S. capitis</i>	HAC189



10	Cheek	<i>S. epidermidis</i>	HAC190
10	Forearm	<i>M. luteus</i>	HAA191
10	Forearm	<i>M. luteus</i>	HAA192
10	Forearm	<i>S. hominis</i>	HAA193
10	Forearm	<i>S. hominis</i>	HAA194
10	Forearm	<i>S. epidermidis</i>	HAA195
10	Back	<i>S. epidermidis</i>	HAB196
10	Back	<i>S. epidermidis</i>	HAB197
10	Back	<i>S. capitis</i>	HAB198
10	Back	<i>S. epidermidis</i>	HAB199
10	Back	<i>S. capitis</i>	HAB200
11	Forehead	<i>S. epidermidis</i>	HAF201
11	Forehead	<i>S. epidermidis</i>	HAF202
11	Forehead	<i>S. epidermidis</i>	HAF203
11	Forehead	<i>S. epidermidis</i>	HAF204
11	Forehead	<i>S. epidermidis</i>	HAF205
11	Cheek	<i>S. epidermidis</i>	HAC206
11	Cheek	<i>S. epidermidis</i>	HAC207
11	Cheek	<i>S. epidermidis</i>	HAC208
11	Cheek	<i>S. epidermidis</i>	HAC209
11	Cheek	<i>S. epidermidis</i>	HAC210
11	Forearm	<i>S. hominis</i>	HAA211
11	Forearm	<i>S. hominis</i>	HAA212
11	Forearm	<i>S. hominis</i>	HAA213
11	Forearm	<i>S. epidermidis</i>	HAA214
11	Forearm	<i>S. hominis</i>	HAA215
11	Back	<i>S. epidermidis</i>	HAB216
11	Back	<i>S. epidermidis</i>	HAB217
11	Back	<i>S. hominis</i>	HAB218
11	Back	<i>S. epidermidis</i>	HAB219
11	Back	<i>S. epidermidis</i>	HAB220
12	Forehead	<i>S. epidermidis</i>	HAF221
12	Forehead	<i>S. epidermidis</i>	HAF222
12	Forehead	<i>S. epidermidis</i>	HAF223
12	Forehead	<i>S. epidermidis</i>	HAF224
12	Forehead	<i>S. epidermidis</i>	HAF225
12	Cheek	<i>S. epidermidis</i>	HAC226

12	Cheek	<i>S. epidermidis</i>	HAC227
12	Cheek	<i>S. epidermidis</i>	HAC228
12	Cheek	<i>S. epidermidis</i>	HAC229
12	Cheek	<i>S. epidermidis</i>	HAC230
12	Forearm	<i>S. epidermidis</i>	HAA231
12	Forearm	<i>S. epidermidis</i>	HAA232
12	Forearm	<i>S. epidermidis</i>	HAA233
12	Forearm	<i>S. epidermidis</i>	HAA234
12	Forearm	<i>S. hominis</i>	HAA235
12	Back	<i>S. epidermidis</i>	HAB236
12	Back	<i>S. epidermidis</i>	HAB237
12	Back	<i>S. epidermidis</i>	HAB238
12	Back	<i>S. epidermidis</i>	HAB239
12	Back	<i>S. epidermidis</i>	HAB240
13	Forehead	<i>S. epidermidis</i>	HAF241
13	Forehead	<i>S. epidermidis</i>	HAF242
13	Forehead	<i>S. epidermidis</i>	HAF243
13	Forehead	<i>S. epidermidis</i>	HAF244
13	Forehead	<i>S. capitis</i>	HAF245
13	Cheek	<i>S. epidermidis</i>	HAC246
13	Cheek	<i>S. epidermidis</i>	HAC247
13	Cheek	<i>S. epidermidis</i>	HAC248
13	Cheek	<i>S. epidermidis</i>	HAC249
13	Cheek	<i>S. epidermidis</i>	HAC250
13	Forearm	<i>S. hominis</i>	HAA251
13	Forearm	<i>S. epidermidis</i>	HAA252
13	Forearm	<i>S. haemolyticus</i>	HAA253
13	Forearm	<i>S. hominis</i>	HAA254
13	Forearm	<i>S. epidermidis</i>	HAA255
13	Back	<i>S. hominis</i>	HAB256
13	Back	<i>S. hominis</i>	HAB257
13	Back	<i>S. epidermidis</i>	HAB258
13	Back	<i>S. epidermidis</i>	HAB259
13	Back	<i>S. capitis</i>	HAB260
14	Forehead	<i>S. epidermidis</i>	HAF261
14	Forehead	<i>S. epidermidis</i>	HAF262
14	Forehead	<i>S. epidermidis</i>	HAF263

14	Forehead	<i>S. capitis</i>	HAF264
14	Forehead	<i>S. epidermidis</i>	HAF265
14	Cheek	<i>S. epidermidis</i>	HAC266
14	Cheek	<i>S. epidermidis</i>	HAC267
14	Cheek	<i>S. epidermidis</i>	HAC268
14	Cheek	<i>S. epidermidis</i>	HAC269
14	Cheek	<i>S. epidermidis</i>	HAC270
14	Forearm	<i>S. warneri</i>	HAA271
14	Forearm	<i>S. hominis</i>	HAA272
14	Forearm	<i>S. hominis</i>	HAA273
14	Forearm	<i>S. hominis</i>	HAA274
14	Forearm	<i>S. epidermidis</i>	HAA275
14	Back	<i>S. capitis</i>	HAB276
14	Back	<i>S. capitis</i>	HAB277
14	Back	<i>S. capitis</i>	HAB278
14	Back	<i>S. hominis</i>	HAB279
14	Back	<i>S. capitis</i>	HAB280
15	Forehead	<i>S. epidermidis</i>	HAF281
15	Forehead	<i>S. epidermidis</i>	HAF282
15	Forehead	<i>S. epidermidis</i>	HAF283
15	Forehead	<i>S. epidermidis</i>	HAF284
15	Forehead	<i>S. epidermidis</i>	HAF285
15	Cheek	<i>S. hominis</i>	HAC286
15	Cheek	<i>S. epidermidis</i>	HAC287
15	Cheek	<i>S. epidermidis</i>	HAC288
15	Cheek	<i>S. epidermidis</i>	HAC289
15	Cheek	<i>S. epidermidis</i>	HAC290
15	Forearm	<i>S. hominis</i>	HAA291
15	Forearm	<i>S. epidermidis</i>	HAA292
15	Forearm	<i>S. epidermidis</i>	HAA293
15	Forearm	<i>S. simulans</i>	HAA294
15	Forearm	<i>S. simulans</i>	HAA295
15	Back	<i>S. simulans</i>	HAB296
15	Back	<i>M. luteus</i>	HAB297
16	Forehead	<i>S. hominis</i>	HAF301
16	Forehead	<i>S. hominis</i>	HAF302
16	Forehead	<i>S. hominis</i>	HAF303

16	Forehead	<i>S. hominis</i>	HAF304
16	Forehead	<i>S. epidermidis</i>	HAF305
16	Cheek	<i>S. epidermidis</i>	HAC306
16	Cheek	<i>S. capitis</i>	HAC307
16	Cheek	<i>S. hominis</i>	HAC308
16	Cheek	<i>S. epidermidis</i>	HAC309
16	Cheek	<i>S. epidermidis</i>	HAC310
16	Forearm	<i>S. haemolyticus</i>	HAA311
16	Forearm	<i>S. hominis</i>	HAA312
16	Forearm	<i>S. warneri</i>	HAA313
16	Forearm	<i>S. haemolyticus</i>	HAA314
16	Forearm	<i>S. epidermidis</i>	HAA315
16	Back	<i>S. epidermidis</i>	HAB316
16	Back	<i>S. epidermidis</i>	HAB317
16	Back	<i>S. epidermidis</i>	HAB318
16	Back	<i>S. epidermidis</i>	HAB319
16	Back	<i>S. epidermidis</i>	HAB320
17	Forehead	<i>S. epidermidis</i>	HAF321
17	Forehead	<i>S. capitis</i>	HAF322
17	Forehead	<i>S. epidermidis</i>	HAF323
17	Forehead	<i>S. epidermidis</i>	HAF324
17	Forehead	<i>S. epidermidis</i>	HAF325
17	Cheek	<i>S. epidermidis</i>	HAC326
17	Cheek	<i>S. epidermidis</i>	HAC327
17	Cheek	<i>S. capitis</i>	HAC328
17	Cheek	<i>S. epidermidis</i>	HAC329
17	Cheek	<i>S. epidermidis</i>	HAC330
17	Forearm	<i>S. epidermidis</i>	HAA331
17	Forearm	<i>S. epidermidis</i>	HAA332
17	Forearm	<i>S. warneri</i>	HAA333
17	Forearm	<i>S. warneri</i>	HAA334
17	Forearm	<i>S. epidermidis</i>	HAA335
17	Back	<i>S. epidermidis</i>	HAB336
17	Back	<i>S. capitis</i>	HAB337
17	Back	<i>S. epidermidis</i>	HAB338
17	Back	<i>S. epidermidis</i>	HAB339
17	Back	<i>S. epidermidis</i>	HAB340

18	Forehead	<i>S. epidermidis</i>	HAF341
18	Forehead	<i>S. epidermidis</i>	HAF342
18	Forehead	<i>S. epidermidis</i>	HAF343
18	Forehead	<i>S. epidermidis</i>	HAF344
18	Forehead	<i>S. epidermidis</i>	HAF345
18	Cheek	<i>S. capitis</i>	HAC346
18	Cheek	<i>S. capitis</i>	HAC347
18	Cheek	<i>S. epidermidis</i>	HAC348
18	Cheek	<i>S. capitis</i>	HAC349
18	Cheek	<i>S. capitis</i>	HAC350
18	Forearm	<i>S. epidermidis</i>	HAA351
18	Forearm	<i>S. hominis</i>	HAA352
18	Forearm	<i>S. epidermidis</i>	HAA353
18	Forearm	<i>S. hominis</i>	HAA354
18	Forearm	<i>S. epidermidis</i>	HAA355
18	Back	<i>S. epidermidis</i>	HAB356
18	Back	<i>S. epidermidis</i>	HAB357
18	Back	<i>S. epidermidis</i>	HAB358
18	Back	<i>S. epidermidis</i>	HAB359
18	Back	<i>S. epidermidis</i>	HAB360
19	Forehead	<i>S. epidermidis</i>	HAF361
19	Forehead	<i>S. epidermidis</i>	HAF362
19	Forehead	<i>S. epidermidis</i>	HAF363
19	Forehead	<i>S. epidermidis</i>	HAF364
19	Forehead	<i>S. epidermidis</i>	HAF365
19	Cheek	<i>S. epidermidis</i>	HAC366
19	Cheek	<i>S. epidermidis</i>	HAC367
19	Cheek	<i>S. epidermidis</i>	HAC368
19	Cheek	<i>S. epidermidis</i>	HAC369
19	Cheek	<i>S. epidermidis</i>	HAC370
19	Forearm	<i>S. epidermidis</i>	HAA371
19	Forearm	<i>S. hominis</i>	HAA372
19	Forearm	<i>S. epidermidis</i>	HAA373
19	Forearm	<i>S. hominis</i>	HAA374
19	Forearm	<i>S. epidermidis</i>	HAA375
19	Back	<i>S. epidermidis</i>	HAB376
19	Back	<i>S. capitis</i>	HAB377

19	Back	<i>M. luteus</i>	HAB378
19	Back	<i>S. epidermidis</i>	HAB379
19	Back	<i>S. epidermidis</i>	HAB380
20	Forehead	<i>S. epidermidis</i>	HAF381
20	Forehead	<i>S. epidermidis</i>	HAF382
20	Forehead	<i>S. epidermidis</i>	HAF383
20	Forehead	<i>S. epidermidis</i>	HAF384
20	Forehead	<i>S. epidermidis</i>	HAF385
20	Cheek	<i>S. epidermidis</i>	HAC386
20	Cheek	<i>S. epidermidis</i>	HAC387
20	Cheek	<i>S. warneri</i>	HAC388
20	Cheek	<i>S. epidermidis</i>	HAC389
20	Cheek	<i>S. warneri</i>	HAC390
20	Forearm	<i>S. hominis</i>	HAA391
20	Forearm	<i>S. hominis</i>	HAA392
20	Forearm	<i>S. epidermidis</i>	HAA393
20	Forearm	<i>S. epidermidis</i>	HAA394
20	Forearm	<i>S. hominis</i>	HAA395
20	Back	<i>S. warneri</i>	HAB396
21	Forehead	<i>S. capitis</i>	HAF401
21	Forehead	<i>S. capitis</i>	HAF402
21	Forehead	<i>S. capitis</i>	HAF403
21	Cheek	<i>S. epidermidis</i>	HAC406
21	Cheek	<i>S. epidermidis</i>	HAC407
21	Cheek	<i>S. epidermidis</i>	HAC408
21	Cheek	<i>S. epidermidis</i>	HAC409
21	Cheek	<i>S. epidermidis</i>	HAC410
21	Forearm	<i>S. hominis</i>	HAA411
21	Forearm	<i>S. hominis</i>	HAA412
21	Forearm	<i>S. epidermidis</i>	HAA413
21	Forearm	<i>S. epidermidis</i>	HAA414
21	Forearm	<i>S. epidermidis</i>	HAA415
21	Back	<i>S. hominis</i>	HAB416
21	Back	<i>S. hominis</i>	HAB417
22	Forehead	<i>S. epidermidis</i>	HAF421
22	Forehead	<i>S. epidermidis</i>	HAF422
22	Forehead	<i>S. epidermidis</i>	HAF423

22	Forehead	<i>S. epidermidis</i>	HAF424
22	Forehead	<i>S. epidermidis</i>	HAF425
22	Cheek	<i>S. epidermidis</i>	HAC426
22	Cheek	<i>S. epidermidis</i>	HAC427
22	Cheek	<i>S. epidermidis</i>	HAC428
22	Cheek	<i>S. epidermidis</i>	HAC429
22	Cheek	<i>S. epidermidis</i>	HAC430
22	Forearm	<i>M. luteus</i>	HAA431
22	Forearm	<i>S. capitis</i>	HAA432
22	Forearm	<i>M. luteus</i>	HAA433
22	Forearm	<i>M. luteus</i>	HAA434
22	Back	<i>S. epidermidis</i>	HAB436
22	Back	<i>S. epidermidis</i>	HAB437
22	Back	<i>S. epidermidis</i>	HAB438
22	Back	<i>S. epidermidis</i>	HAB439
22	Back	<i>S. epidermidis</i>	HAB440
23	Forehead	<i>S. epidermidis</i>	HAF441
23	Forehead	<i>S. epidermidis</i>	HAF442
23	Forehead	<i>S. epidermidis</i>	HAF443
23	Forehead	<i>S. epidermidis</i>	HAF444
23	Forehead	<i>S. epidermidis</i>	HAF445
23	Cheek	<i>S. epidermidis</i>	HAC446
23	Cheek	<i>S. epidermidis</i>	HAC447
23	Cheek	<i>S. epidermidis</i>	HAC448
23	Cheek	<i>S. epidermidis</i>	HAC449
23	Cheek	<i>S. epidermidis</i>	HAC450
23	Forearm	<i>S. epidermidis</i>	HAA451
23	Forearm	<i>S. epidermidis</i>	HAA452
23	Forearm	<i>S. epidermidis</i>	HAA453
23	Forearm	<i>S. epidermidis</i>	HAA454
23	Forearm	<i>S. haemolyticus</i>	HAA455
23	Back	<i>S. hominis</i>	HAB456
23	Back	<i>S. epidermidis</i>	HAB457
23	Back	<i>S. capitis</i>	HAB458
23	Back	<i>S. capitis</i>	HAB459
23	Back	<i>S. capitis</i>	HAB460
24	Forehead	<i>S. hominis</i>	HAF461

24	Forehead	<i>S. capitis</i>	HAF462
24	Forehead	<i>S. hominis</i>	HAF463
24	Forehead	<i>S. hominis</i>	HAF464
24	Forehead	<i>S. epidermidis</i>	HAF465
24	Cheek	<i>S. hominis</i>	HAC466
24	Cheek	<i>S. hominis</i>	HAC467
24	Cheek	<i>S. hominis</i>	HAC468
24	Cheek	<i>S. hominis</i>	HAC469
24	Cheek	<i>S. capitis</i>	HAC470
24	Forearm	<i>S. haemolyticus</i>	HAA471
24	Forearm	<i>S. haemolyticus</i>	HAA472
24	Forearm	<i>S. hominis</i>	HAA473
24	Forearm	<i>S. haemolyticus</i>	HAA474
24	Forearm	<i>S. haemolyticus</i>	HAA475
24	Back	<i>S. hominis</i>	HAB476
24	Back	<i>S. epidermidis</i>	HAB477
24	Back	<i>S. hominis</i>	HAB478
24	Back	<i>S. hominis</i>	HAB479
24	Back	<i>S. haemolyticus</i>	HAB480
25	Forehead	<i>S. epidermidis</i>	HAF481
25	Forehead	<i>S. epidermidis</i>	HAF482
25	Forehead	<i>S. epidermidis</i>	HAF483
25	Forehead	<i>S. epidermidis</i>	HAF484
25	Forehead	<i>S. epidermidis</i>	HAF485
25	Cheek	<i>S. epidermidis</i>	HAC486
25	Cheek	<i>S. epidermidis</i>	HAC487
25	Cheek	<i>S. epidermidis</i>	HAC488
25	Cheek	<i>S. haemolyticus</i>	HAC489
25	Cheek	<i>S. epidermidis</i>	HAC490
25	Forearm	<i>S. haemolyticus</i>	HAA491
25	Forearm	<i>S. epidermidis</i>	HAA492
25	Forearm	<i>S. hominis</i>	HAA493
25	Forearm	<i>S. epidermidis</i>	HAA494
25	Forearm	<i>S. epidermidis</i>	HAA495
25	Back	<i>S. epidermidis</i>	HAB496
25	Back	<i>S. epidermidis</i>	HAB497
25	Back	<i>S. epidermidis</i>	HAB498



25	Back	<i>S. epidermidis</i>	HAB499
25	Back	<i>S. epidermidis</i>	HAB500
26	Forehead	<i>S. capitis</i>	HAF501
26	Forehead	<i>S. epidermidis</i>	HAF502
26	Forehead	<i>S. epidermidis</i>	HAF503
26	Forehead	<i>S. capitis</i>	HAF504
26	Forehead	<i>S. epidermidis</i>	HAF505
26	Cheek	<i>S. capitis</i>	HAC506
26	Cheek	<i>S. capitis</i>	HAC507
26	Cheek	<i>S. capitis</i>	HAC508
26	Cheek	<i>S. capitis</i>	HAC509
26	Cheek	<i>S. capitis</i>	HAC510
26	Forearm	<i>S. hominis</i>	HAA511
26	Forearm	<i>S. epidermidis</i>	HAA512
26	Forearm	<i>S. hominis</i>	HAA513
26	Forearm	<i>S. hominis</i>	HAA514
26	Forearm	<i>S. epidermidis</i>	HAA515
26	Back	<i>S. capitis</i>	HAB516
26	Back	<i>S. hominis</i>	HAB517
26	Back	<i>S. hominis</i>	HAB518
26	Back	<i>S. hominis</i>	HAB519
26	Back	<i>S. hominis</i>	HAB520
27	Forehead	<i>S. epidermidis</i>	HAF521
27	Forehead	<i>S. epidermidis</i>	HAF522
27	Forehead	<i>S. epidermidis</i>	HAF523
27	Forehead	<i>S. epidermidis</i>	HAF524
27	Forehead	<i>S. epidermidis</i>	HAF525
27	Cheek	<i>S. epidermidis</i>	HAC526
27	Cheek	<i>S. epidermidis</i>	HAC527
27	Cheek	<i>S. epidermidis</i>	HAC528
27	Cheek	<i>S. epidermidis</i>	HAC529
27	Cheek	<i>S. epidermidis</i>	HAC530
27	Forearm	<i>S. epidermidis</i>	HAA531
27	Forearm	<i>S. epidermidis</i>	HAA532
27	Forearm	<i>S. epidermidis</i>	HAA533
27	Forearm	<i>S. epidermidis</i>	HAA534
27	Forearm	<i>S. epidermidis</i>	HAA535

27	Back	<i>S. epidermidis</i>	HAB536
27	Back	<i>S. epidermidis</i>	HAB537
27	Back	<i>S. epidermidis</i>	HAB538
27	Back	<i>S. epidermidis</i>	HAB539
27	Back	<i>S. epidermidis</i>	HAB540
28	Forehead	<i>S. epidermidis</i>	HAF541
28	Forehead	<i>S. epidermidis</i>	HAF542
28	Forehead	<i>S. epidermidis</i>	HAF543
28	Forehead	<i>S. capitis</i>	HAF544
28	Forehead	<i>S. epidermidis</i>	HAF545
28	Cheek	<i>S. epidermidis</i>	HAC546
28	Cheek	<i>S. epidermidis</i>	HAC547
28	Cheek	<i>S. epidermidis</i>	HAC548
28	Cheek	<i>S. epidermidis</i>	HAC549
28	Cheek	<i>S. epidermidis</i>	HAC550
28	Forearm	<i>S. epidermidis</i>	HAA551
28	Forearm	<i>S. hominis</i>	HAA552
28	Forearm	<i>S. hominis</i>	HAA553
28	Forearm	<i>S. hominis</i>	HAA554
28	Forearm	<i>S. hominis</i>	HAA555
28	Back	<i>S. epidermidis</i>	HAB556
28	Back	<i>S. epidermidis</i>	HAB557
28	Back	<i>S. epidermidis</i>	HAB558
28	Back	<i>S. epidermidis</i>	HAB559
28	Back	<i>S. epidermidis</i>	HAB560
29	Forehead	<i>S. epidermidis</i>	HAF561
29	Forehead	<i>S. epidermidis</i>	HAF562
29	Forehead	<i>S. epidermidis</i>	HAF563
29	Forehead	<i>S. epidermidis</i>	HAF564
29	Forehead	<i>S. epidermidis</i>	HAF565
29	Cheek	<i>S. epidermidis</i>	HAC566
29	Cheek	<i>S. epidermidis</i>	HAC567
29	Cheek	<i>S. epidermidis</i>	HAC568
29	Cheek	<i>S. epidermidis</i>	HAC569
29	Cheek	<i>S. epidermidis</i>	HAC570
29	Forearm	<i>S. hominis</i>	HAA571
29	Forearm	<i>S. epidermidis</i>	HAA572

---

29	Forearm	<i>S. hominis</i>	HAA573
29	Forearm	<i>S. epidermidis</i>	HAA574
29	Forearm	<i>S. epidermidis</i>	HAA575
29	Back	<i>S. epidermidis</i>	HAB576
29	Back	<i>S. epidermidis</i>	HAB577
29	Back	<i>S. epidermidis</i>	HAB578
29	Back	<i>S. epidermidis</i>	HAB579
29	Back	<i>S. haemolyticus</i>	HAB580
30	Forehead	<i>S. hominis</i>	HAF581
30	Forehead	<i>S. epidermidis</i>	HAF582
30	Forehead	<i>S. epidermidis</i>	HAF583
30	Forehead	<i>S. hominis</i>	HAF584
30	Forehead	<i>S. epidermidis</i>	HAF585
30	Cheek	<i>S. hominis</i>	HAC586
30	Cheek	<i>S. epidermidis</i>	HAC587
30	Cheek	<i>S. epidermidis</i>	HAC588
30	Cheek	<i>S. capitis</i>	HAC589
30	Cheek	<i>S. epidermidis</i>	HAC590
30	Forearm	<i>S. hominis</i>	HAA591
30	Forearm	<i>S. capitis</i>	HAA592
30	Forearm	<i>S. hominis</i>	HAA593
30	Forearm	<i>S. epidermidis</i>	HAA594
30	Forearm	<i>S. hominis</i>	HAA595

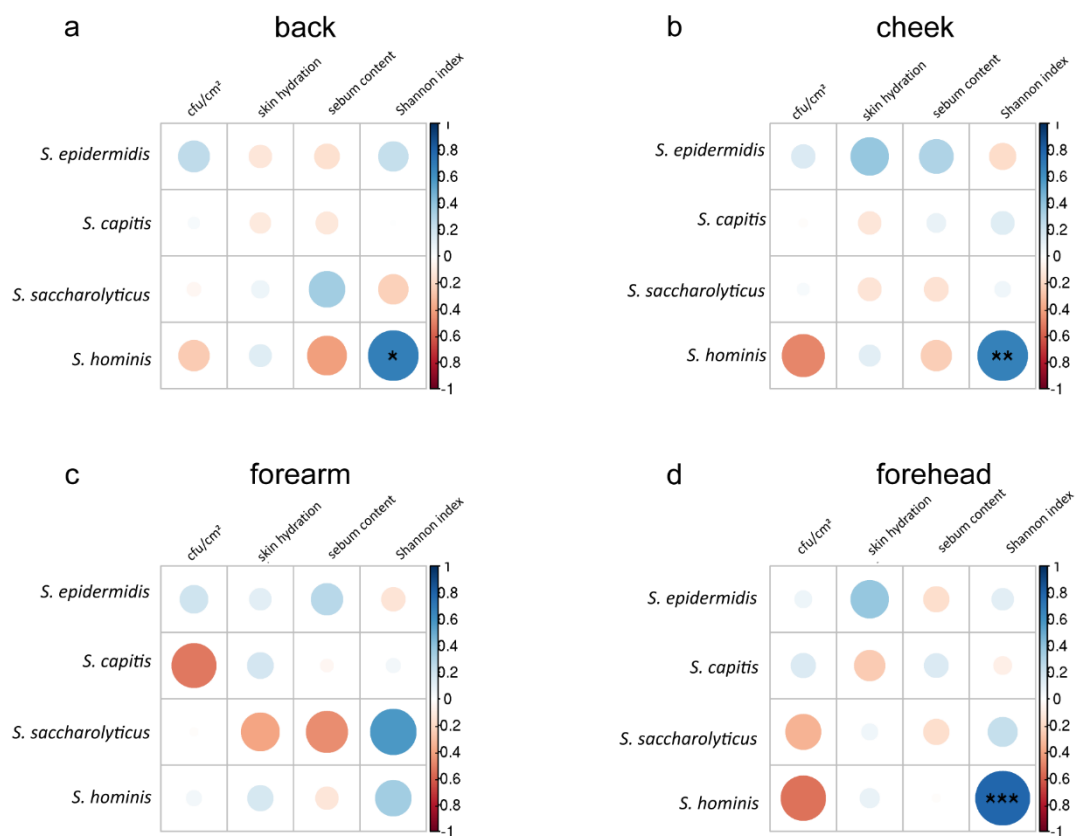
**Additional File 2: GenBank accession numbers and origin of indicator strains**

Indicator strains	SLST-type	Accession number	origin
<i>S. aureus</i> DSM799	-	JXHV000000000	Germany, DSMZ
<i>C. acnes</i> DSM1897	A1	AWZZ000000000	Germany, DSMZ
<i>C. acnes</i> 12.1.L1	A1	CP012354	Scholz et al. 2016 <sup>1</sup>
<i>C. acnes</i> 15.1.R1	C1	CP012355 (chromosome); CP012356 (plasmid)	Scholz et al. 2016 <sup>1</sup>
<i>C. acnes</i> 30.2.L1	D1	CP012350	Scholz et al. 2016 <sup>1</sup>
<i>C. acnes</i> 09-193	D1	LKVE010000000	Davidsson et al. 2017 <sup>2</sup>
<i>C. acnes</i> 11-90	H1	MVCG000000000	Davidsson et al. 2017 <sup>2</sup>
<i>C. acnes</i> KPA171202	H2	AE017283	Brüggemann et al. 2004 <sup>3</sup>
<i>C. acnes</i> 21.1.L1	H1	CP012351	Scholz et al. 2016 <sup>1</sup>
<i>C. acnes</i> 11-49	K1	MVCN000000000	Davidsson et al. 2017 <sup>2</sup>
<i>C. acnes</i> 11-79	K2	MVCO000000000	Davidsson et al. 2017 <sup>2</sup>
<i>C. acnes</i> PMH5	L1	LJAS000000000	Petersen et al. 2015 <sup>4</sup>

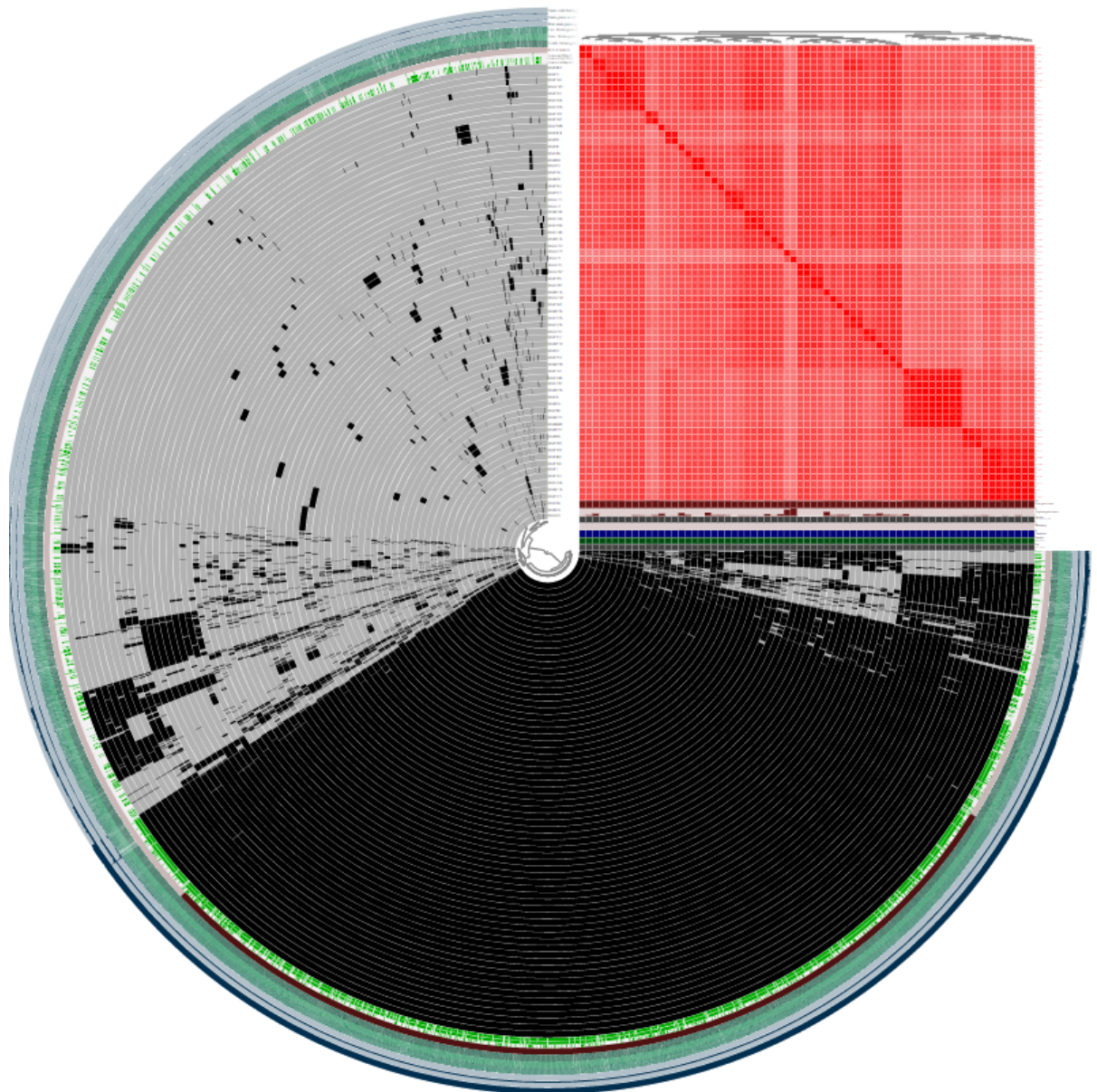
1. Scholz CF, Brüggemann H, Lomholt HB, Tettelin H, Kilian M. Genome stability of *Propionibacterium acnes*: a comprehensive study of indels and homopolymeric tracts. *Sci Rep* **6**, 20662 (2016).
2. Davidsson S, et al. Prevalence of Flp Pili-Encoding Plasmids in *Cutibacterium acnes* Isolates Obtained from Prostatic Tissue. *Front Microbiol* **8**, 2241 (2017).
3. Brüggemann H, et al. The complete genome sequence of *Propionibacterium acnes*, a commensal of human skin. *Science* **305**, 671-673 (2004).
4. Petersen R, Lomholt HB, Scholz CF, Brüggemann H. Draft Genome Sequences of Two *Propionibacterium acnes* Strains Isolated from Progressive Macular Hypomelanosis Lesions of Human Skin. *Genome Announc* **3**, (2015).

**Additional File 3: ANCOM-BC results (coefficient and adjusted p-value) for differences in abundances of staphylococcal species between skin sites (back = Ba, Ch = Cheek, Fa = Forearm, Fh = Forehead)**

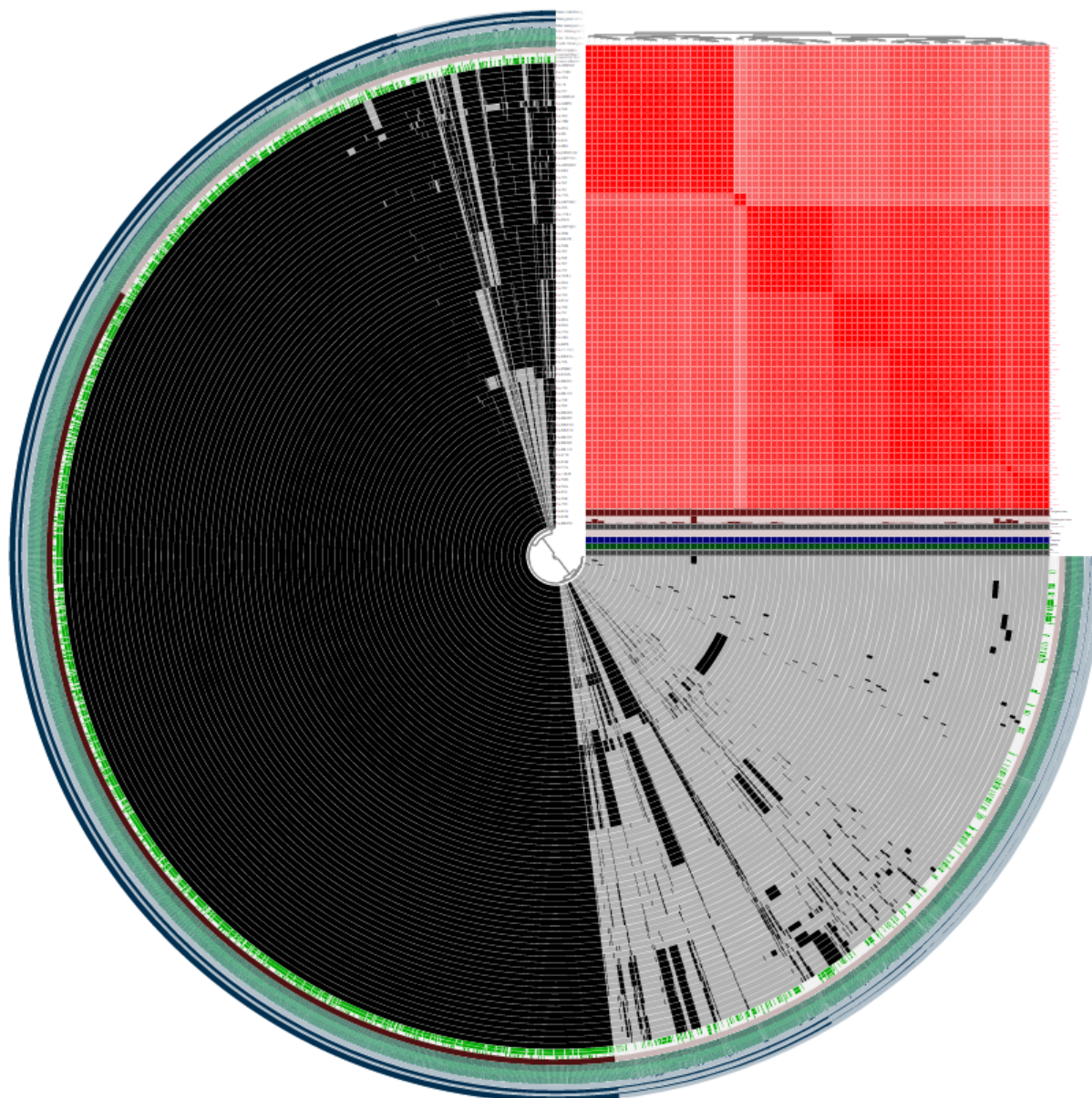
	Ba - Ch		Ba - Fa		Ba - Fh		Ch - Fa		Ch - Fh		Fa - Fh	
	coeff.	adj. p	coeff.	adj. p	coeff.	adj. p	coeff.	adj. p	coeff.	adj. p	coeff.	adj. p
<i>S. epidermidis</i>	0.13	0.35	0.06	1.00	0.13	0.45	-0.12	0.68	-0.01	1.00	0.07	1.00
<i>S. capitis</i>	0.01	1.00	0.00	1.00	0.01	1.00	-0.06	1.00	-0.02	1.00	-0.01	1.00
<i>S. saccharolyticus</i>	-0.10	0.42	-0.03	1.00	-0.06	1.00	0.03	1.00	0.04	1.00	-0.04	1.00
<i>S. hominis</i>	-0.05	0.63	0.18	0.00	-0.02	1.00	0.19	0.03	0.01	1.00	-0.22	0.00
below threshold	0.00	1.00	0.10	0.00	0.00	1.00	0.06	0.68	-0.01	1.00	-0.11	0.02



**Additional File 4: Spearman correlation between staphylococcal species abundances (determined by amplicon-based NGS) and skin parameters. This analysis was performed for each skin site separately: a back b cheek c forearm d forehead (FDR-adjusted p-value, \* $p \leq 0.05$ , \*\* $p \leq 0.01$ , \*\*\* $p \leq 0.001$ ).**



**Additional File 5: Pan-genome of 69 *S. epidermidis* strains isolated in this study.** Pan-genome analysis of the 69 strains was done with ANVIO. The pan-genome is composed of the core genome (i.e. genes shared by all strains) and a large accessory genomes (i.e. genes specific to single strains or subset of strains). Presence (black) and absence (grey) of gene clusters are depicted. The strains are sorted according to their average nucleotide identity (ANI) (red square; a higher ANI is depicted by a darker red color).



**Additional File 6: Pan-genome of 75 *C. acnes* strains covering all SLST classes.** Pan-genome analysis of the 75 strains was done with ANVIO. The 75 strains were chosen among all published *C. acnes* genomes and included strains from all 10 SLST classes (Supplementary data 7). The pan-genome is composed of the core genome (i.e. genes shared by all strains) and a large accessory genomes (i.e. genes specific to single strains or subset of strains). Presence (black) and absence (grey) of gene clusters are depicted. The strains are sorted according to their average nucleotide identity (ANI) (red square; a higher ANI is depicted by darker red).

**Additional File 7: ANCOM-BC results (coefficient and adjusted p-value) for differences in abundances of *C. acnes* SLST classes (A, C, D, E, F, H, G, K, L) between skin sites (back = Ba, Ch = Cheek, Fa = Forearm, Fh = Forehead)**

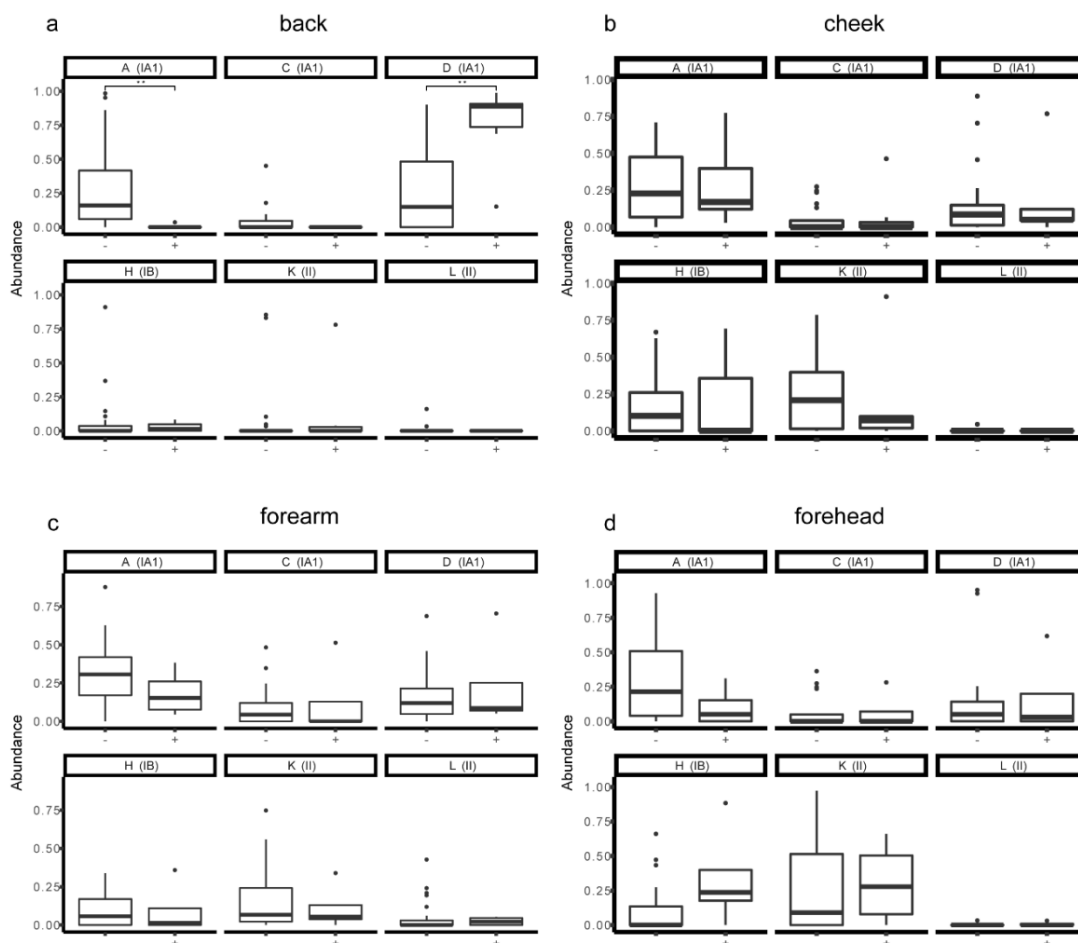
	Ba - Ch		Ba - Fa		Ba - Fh		Ch - Fa		Ch - Fh		Fa - Fh	
	coeff.	adj. p	coeff.	adj. p	coeff.	adj. p	coeff.	adj. p	coeff.	adj. p	coeff.	adj. p
A (IA1)	0.04	1.00	0.04	1.00	0.03	1.00	0.00	1.00	-0.01	1.00	-0.01	1.00
C (IA1)	0.02	1.00	0.03	1.00	0.02	1.00	0.01	1.00	-0.01	1.00	-0.02	1.00
D (IA1)	-0.15	0.08	-0.16	0.03	-0.18	0.03	0.00	1.00	-0.02	1.00	-0.02	1.00
E (IA1)	-0.06	0.74	-0.06	0.75	-0.05	1.00	0.00	1.00	0.00	1.00	0.00	1.00
F (IA2)	-0.01	1.00	-0.03	1.00	0.00	1.00	-0.01	1.00	0.01	1.00	0.02	1.00
H (IB)	0.10	0.19	0.02	1.00	0.05	1.00	-0.07	0.50	-0.04	1.00	0.03	1.00
G (IC)	0.00	1.00	0.00	1.00	0.00	1.00	0.00	1.00	0.00	1.00	0.00	1.00
K (II)	0.11	0.23	0.04	1.00	0.15	0.09	-0.06	1.00	0.04	1.00	0.10	0.56
L (III)	0.00	1.00	0.02	1.00	0.00	1.00	0.03	0.99	0.00	1.00	-0.03	1.00
unknown	0.00	1.00	-0.02	0.00	0.00	1.00	-0.02	0.00	0.00	1.00	0.02	0.00

**Additional File 8: Antimicrobial activity of staphylococcal strains against *S. aureus* DSM799, *C. acnes* DSM1897 and *C. acnes* 30.2.L1**

indicator strain \ staphylococcal strain	<i>S. aureus</i> DSM 799	<i>C. acnes</i> DSM 1897	<i>C. acnes</i> 30.2.L1
<i>S. capitis</i> HAB177	-	+	-
<i>S. capitis</i> HAB198	-	+	-
<i>S. capitis</i> HAB200	-	+	-
<i>S. capitis</i> HAB276	-	+	-
<i>S. capitis</i> HAB277	-	+	-
<i>S. capitis</i> HAB278	-	+	-
<i>S. capitis</i> HAB280	-	+	-
<i>S. capitis</i> HAB56	-	+	-
<i>S. capitis</i> HAC49	-	+	-
<i>S. capitis</i> HAC509	-	+	-
<i>S. epidermidis</i> HAA531	+	-	-



<i>S. epidermidis</i> HAA534	+	-	-
<i>S. epidermidis</i> HAB357	+	-	-
<i>S. epidermidis</i> HAB358	+	-	-
<i>S. epidermidis</i> HAB359	+	-	-
<i>S. epidermidis</i> HAB360	+	-	-
<i>S. epidermidis</i> HAB440	+	-	-
<i>S. epidermidis</i> HAC26	+	+	+
<i>S. epidermidis</i> HAC526	+	-	-
<i>S. epidermidis</i> HAC527	+	-	-
<i>S. epidermidis</i> HAC528	+	-	-
<i>S. epidermidis</i> HAC529	+	-	-
<i>S. epidermidis</i> HAC530	+	-	-
<i>S. epidermidis</i> HAC588	-	+	-
<i>S. epidermidis</i> HAC590	-	+	-
<i>S. epidermidis</i> HAF242	-	+	-
<i>S. epidermidis</i> HAF243	+	-	-
<i>S. epidermidis</i> HAF424	-	+	-
<i>S. epidermidis</i> HAF521	+	-	-
<i>S. epidermidis</i> HAF522	+	-	-
<i>S. epidermidis</i> HAF523	+	-	-
<i>S. epidermidis</i> HAF525	+	-	-
<i>S. hominis</i> HAA254	-	+	-
<i>S. hominis</i> HAA272	-	+	-
<i>S. hominis</i> HAA273	-	+	-
<i>S. hominis</i> HAA274	-	+	-
<i>S. hominis</i> HAB257	-	+	-
<i>S. hominis</i> HAC286	+	+	-
<i>S. warneri</i> HAA271	+	-	-
<i>S. warneri</i> HAA333	+	+	-
<i>S. warneri</i> HAA334	+	+	-



**Additional File 9: Staphylococcal strains with antimicrobial activity influence *C. acnes* populations.** Depicted are relative abundances of six *C. acnes* SLST classes (A, C, D, H, K, L) on a back b cheek c forearm d forehead skin sites with (+) or without (-) staphylococcal strains with antimicrobial activity (FDR-adjusted p-value, \*\* $p \leq 0.01$ . Unpaired Wilcoxon test).

**Additional File 10: Differentially expressed genes of *S. epidermidis* HAF242 (SE): growth of SE in co-culture with *C. acnes* 30.2.L1 (D-class) versus growth of SE in co-culture with *C. acnes* DSM1897 (A-class) (FDR-adjusted p-value, cut off:  $p \leq 0.05$ ; fold-change range  $>2$  or  $<-2$ ).**

Locus tag	curated annotation	log2 fold-change	padj
HBRUn20_25290	Hydrogen peroxide-inducible genes activator (oxyR)	4,55	9,59E-03
HBRUn20_14010	Extracellular matrix-binding protein (ebh)	4,13	2,26E-02
HBRUn20_09740	helix-turn-helix transcriptional regulator	3,96	9,59E-03
HBRUn20_03290	Staphylococcal secretory antigen (ssaA)	1,25	9,92E-04
HBRUn20_19070	sulfite exporter TauE/SafE family protein	1,22	2,04E-02
HBRUn20_12040	ACT domain-containing protein	1,06	1,39E-02

HBRUn20_17570	Amidophosphoribosyltransferase	-1,11	3,40E-03
HBRUn20_13570	FMN	-1,13	2,72E-02
HBRUn20_03800	N-acetyltransferase	-1,14	3,79E-04
HBRUn20_17630	N5-carboxyaminoimidazole ribonucleotide mutase	-1,24	2,68E-02
HBRUn20_22650	Phosphoglycolate phosphatase	-1,24	9,59E-03
HBRUn20_00990	lipase (gehD)	-1,25	2,72E-02
HBRUn20_17640	Bifunctional protein Fold protein	-1,26	4,01E-03
HBRUn20_16750	phenol-soluble modulin beta 2	-1,39	5,23E-03
HBRUn20_02980	hypothetical protein	-1,39	2,36E-03
HBRUn20_13620	elastin-binding protein EbpS	-1,42	3,30E-02
HBRUn20_11060	hypothetical protein	-1,44	3,54E-02
HBRUn20_17580	Phosphoribosylformylglycinamide synthase subunit	-1,52	2,55E-04
HBRUn20_16740	phenol-soluble modulin beta 1	-1,57	4,97E-03
HBRUn20_11220	Formate-tetrahydrofolate ligase	-1,57	1,29E-04
HBRUn20_17620	N5-carboxyaminoimidazole ribonucleotide synthase	-1,66	2,36E-03
HBRUn20_05110	ABC transporter ATP-binding protein	-1,77	4,92E-02
HBRUn20_20370	DUF4887 domain-containing protein	-1,78	3,04E-02
HBRUn20_08240	agr autoinducing peptide	-1,81	2,46E-03
HBRUn20_08440	hypothetical protein	-1,82	5,23E-03
HBRUn20_02240	Mannose-6-phosphate isomerase (manA)	-1,82	1,33E-02
HBRUn20_05100	putative ABC transporter permease	-1,83	4,55E-02
HBRUn20_17610	Phosphoribosylaminoimidazole-succinocarboxamide synthase	-1,96	2,46E-03
HBRUn20_09670	hypothetical protein	-1,99	1,39E-02
HBRUn20_24850	lantibiotic epidermin (epiA)	-2,07	2,82E-02
HBRUn20_16760	phenol-soluble modulin beta 3	-2,65	1,99E-02
HBRUn20_19890	Ribonuclease M5	-2,65	3,89E-03
HBRUn20_17470	glycopeptide resistance-associated protein (graF)	-4,60	1,33E-02

**Additional File 11: Differentially expressed genes of *S. epidermidis* HAF242 (SE): growth of SE in co-culture with *C. acnes* DSM1897 (A-class) versus growth of SE in monoculture (FDR-adjusted p-value, cut off:  $p \leq 0.05$ ; fold-change range  $>2$  or  $<-2$ ).**

locus tag	curated annotation	log2 fold-change	padj
HBRUn20_25290	Hydrogen peroxide-inducible genes activator (oxyR)	-4,84	1,61E-03
HBRUn20_21940	hypothetical protein	-4,53	3,34E-03
HBRUn20_09740	helix-turn-helix transcriptional regulator	-4,08	2,18E-03
HBRUn20_14010	Extracellular matrix-binding protein (ebh)	-3,98	9,60E-03
HBRUn20_23870	Cystathionine gamma-lyase	-2,49	4,89E-02
HBRUn20_01500	HTH-type transcriptional regulator SsuR	-2,35	5,69E-03
HBRUn20_16250	Thiamine pyrophosphokinase	-1,66	3,61E-02
HBRUn20_04570	L-cystine-binding protein TcyA	-1,64	3,77E-02
HBRUn20_02890	Oxygen-dependent choline dehydrogenase	-1,40	8,19E-04
HBRUn20_03290	Staphylococcal secretory antigen SsaA	-1,38	2,74E-05
HBRUn20_14030	Chromosome partition protein Smc	-1,37	4,05E-03
HBRUn20_11890	T-box domain containing protein	-1,36	2,02E-02
HBRUn20_03430	3-hydroxy-3-methylglutaryl-coenzyme A reductase	-1,35	1,81E-04
HBRUn20_21890	Na(+)/H(+) antiporter subunit B	-1,34	1,12E-02
HBRUn20_03560	YitT family protein	-1,21	3,79E-02
HBRUn20_16730	Putative HAD-hydrolase YfnB	-1,19	2,19E-02
HBRUn20_05750	Staphylococcal secretory antigen SsaA	-1,16	6,29E-04
HBRUn20_01560	Lipase	-1,15	3,11E-02
HBRUn20_16280	Serine/threonine-protein kinase PrkC	-1,13	1,90E-05
HBRUn20_15400	HTH-type transcriptional regulator GlnR	-1,12	1,13E-02
HBRUn20_18800	Na(+)/H(+) antiporter subunit C1	-1,10	3,86E-02
HBRUn20_03660	Ribokinase	-1,09	1,12E-03
HBRUn20_05170	Colistin resistance protein EmrA	-1,09	1,77E-02
HBRUn20_21440	Sugar efflux transporter C	-1,07	2,62E-03
HBRUn20_12990	putative metallo-hydrolase	-1,03	3,21E-03
HBRUn20_20930	Energy-dependent translational throttle protein EttA	-1,02	9,06E-04

HBRUn20_21320	Vitamin B12 import ATP-binding protein BtuD	-1,02	6,05E-04
HBRUn20_10910	Riboflavin biosynthesis protein RibBA	-1,00	4,27E-05
HBRUn20_23090	Pyridoxal 5'-phosphate synthase subunit PdxS	1,00	6,71E-04
HBRUn20_03090	L-lactate dehydrogenase 2	1,01	2,67E-08
HBRUn20_04830	HTH-type transcriptional regulator SarZ	1,01	5,92E-04
HBRUn20_00090	Serine--tRNA ligase	1,01	9,44E-05
HBRUn20_20340	Glyceraldehyde-3-phosphate dehydrogenase 1	1,03	2,75E-04
HBRUn20_08600	thioredoxin family protein	1,03	1,84E-02
HBRUn20_03100	Acetolactate synthase	1,04	2,58E-09
HBRUn20_11190	YtxH domain-containing protein	1,04	4,05E-03
HBRUn20_11220	Formate--tetrahydrofolate ligase	1,06	2,27E-03
HBRUn20_01900	putative poly-beta-N-acetyl-D-glucosamine export protein	1,06	3,01E-03
HBRUn20_19650	hypothetical protein	1,06	2,83E-02
HBRUn20_20390	Epimerase family protein	1,07	1,08E-03
HBRUn20_09820	YtxH domain-containing protein	1,08	4,07E-03
HBRUn20_02450	MarR family winged helix-turn-helix transcriptional regulator	1,08	2,14E-03
HBRUn20_16710	putative N-acetyltransferase	1,09	2,39E-03
HBRUn20_09660	Glucosamine-6-phosphate deaminase	1,10	2,18E-03
HBRUn20_23730	Bacteria_large_SRP	1,10	5,41E-03
HBRUn20_21140	Putative glycosyltransferase CsbB	1,11	1,54E-03
HBRUn20_16690	Transcriptional regulator MraZ	1,11	2,91E-03
HBRUn20_05460	PTS system maltose-specific EIICB component	1,12	2,58E-02
HBRUn20_20330	Phosphoglycerate kinase	1,12	1,81E-04
HBRUn20_14530	N-acetylcysteine deacetylase	1,14	2,18E-03
HBRUn20_00810	putative malate:quinone oxidoreductase 2	1,15	7,25E-03
HBRUn20_01080	Diacetyl reductase [(S)-acetoin forming]	1,17	6,57E-04
HBRUn20_09130	type 1 glutamine amidotransferase	1,18	2,10E-04
HBRUn20_02240	Mannose-6-phosphate isomerase ManA	1,19	2,10E-02

HBRUn20_21150	putative oxidoreductase	1,20	4,05E-03
HBRUn20_10950	HTH-type transcriptional regulator	1,21	5,92E-04
HBRUn20_04160	Guanosine-5'-triphosphate-3'-diphosphate pyrophosphatase	1,23	1,05E-04
HBRUn20_03000	NADH peroxidase	1,25	7,38E-03
HBRUn20_05400	flavin reductase family protein	1,25	3,81E-04
HBRUn20_14540	Tetrahydropyridine-dicarboxylate N- acetyltransferase	1,28	1,12E-04
HBRUn20_23460	Putative septation protein SpoVG	1,28	6,71E-04
HBRUn20_24720	YIP1 family protein	1,30	2,88E-02
HBRUn20_03350	General stress protein 39	1,33	1,29E-03
HBRUn20_08990	aromatic acid exporter family protein	1,34	1,17E-03
HBRUn20_23470	2-iminobutanoate/2-iminopropanoate deaminase	1,35	1,04E-05
HBRUn20_00140	Homoserine O-acetyltransferase	1,36	4,60E-02
HBRUn20_14520	Alanine racemase	1,38	1,12E-04
HBRUn20_22170	Aldo-keto reductase IolS	1,40	1,12E-04
HBRUn20_05540	PTS system EIIBC component	1,45	1,06E-16
HBRUn20_07170	DCC1-like thiol-disulfide oxidoreductase family protein	1,46	1,12E-04
HBRUn20_04910	general stress protein 26	1,46	1,12E-04
HBRUn20_19890	Ribonuclease M5	1,50	2,04E-02
HBRUn20_22100	Lactate racemase	1,50	2,09E-02
HBRUn20_05370	Formimidoylglutamase	1,51	1,90E-05
HBRUn20_14560	4-hydroxy-tetrahydrodipicolinate synthase	1,52	1,20E-04
HBRUn20_06850	Heme oxygenase (staphylobilin-producing) 2	1,53	1,24E-02
HBRUn20_14550	4-hydroxy-tetrahydrodipicolinate reductase	1,55	2,10E-04
HBRUn20_05530	putative HTH-type transcriptional regulator YbbH	1,58	1,29E-10
HBRUn20_25110	rli28	1,60	2,21E-05
HBRUn20_04170	Levodione reductase	1,70	5,24E-04
HBRUn20_24700	putative ABC transporter ATP-binding protein YknY	1,72	1,80E-03

HBRUn20_19810	DUF368 domain-containing protein	1,74	1,61E-07
HBRUn20_05390	putative oxidoreductase YghA	1,75	2,50E-04
HBRUn20_03800	putative protein YjdJ	1,95	6,76E-14
HBRUn20_06860	hypothetical protein	2,08	2,28E-09
HBRUn20_03440	hypothetical protein	2,24	4,25E-10
HBRUn20_01110	ABC transporter permease	2,50	2,31E-04
HBRUn20_01100	ABC transporter permease	2,77	1,87E-06
HBRUn20_19990	sterile alpha motif-like domain-containing protein	4,06	8,14E-06

**Additional File 12: Differentially expressed genes of *S. epidermidis* HAF242 (SE): growth of SE in co-culture with *C. acnes* 30.2.L1 (D-class) versus growth of SE in monoculture (FDR-adjusted p-value, cut off:  $p \leq 0.05$ ; fold-change range  $>2$  or  $<-2$ ).**

<b>locus tag</b>	<b>curated annotation</b>	<b>log2 fold-change</b>	<b>padj</b>
HBRUn20_25190	CsbD family protein	-5,05	3,58E-03
HBRUn20_16760	phenol-soluble modulins beta 3	-3,37	4,85E-04
HBRUn20_05440	SRPBCC domain-containing protein	-2,98	3,67E-06
HBRUn20_23700	Nucleoid-associated protein	-2,31	5,76E-04
HBRUn20_15380	phage head morphogenesis protein	-2,22	7,41E-03
HBRUn20_16740	phenol-soluble modulins beta 1	-2,14	2,43E-05
HBRUn20_20370	DUF4887 domain-containing protein	-2,10	6,15E-03
HBRUn20_15070	DUF896 domain-containing protein	-2,04	9,36E-03
HBRUn20_00170	50S ribosomal protein	-2,01	6,16E-04
HBRUn20_10050	helix-turn-helix domain-containing protein	-1,93	2,76E-02
HBRUn20_10030	hypothetical protein	-1,90	1,22E-02
HBRUn20_16750	phenol-soluble modulins beta 2	-1,86	1,84E-06
HBRUn20_15830	Ribosome maturation factor RimP	-1,75	1,59E-02
HBRUn20_05280	DUF4097 family beta strand repeat-containing protein	-1,71	2,62E-02
HBRUn20_11890	T-box domain-containing protein	-1,68	5,49E-04
HBRUn20_17580	Phosphoribosylformylglycinamide synthase subunit PurL	-1,61	4,57E-06
HBRUn20_24670	Lipase 2 (gehD)	-1,59	1,10E-04

HBRUn20_10020	hypothetical protein	-1,57	4,77E-03
HBRUn20_22200	hypothetical protein	-1,55	6,71E-04
HBRUn20_00830	hypothetical protein	-1,55	2,95E-02
HBRUn20_07820	Holo-[acyl-carrier-protein] synthase	-1,50	3,29E-02
HBRUn20_14150	Peptide methionine sulfoxide reductase MsrA 2	-1,47	1,04E-02
HBRUn20_08440	phage termise small subunit P27 family	-1,44	5,42E-03
HBRUn20_10710	Putative 8-oxo-dGTP diphosphatase YtkD	-1,43	1,47E-03
HBRUn20_17550	Phosphoribosylglycinamide formyltransferase	-1,40	1,39E-02
HBRUn20_00390	putative protein YdhK	-1,34	2,66E-02
HBRUn20_02200	Organic hydroperoxide resistance protein- like protein	-1,34	4,74E-03
HBRUn20_10660	hypothetical protein	-1,30	2,66E-02
HBRUn20_06930	Iron-sulfur cluster carrier protein	-1,17	2,64E-03
HBRUn20_02890	Oxygen-dependent choline dehydrogenase	-1,13	6,15E-03
HBRUn20_03780	TM2 domain-containing protein	-1,12	2,66E-02
HBRUn20_17420	Phosphocarrier protein HPr	-1,09	1,93E-02
HBRUn20_00380	Multicopper oxidase mco	-1,08	6,37E-03
HBRUn20_15400	HTH-type transcriptional regulator GlnR	-1,08	1,41E-02
HBRUn20_14080	NifU N-termil domain-containing protein	-1,07	1,92E-02
HBRUn20_16380	Guanylate kinase	-1,04	5,02E-03
HBRUn20_17570	Amidophosphoribosyltransferase	-1,04	1,34E-03
HBRUn20_16850	Thioredoxin	-1,04	1,58E-04
HBRUn20_07170	DCC1-like thiol-disulfide oxidoreductase family protein	1,01	6,15E-03
HBRUn20_05530	MurR/RpiR family transcriptiol regulator	1,02	4,99E-05
HBRUn20_16890	cell division protein ZapA	1,06	3,14E-02
HBRUn20_05510	hypothetical protein	1,07	1,69E-03
HBRUn20_19810	hypothetical protein	1,11	6,16E-04
HBRUn20_01360	S35	1,20	2,66E-02
HBRUn20_01090	ABC transporter ATP-binding protein	1,21	1,68E-02
HBRUn20_06860	hypothetical protein	1,22	6,54E-04
HBRUn20_03440	CHAP domain-containing protein	1,74	4,40E-07



---

HBRUn20_01100	ABC transporter permease	1,90	4,37E-04
HBRUn20_19990	sterile alpha motif-like domain-containing protein	2,03	1,92E-02

## Danksagung

Zum Abschluss der Arbeit, möchte ich mich einmal bei allen Menschen bedanken, die mich auf dem Weg hierhin begleitet und unterstützt haben.

Zuerst möchte ich mich bei Assoc. Prof. Dr. Holger Brüggemann bedanken, dessen wissenschaftlicher Input und Diskussionen das Projekt gestützt haben. Danke, für alles was ich in den letzten Jahren von Dir lernen durfte.

Prof. Dr. Wolfgang Streit danke ich für die gute Betreuung, die Unterstützung meines Projektes, den guten wissenschaftlichen Austausch und die hilfreichen Ratschläge.

Mein besonderer Dank gilt Dr. Jennifer Hüpeden, die sich schon während meiner Masterarbeit immer für mich eingesetzt hat. Danke, dass Du in den letzten Jahren meine Ansprech- und Diskussionspartnerin warst und bei allen Fragen und Problemen ein offenes Ohr für mich hattest.

Ich bedanke mich bei Heike Fölster und Dr. Hendrik Reuter für die Ermöglichung und Unterstützung meines Projektes. Außerdem bedanke ich mich bei Andrea, Sandra, Mirja, Petra, Tina, Laura, Karen und Melli für die gute Zeit, während und zwischen den Arbeitszeiten. Danke, dass Ihr mir bei allen Fragen und Problemen immer weitergeholfen habt.

Vielen Dank an Katrin, Jana, Claudia, Kira, Leonie und Anina, die mich aufgemuntert haben, wenn es mal nicht gut lief.

Vor allem danke ich Fabi, der mich immer unterstützt hat. Danke, dass Du mich in schlechten Phasen gehalten und dich in guten Phasen mitgefremt hast.

Danke auch an meine Eltern und Clara, die für mich immer ein Ruhepol sind.